Gene Therapy for Muscular Dystrophy using Secondary Modifiers of the Dystrophic Phenotype

DISSERTATION ZUR ERLANGUNG DES DOKTORGRADES
DER NATURWISSENSCHAFTEN (DR. RER. NAT.) DER
NATURWISSENSCHAFTLICHEN FAKULTÄT III - BIOLOGIE UND
VORKLINISCHE MEDIZIN DER UNIVERSITÄT REGENSBURG

vorgelegt von
Simone Abmayr aus München

Februar 2004

Das Promotionsgesuch wurde eingereicht am 11.2.2004

Die Arbeit wurde angeleitet von Prof. Dr. Jeffrey Chamberlain

Prüfungsausschuß:

Vorsitzender:

1. Prüfer:	Prof. Dr. Ch. Aslanidis
2. Prüfer:	Prof. Dr. J. Chamberlain
3. Prüfer:	Prof. Dr. R. Warth

TABLE OF CONTENTS

ABBREVIATIONS

AAV	adeno-associated virus
ABD	actin-binding domain
AD	adenovirus
APAF-I	apoptotic protease activating factor-I
ARC	apoptosis repressor interacting with CARD
ATP	adenosine triphosphate
BMD	Becker muscular dystrophy
BSA	bovine serum albumin
CARD	caspase recruitment domain
CD	cluster of differentiation
CK	creatine kinase
CMD	congenital muscular dystrophy
CMV	cytomegalovirus
CPE	cytopathic effect
COX	cytochrome oxidase
DB	dystrobrevin
DED	death effector domain
DG	dystroglycan
DGC	dystrophin glycoprotein complex
DMD	Duchenne muscular dystrophy
DMEM	Dulbecco's modified Eagles medium
DNase	desoxyribonuclease
dko	double knock-out
EST	expressed-sequence tags
FBS	fetal bovine serum
GalNAc	N-acetylgalactosamine
GAPDH	glyceraldehyde-phosphate dehydrogenase
bGHpA	bovine growth hormone polyadenylation site
hGHpA	human growth hormone polyadenylation site
HEK	human embryonic kidney
HSA	human α-skeletal actin
H&E	hematoxylin and eosin
Igf-I	Insulin-like growth factor I
LGMD	limb-girdle muscular dystrophy
MAPK	mitogen activated protein kinase

mdx	X-chromosome linked muscular dystrophy
MHC	myosin-heavy chain
MOI	multiplicity of infection
nNOS	neuronal nitric oxide synthase
NO	nitric oxide
NMJ	neuromuscular junction
PI3K	phosphatidylinositol 3-phosphate
P/E	prolin-glutamic acid
PDZ	domain found in postsynaptic density protein-95, discs large, and zonula occludens-1 proteins
NT	N-terminal
RAIDD	RIP-associated ICH-I homologous protein with a death domain
RNase	ribonuclease
SAPK3	stress-activated protein kinase-3
SG	sarcoglycan
SV40	simian virus 40
SH2/SH3	Src homology 2 and 3
TA	*tibialis anterior*
TUNEL	terminal desoxynucleotidyl transferase (TdT)-mediated dUTP nick endlabeling
UGC	utrophin glycoprotein complex
vg	vector genomes
μdys	micro-dystrophin

1. SUMMARY

Duchenne muscular dystrophy (DMD) is an x-linked recessive disorder, primarily characterized by progressive muscle weakness and wasting. Although the disease is caused by mutations in the dystrophin gene, the precise molecular mechanisms leading to muscle pathology are poorly understood. Dystrophin is thought to play a structural role by providing a link between the intracellular actin cytoskeleton and the extracellular matrix *via* its interaction with a complex of peripheral and integral membrane proteins called "the dystrophin-glycoprotein complex" (DGC). Disruption of this linkage results in membrane instability and renders dystrophic muscle fibers highly susceptible to contraction-induced injury. Several members of the DGC play a role in cell signaling rather than contributing to mechanical stability. Altered cell signaling is thought to increase the susceptibility of muscle fibers to secondary triggers of damage, such as functional ischemia and oxidative stress. Understanding the connection between signaling and mechanical dysfunction is important to further understand the function of dystrophin and the DGC and for finding improved therapies for DMD.

Recent studies have identified ARC (apoptosis repressor with caspase recruitment domain) as an abundant protein in human muscle that can inhibit both hypoxia and caspase-8 induced apoptosis as well as protect cells from oxidative stress. To explore a potential role for ARC in protecting muscle fibers from dystrophic breakdown, we have cloned and characterized murine ARC and studied its expression in normal and dystrophic mouse *mdx* muscles. Similarly to ARC mRNA expression in human and rat tissues, mouse ARC mRNA was found to be highly expressed in skeletal muscle and heart, and at a lower level in brain and testis. We further examined ARC protein expression in striated muscles and found that ARC displayed fiber-type restricted expression patterns and co-localized with the mitochondrial marker cytochrome oxidase (COX). These studies further explored ARC expression and localization in a dystrophic background. ARC was expressed at essentially the same levels in normal and dystrophic *mdx* muscles and appeared to be predominantly cytoplasmic in localization. However, we were able to demonstrate differences in the intracellular localization pattern of ARC between normal and dystrophic *mdx* muscle. ARC expression in normal muscle showed a distinct regular pattern of ARC positive and negative

fibers, while ARC expression in dystrophic *mdx* muscle appeared as a less distinct, irregular pattern. These differences could be a consequence of altered mitochondrial protein expression, which is a characteristic feature of dystrophic muscle. However, it remains unclear if apoptosis is a primary or secondary effect of muscle fiber breakdown. We found activated caspases in degenerating muscle fibers, suggesting that apoptosis is a secondary consequence resulting from the loss of membrane integrity. Our observations suggest a sequence of molecular events in which an initial membrane-damaging event is subsequently followed by up-regulation of caspase-3 and loss of ARC expression. To gain further insights in the role of ARC in dystrophic *mdx* muscle, we generated transgenic *mdx* mice that over-expressed ARC under a tissue-specific promoter. These mice demonstrated high expression levels of transgenic ARC in all, oxidative and glycolytic, muscle fibers. Despite the over-expression of ARC in *mdx* skeletal muscle, these mice developed a dystrophic phenotype. We evaluated muscle morphology in ARC transgenic/*mdx* in comparison with *mdx* animals and did not observe an amelioration of the dystrophic pathology in ARC transgenic/*mdx* mice in various muscles at different ages. In summary, these studies suggested that the apoptotic pathways regulated by ARC do not significantly contribute to myofiber death in muscular dystrophy.

In a complementary approach we have cloned cDNAs for two murine muscle-specific Insulin-like growth factor-I (Igf-I) isoforms (Igf-I Ea and Igf-I Eb) and characterized their expression in normal and dystrophic *mdx* muscles. Although Igf-I is primarily synthesized by the liver in response to growth hormone secretion, this growth factor is also produced locally in tissues where it exerts autocrine and paracrine effects. We have developed assays to quantitate expression of both Igf-I mRNA isoforms in normal and dystrophic *mdx* muscles. Quantitative analysis of Igf-I mRNA expression showed that both Igf-I isoforms were expressed in normal and *mdx* muscles and revealed no significant differences in their relative expression levels between normal and *mdx* muscles of nine month-old male mice. These analyses further showed that the more abundant Igf-I isoform, Igf-I Ea, was expressed at approximately seven times higher levels than the other isoform, Igf-I Eb at our tested age group. To determine if the cloned muscle-specific Igf-I cDNAs encoded functional proteins, we generated recombinant adenoviral vectors that expressed either Igf-I Ea or Igf-I Eb. We utilized an *in vitro* myoblast differentiation assay to show that both Igf-I cDNAs were

functional and enhanced L6 myoblast differentiation, similarly to that observed following treatment of the cultures with recombinant Igf-I protein.

In contrast to ARC, the effects of Igf-I have been widely studied in various cell types and tissues. In particular, during mammalian growth and development Igf-I has been shown to play an important role in regulating tissue growth and differentiation. Overexpression of Igf-I in transgenic *mdx* muscles has been shown to protect the animals from the loss of muscle mass and function and to enhance muscle repair mechanisms. To determine if the beneficial effects of Igf-I are synergistic with the protective effects of dystrophin in ameliorating muscular dystrophy, we compared the effects of delivering Igf-I alone versus co-delivering both Igf-1 and dystrophin to adult, dystrophic *mdx* mouse muscles. For this purpose, we generated recombinant adeno-associated viral (AAV) vectors expressing Igf-I (AAV-Igf-I) or a functional micro-dystrophin (AAV-μdys) from a muscle-specific promoter. *Tibialis anterior* muscles of adult *mdx* mice were injected with AAV-Igf-I, AAV-μdys or a combination of both. Four months post injection, immunohistochemical analysis demonstrated persistent expression of dystrophin that reached an average of 40% of the total muscle cross sectional area. mRNA analysis further revealed Igf-I overexpression with levels ranging from 50-100 fold in AAV-Igf-I treated and up to 400 fold in AAV-Igf-I and AAV-μdys co-treated muscles. By analyzing muscle histology as well as functional properties four months post-injection, we were able to show that these treatments were beneficial in reversing the dystrophic pathology. Histological analysis of AAV-Igf-I, AAV-μdys and co-treated animals revealed that each treatment provided protection from at least some aspects of muscle degeneration. Measurement of mechanical properties in the injected muscles demonstrated that AAV-Igf-I treated muscles displayed an increase in muscle mass, but were not significantly protected from contraction-induced injuries. In contrast, AAV-μdys treated animals demonstrated increased protection from contraction-induced injury after two lengthening contractions but did not display increases in mass or force generation. However, the combined treatment of both AAV-Igf-I and AAV-μdys showed an increase in muscle strength in conjunction with a protection from contraction-induced injury, suggesting that Igf-I and dystrophin acted synergistically and that co-treatment was more beneficial for dystrophic muscle than treatment with either protein alone.

In summary, characterization of proteins that inhibit apoptosis and/or enhance muscle strength and repair in dystrophic muscle has provided further insights into the complexity of the dystrophic pathology and the potential for gene replacement therapy in conjunction with treatment of secondary pathological features of the disease.

2. ZUSAMMENFASSUNG

Muskeldystrophie Duchenne ist eine rezessive Erbkrankheit, die durch fortschreitende Muskelschwäche und Muskelschwund gekennzeichnet ist. Mit einer Inzidenz von einer unter 3500 Knabengeburten ist sie die häufigste vererbbare Myopathie. Die ersten Symptome treten typischerweise um das dritte Lebensjahr auf, in der frühen Jugend kommt es im allgemeinen zum Verlust der Gehfähigkeit und die Lebenserwartung liegt selten über 25 Jahren. Die Krankheit wird durch Mutationen im Dystrophingen verursacht, wobei die genauen molekularen Zusammenhänge zwischen Gendefekt und Krankheitsverlauf bisher nur sehr unzureichend erklärt werden konnten. Dystrophin besitzt vermutlich eine wichtige Strukturfunktion im Muskel, indem es eine Quervernetzung zwischen dem intrazellulären Aktin-Zytoskelett und der extrazellulären Matrix herstellt. Dystrophin interagiert mit einer Vielzahl von peripheren und integralen Membranproteinen, die den Dystrophin-Glykoprotein Komplex (DGC) bilden. Die Zerstörung dieser Querverknüpfung führt zum Verlust des DGC und zur Instabilität von Muskelmembranen, die somit leicht durch Muskelkontraktionen beschädigt werden können. Es wurde gezeigt, dass einige DGC Proteine wesentlich zur Stabilität der Muskelmembran beitragen, während andere DGC Proteine eine Rolle bei der Signaltransduktion spielen. Die Abwesenheit des DGC könnte daher wesentliche Mechanismen der Signaltransduktion beeinträchtigen und die Sensitivität von Muskelzellen gegenüber sekundären Reizen wie Ischämie und oxidativem Stress erhöhen. Um verbesserte Therapieansätze für DMD zu entwickeln, ist es daher notwendig, eine genaues Verständnis für die Struktur- und Signalfunktion von Dystrophin und des DGC zu gewinnen.

Neue Studien haben gezeigt, dass das Protein ARC (apoptosis repressor interacting with caspase recruitment domain) in hohen Mengen im humanen Skelett- und Herzmuskel vorkommt, und dass die Überexpression von ARC in Herzmuskelzellen vor Hypoxie und Caspase-8 induzierter Apoptose schützen kann. In der vorliegenden Arbeit wurde untersucht, ob ARC eine Rolle in der Pathologie der Dystrophie spielt und ob es vor Zerstörung von Muskelfasern schützen kann. Daher wurde murines ARC kloniert und seine Expression im gesunden und dystrophischen *mdx* Muskel charakterisiert. Murines ARC zeigte hohe mRNA Expression im Skelett- und Herzmuskel und niedrige Expression im Gehirn- und Hodengewebe. Immunohistologische Untersuchungen ergaben, dass ARC faserspezifisch im

quergestreiften Muskel exprimiert ist, wo es hauptsächlich in oxidativen Muskelfasern vorkommt und mit dem mitochondrien-spezifischen Marker Cytochromoxidase (COX) kolokalisiert. Endogenes ARC zeigte eine vergleichbare Expressionsstärke im gesunden und dystrophischen *mdx* Gewebe, jedoch war die intrazelluläre Lokalisation von ARC in diesen Geweben unterschiedlich. So zeigte ARC im gesunden Gewebe ein regelmäßiges Expressionsmuster von ARC positiven und negativen Muskelfasern, während dieses Muster im dystrophischen *mdx* Gewebe stark unregelmäßig und weniger deutlich ausgeprägt war. Diese Unterschiede könnten die Folge einer veränderter Expression von mitochondrialen Proteinen sein, die im allgemeinen symptomatisch für dystrophisches Gewebe ist. Es bleibt jedoch unklar, ob Apoptose die Ursache oder die Folge der Zerstörung von Muskelfasern ist. In dieser Studie wurde eine erhöhte Caspaseaktivität in degenerierten Muskelfasern gemessen, die eine direkte Folge des Verlusts der Membranintegrität sein könnte. Initiale Schäden an der Membran könnten eine Abfolge von molekularen Ereignissen auslösen, die zu einer erhöhten Expression von Caspase-3 und einem einhergehenden Verlust von ARC führen. Um weitere Einsichten über die Rolle von ARC im dystrophischen Muskel zu gewinnen, wurden transgene *mdx* Mäuse generiert, die ARC unter einem gewebespezifischen Promoter überexprimieren. Diese Mäuse wiesen eine hohe Expression von transgenem ARC in oxidativen und glykolytischen Muskelfasern auf, und entwickelten trotz ARC Überexpression einen dystrophischen Krankheitsverlauf. Die Morphologie unterschiedlicher Muskeln von ARC transgenen *mdx* Mäusen aus verschiedenen Altersstufen wurde anschließend untersucht und mit der *mdx* Muskelmorphologie verglichen, zeigte jedoch keine Verbesserung des dystrophischen Pathologiebildes. Es wurde daraus geschlossen, dass apoptotische Regulationsmechanismen, die durch ARC kontrolliert werden, nicht signifikant zur Muskelpathologie in dystrophischem Gewebe beitragen.

In einem komplementären Ansatz wurden die cDNAs für zwei muskelspezifische Isoformen des insulin-ähnlichen Wachstumsfaktor I (*Insulin-like growth factor-I,* Igf-I) kloniert und die Expression in normalem und dystrophischem *mdx* Muskelgewebe charakterisiert. Igf-I wird hauptsächlich von der Leber gebildet und in die Blutbahn abgegeben, kann aber auch lokal in extrahepatischem Gewebe erzeugt werden und einen direkten Effekt auf das jeweilige Gewebe ausüben, und dadurch eine essentielle Rolle in der Regulation von Zellwachstum und –differenzierung übernehmen. In der vorliegenden Arbeit

wurden Tests für die Quantifizierung der Igf-I mRNA entwickelt, die zwischen beiden Isoformen unterscheiden können. Mit Hilfe dieser Tests wurden die Stärke der Expression von beiden Igf-I Isoformen in normalen und dystrophischen Muskeln gemessen. Die quantitative PCR-Analyse zeigte, dass es keinen signifikanten Unterschied in den relativen Igf-I Expressionsstärken zwischen normalen und dystrophischen Muskeln bei Mäusen im Alter von neun Monaten gibt. Diese Analyse zeigte auch, dass die Igf-I Ea Isoform in den untersuchten Mäusen ungefähr sieben Mal höher exprimiert ist als die Igf-I Eb Isoform. Weiter wurde untersucht, ob beide Igf-I Isoformen für funktionelle Proteine kodieren. Dazu wurden rekombinante adenovirale Vektoren generiert, die entweder Igf-I Ea oder Igf-I Eb exprimieren. In einem Myoblastendifferenzierungsassay wurde daraufhin gezeigt, dass beide Proteine funktionsfähig sind und die Myoblastendifferenzierung von L6 Zellen beschleunigen.

Im Gegensatz zu ARC ist die Rolle von Igf-I in verschiedenen Zell- und Gewebetypen in früheren Studien ausgiebig charakterisiert worden. Die Überexpression von Igf-I im *mdx* Skelettmuskel mildert den dystrophischen Phänotyp, indem es die Muskelmasse vergrößert und Reparaturmechanismen des Muskels fördert. In der vorliegenden Arbeit wurden adulte *mdx* Muskeln gentherapeutisch mit Igf-I alleine und in Kombination mit Dystrophin behandelt, um zu untersuchen, ob Igf-I synergistisch mit Dystrophin wirkt und das Krankheitsbild von Muskeldystrophie verbessern kann. Dafür wurden rekombinante adeno-assoziierte virale (AAV) Vektoren generiert, die unter einem muskelspezifischen Promotor entweder Igf-I (AAV-Igf-I) oder eine funktionelle Mikroversion von Dystrophin (AAV-μdys) exprimierten. Diese rekombinanten Vektoren wurden einzeln oder in Kombination in den *Musulus tibialis anterior* von neun Monate alten *mdx* Mäusen gespritzt. Die behandelten Muskeln und Kontrollmuskeln wurden vier Monaten später auf Expression von Dystrophin und Igf-I getestet und anschließend auf Muskelhistologie und Muskelfunktion untersucht. Die Expression von Dystrophin wurde mit Hilfe von Immunfluoreszenz visualisiert und anhand von digitaler Bildverarbeitung quantifiziert. Auf diese Weise konnte festgestellt werden, dass 40% der Muskelzellen eines Muskelschnittes Dystrophin exprimierten. Die Expression von Igf-I wurde mit Hilfe der quantitativen RNA Analyse gemessen, wobei gezeigt werden konnte, dass Igf-I in der Kombinationsbehandlung bis zu 400-fach, und in der Einzelbehandlung etwa 50-100-fach, überexprimiert wurde. Sowohl histologische als auch

funktionelle Analysen demonstrierten, dass jeder behandelte Muskel im Vergleich zu unbehandelten *mdx* Muskeln den dystrophischen Krankheitsverlauf verbesserte. Die Behandlung mit AAV-Igf-I, AAV-µdys und die Kombinationsbehandlung schützte vor Muskeldegeneration, wodurch beispielsweise eine verminderten Anzahl von regenerierenden Muskelfasern auftrat. Funktionelle Studien zeigten weiter, dass die mit AAV-µdys behandelten Muskeln vor Verletzungen durch Muskelkontraktionen geschützt waren, jedoch keine größere Muskelmasse und Muskelkraft aufwiesen. AAV-Igf-I behandelte Muskeln hingegen waren nicht vor Verletzungen durch Muskelkontraktionen geschützt, wiesen aber eine größere Muskelmasse auf. Im Gegensatz dazu zeigte die Kombinationsbehandlung sowohl einen Schutz vor Verletzungen durch Muskelkontraktionen, als auch eine erhöhte Muskelmasse und Muskelkraft. Aus diesem Ergebnis konnte geschlußfolgert werden, dass Dystrophin und Igf-I synergistisch wirkten und die Kombinationsbehandlung den Krankheitsverlauf stärker abschwächte als die jeweiligen Einzelbehandlungen.

Zusammenfassend läßt sich sagen, dass die Charakterisierung von Apoptoseinhibitoren bzw. Proteinen, die Reparaturmechanismen des Muskels fördern weitere Aufschlüsse über die Komplexität des dystrophischen Krankheitsbildes geben konnten. Weiter konnte gezeigt werden, dass die kombinierte Gentherapie, bei der Dystrophin im dystrophischen Muskel ersetzt wird und zusätzlich sekundäre pathologische Symptome behandelt werden, einen neuen vielversprechenden Ansatz für die Behandlung von Muskeldystrophie darstellt.

3. INTRODUCTION

3.1. Duchenne Muscular Dystrophy (DMD)

Duchenne muscular dystrophy (DMD) and the allelic Becker muscular dystrophy (BMD) are X-linked recessive disorders, caused by mutations in the dystrophin gene (Koenig et al., 1987). DMD/BMD are among the most common human genetic diseases with a worldwide incidence of approximately 1 in 3500 male births, one-third of which arise from *de novo* mutations (Emery, 1993; Moser, 1984). While DMD results from the absence of dystrophin, most BMD patients express a partially functional dystrophin protein (Baumbach et al., 1989; Hoffman et al., 1987).

DMD patients are clinically healthy at birth. The first symptoms are characterized by a delayed ability to walk, excessive clumsiness and difficulty running. By the age of four to six, patients develop muscle pseudohypertrophy, proximal muscle weakness and have increasing difficulty rising to a standing position from a seated position on the floor. To assist in standing, DMD patients invariably stand up by using their hands to push up along the legs, known as a Gower's sign (Emery, 1993). With time, a progressive muscular weakness takes place, which results in a wheelchair dependency by the age of 8-11 years. In addition to skeletal muscle degeneration, most of the patients develop cardiomyopathy and one third display cognitive defects characterized by variable degrees of mental retardation (Bresolin et al., 1994). The majority of DMD patients die in their early to late twenties from respiratory or cardiac failure (Emery, 1993). BMD patients, on the other hand, display similar clinical symptoms, however the onset and the progression of the disease are delayed (Baumbach et al., 1989; Monaco et al., 1988). These patients usually begin using a wheelchair beyond age 16 and survive beyond age 30. An extremely mild case of BMB has been reported where a patient was still walking in his late seventieth (England et al., 1990).

Histological analysis of muscle biopsies from DMD/BMD patients display an extensive muscle degeneration/regeneration process, characterized by centrally located nuclei, a wide variation in myofiber size and immune cell infiltration. With age, muscle fibers progressively fail to regenerate and are gradually replaced by adipose and connective tissue

(fibrosis). As a consequence of muscle degeneration, patients display high levels of muscle enzymes in their circulatory system. Elevated levels of muscle creatine kinase can be used for early DMD diagnosis. Approximately 50% of newborn males that display elevated creatine kinase levels develop DMD.

Two-thirds of DMD and BMD cases result from various deletions in the dystrophin gene. Partial gene duplications make up 5-10% of the cases and the remaining cases are due to point mutations or translocations (Amalfitano et al., 1997). The vast majority of patients are boys, while only a low number of females are affected due to X-autosomal translocations (Ray et al., 1985). Carrier females generally do not display any symptoms, however some have been reported to show abnormalities in cardiac function after exercise (Mathews and Moore, 2003; Nolan et al., 2003). Deletions in DMD/BMD boys and carrier females can be screened by multiplex PCR, which is the most widely used DNA diagnostic test for DMD/BMD (Chamberlain et al., 1992; Chamberlain et al., 1988a).

3.2. Animal models for DMD

Several animal models (mouse, dog, cat, chicken) for DMD have been identified (Nonaka, 1998). The best characterized is the *mdx* (X-chromosome-linked muscular dystrophy) mouse model, which has a point mutation in exon 23, resulting in a premature STOP codon (Sicinski et al., 1989). The N-terminus of dystrophin upstream of the mutation is synthesized, but it does not localize to the sarcolemma and is rapidly degraded. Only a very small percentage of revertant, dystrophin expressing fibers can be detected in *mdx* muscle, which are the result of exon skipping and alternative splicing patterns (Crawford et al., 2001; Lu et al., 2000). Additional mutations in mice have been described, which differentially affect expression of dystrophin isoforms in various tissues (Chapman et al., 1989; Cox et al., 1993b; Im et al., 1996).

Mdx mice develop a milder form of muscular dystrophy than DMD patients, but their muscles are highly susceptible to contraction-induced injury and display morphological changes similar to the human disease (Brooks, 1998; DelloRusso et al., 2001). The clinical onset of muscle pathology occurs at about two to three weeks of age and reaches its peak at

five to six weeks (Torres and Duchen, 1987). Affected mice, *mdx*/Y males and *mdx/mdx* females show a variety of histological changes, including extensive degeneration and regeneration of muscle fibers, increased proportion of myofibers with centrally located nuclei, large variations in myofiber size, fibrosis, immune cell infiltration and elevated serum levels of muscle enzymes such as creatine kinase. In contrast to DMD patients, *mdx* mice demonstrate a successful regeneration process and do not show overt signs of muscular weakness until two years of age (Lynch et al., 2001b; Torres and Duchen, 1987). The exception is the diaphragm muscle, which shows a significant weakness, fibrosis and adipose tissue accumulation in young animals and therefore more closely resembles the human disease (Cox et al., 1993b; Stedman et al., 1991).

3.3. The molecular basis of DMD

The dystrophin gene is the largest known gene, spanning at least 2.4 Mb of X chromosome (Hoffman et al., 1987; Koenig et al., 1987; Koenig et al., 1988). The DMD gene was the first to be identifed by positional cloning methods, whereby cytogenetically detectable abnormalities in a male DMD patient ("BB") with a large deletion localized the gene to the band Xp21 (Francke et al., 1985). Consequently, multiple X-linked probes were identified by subtractive hybridization between 49XXXXY DNA and patient BB-DNA to select potential clones that might map to the deletion (Kunkel et al., 1985). One of seven isolated deletion-specific clones (DXS164) was found to be deleted in ~10 % of all DMD and BMB patients, suggesting its linkage to the DMD gene (Kunkel, 1986). This clone was used for chromosome walking, leading to the isolation of 220 kb of genomic DNA from a cosmid library. Conserved sequences were identified and used to screen a muscle cDNA library (Monaco et al., 1986). Finally, after isolation of several partial cDNAs, the full-length, 14 kb DMD cDNA was cloned (Koenig et al., 1987). The gene contains 79 exons, which have been well conserved throughout vertebrate evolution (Roberts et al., 1993).

Seven promoters driving expression of different dystrophin transcripts have been identified (figure 1). Three promoters give rise to full-length transcripts, primarily in skeletal muscle (M), cerebal cortex (C) and cerebellar Purkinje cells (P) (Chamberlain et al., 1988b;

Nudel et al., 1989). These full-length dystrophin transcripts contain unique first exons, but share the second and proceeding exons. Additional internal promoters allow the generation of shorter dystrophin transcripts in retina (R): 10 kb, brain (B3): 7.5 kb, Schwann cells (S): 5.5 kb and in many non-muscle tissue (G): 4.8 kb (Byers et al., 1993; Cox et al., 1993b; D'Souza et al., 1995; Lederfein et al., 1992; Lidov et al., 1995). The transcription of these smaller mRNAs is initiated from unique first exons, which splice into exon 30, 45, 56 or 63. The 14 kb dystrophin mRNA encodes a protein of 427 kDa. The internal promoters lead to production of proteins with molecular weights of 260 kDa, 140 kDa, 116 kDa and 71 kDa (figure 1).

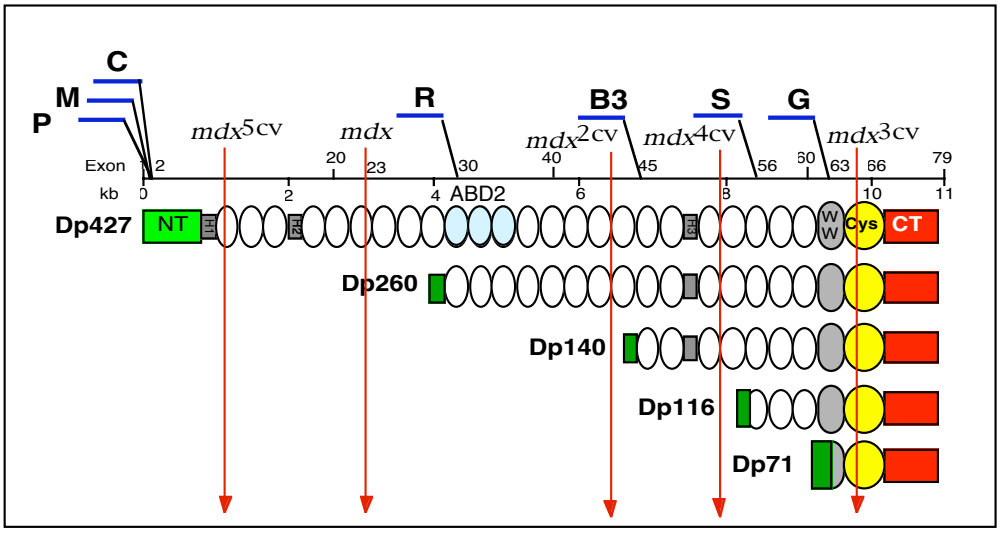

Figure 1. Dystrophin gene and dystrophin isoforms. The gene has 79 exons linked to seven promoters. Three upstream promoters are active in muscle (M), cortical neurons (C) and Purkinje cells (P). Internal promoters are expressed in retina (R), glial cells and kidney (B3), Schwann cells (S), and in non-muscle or general (G) regions. These seven promoters generate five sizes of the protein (Dpxxx). 'Dp' indicates isoform size in kDa. The five forms of dystrophin are aligned by shared domains. Indicated are the two actin binding domains (NT & ABD), the central rod (ovals) domain, the WW and cysteine-rich (Cys) domain and the C-terminal (CT) domain. Five strains of *mdx* mice express different subsets of these isoforms. Red vertical lines indicate the sites of the five *mdx* mouse mutations.

The muscle isoform of dystrophin is primarily expressed in skeletal, cardiac and smooth muscle tissue (Hoffman et al., 1988). The dystrophin protein is localized at the muscle sarcolemma and is enriched at neuromuscular junctions (Shimizu et al., 1989; Zubrzycka-Gaarn et al., 1988). The structure of the protein can be divided into four distinct domains (figure 1). (1) a N-terminal domain (encoded by exons 1-8), which shows high homology with a family of actin binding proteins including β-spectrin and α-actinin (Levine et al., 1990); (2) a long central rod-domain (encoded by exons 9-61), consisting of 24 homologous spectrin-like repeats interrupted by four hinge or spacer domains (Koenig and Kunkel, 1990; Koenig et al., 1988); (3) a WW domain and cysteine-rich region (encoded by exons 62-67), that contains two EF-hand like Ca^{2+}-binding motifs (Bork and Sudol, 1994) and (4) the extreme C-terminal region (encoded by exons 68-79), which consists of an alternatively-spliced domain and two leucine zipper motifs.

3.4. Dystrophin and the DGC complex

Dystrophin binds *via* its N-terminal and portions of the rod domain (ABD2) to the cytoskeletal component F (filamentous)-actin and interacts via its C-terminus, composed of the cysteine-rich and the extreme C-terminal domain, with a large complex of integral and peripheral membrane proteins called the dystrophin-glycoprotein complex (DGC) (Henry and Campbell, 1996) (figure 2). The DGC consists of four core components (the dystroglycans, sarcoglycans, syntrophins and dystrobrevins) and several accessory proteins (neuronal nitric oxide synthase (nNOS), serine/threonine kinases, calmodulin, caveolin-3, Grb2, aquaporin-4, voltage-gated sodium channel), which display direct or indirect interactions with dystrophin (Ahn and Kunkel, 1993; Amalfitano et al., 1997). A homologue of dystrophin, called utrophin, is enriched at neuromuscular junctions (NMJ) and is found along the sarcolemma in dystrophic and regenerating fibers (Khurana et al., 1990; Tinsley et al., 1992). Utrophin also binds actin and interacts with a similar complex to that of dystrophin, known as the utrophin-glycoprotein complex (UGC).

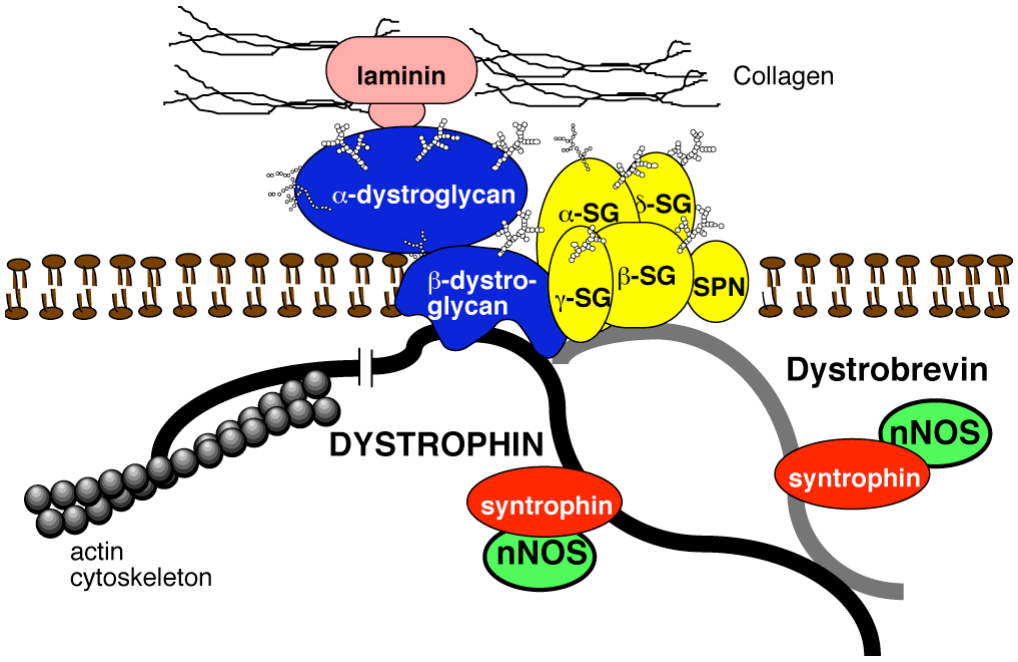

Figure 2. **Model for dystrophin and the DGC**. Dystrophin, binds actin filaments in the subsarcolemmal cytoskeleton *via* the N-terminal actin binding domain and *via* a portion of the central rod domain (most of which is not shown //). The C-terminal portions of dystrophin bind to β-dystroglycan, which binds α-dystroglycan, which binds laminin in the extracellular matrix. The dystroglycan subunits are attached to the four sarcoglycans (SG) and to sarcospan (SPN) (Crawford et al., 2000).

The extreme C-terminal portion of dystrophin binds the peripheral DGC members syntrophin and dystrobrevin. Syntrophin also binds neuronal nitric oxide synthase (nNOS).

Dystroglycan forms the core of the DGC/UGC complex and is post-translationally cleaved into α and β subunits (Deyst et al., 1995; Ervasti et al., 1990). α-DG is located at the extracellular membrane and binds to α1-laminin and agrin in the extracellular matrix (Sunada and Campbell, 1995). β-dystroglycan is an integral membrane protein that binds α-DG and interacts intracellularly with the WW domain and cysteine-rich regions of dystrophin (Jung et al., 1995). Mutations in the dystroglycan gene lead to an early embryonic death, as a result of insufficient formation of basement membranes (Williamson et al., 1997). However, functional studies have been performed on chimeric knock-out mice that expressed almost no dystroglycan in muscle tissue (Côté et al., 1999). These mice did not retain dystrophin at the sarcolemma and developed a severe muscular dystrophy (Côté et al., 1999). In addition,

dystroglycan chimeric knock-out mice demonstrated that dystroglycan is important for the formation of neuromuscular junctions (NMJ), but it is not crucial for the expression of extracellular matrix proteins. Thus, these data suggest that dystroglycan plays an essential role in maintaining the link to dystrophin and in protecting fibers from mechanical injury, although dystroglycan is not required for the formation of basement membranes in muscle tissue. Further studies on conditional dystroglycan knock-out mice that did not express dystroglycan in mature muscle fibers, but in satellite cells, revealed a role for dystroglycan in muscle regeneration. These conditional dystroglycan knock-out mice displayed a mild dystrophic phenotype that was linked to the constant activation of satellite cells and a subsequent efficient muscle regeneration (Cohn et al., 2002).

The sarcoglycans (α, β, γ, δ, ε) and sarcospan are integral membrane proteins that associate with dystroglycan and are thought to play a role in stabilizing the interaction between the α- and β-dystroglycan subunits (Araishi et al., 1999; Crosbie et al., 2000; Noguchi et al., 1995). Mutations of individual sarcoglycans demonstrated a decrease or absence of the other sarcoglycan complex members and some mutations resulted in a secondary loss of dystrophin, dystroglycan, syntrophin or dystrobrevin expression (Hack et al., 2000). Likewise, mutations that directly or indirectly affect the expression of dystroglycan resulted in the loss of the entire sarcoglycan complex (Rafael et al., 1996). In addition to their structural role, the sarcoglycans were implicated in cell signaling processes (Hack et al., 1999; Hack et al., 1998; Yoshida et al., 2000). Disruption of the sarcoglycan complex resulted in a secondary reduction of nNOS, despite the presence of normal dystrophin and syntrophin expression levels and localization (Crosbie et al., 2002a). Mutations in any of the sarcoglycan genes α, β, γ and δ cause at least four different types of autosomal recessive limb-girdle muscular dystrophy (LGMD) (Lim and Campbell, 1998).

The syntrophins (α-1, β-1, β-2, γ-1,γ-2) are a family of peripheral membrane proteins that interact with dystrophin, utrophin and dystrobrevin. α-1, the major isoform in adult skeletal muscle, is localized at the sarcolemma and is primarily associated with dystrophin, whereas β-2 syntrophin is only found at the NMJ and binds to utrophin (Peters et al., 1994). β-1 syntrophin is predominantly expressed in fast, glycolytic muscle fibers and binds to dystrophin and utrophin (Ahn et al., 1996; Peters et al., 1997). γ-1 and γ-2 syntrophins are expressed in neuronal cells (Piluso et al., 2000). All isoforms contain a PDZ domain, which

enables binding of a variety of signaling proteins, including nNOS, voltage gated sodium channels, aquaporin-4, calmodulin, Grb2 and serine/threonine kinases (Adams et al., 2001; Brenman et al., 1996; Gee et al., 1998; Lumeng et al., 1999). Interestingly, neither α-1 syntrophin nor nNOS knock-out mice developed a dystrophic phenotype, however mice displayed abnormal NMJs (Adams et al., 2000; Kameya et al., 1999). In addition, mice with mutant α-1 syntrophin genes demonstrated highly reduced expression of utrophin (Adams et al., 2000) and displayed a mild defect in regeneration (Hosaka et al., 2002). The syntrophins may therefore function as modular adaptors providing a crucial link between the DGC and signaling networks.

The dystrobrevins (α, β) are another family of peripheral membrane proteins that interact with dystrophin, although only α-dystrobrevin is expressed in skeletal muscle. Alternative splicing of the dystrobrevin gene generates three major isoforms of α-dystrobrevin, which differ by the length of their C-terminus (Blake et al., 1996; Peters et al., 1998). The C-terminus of α-dystrobrevin shares sequence homology with dystrophin and binds to dystrophin through a conserved coiled-coil domain (Sadoulet-Puccio et al., 1997). Dystrobrevin also interacts with syntrophin and with the filamentous proteins syncoilin and desmuslin (Mizuno et al., 2001; Newey et al., 2001). In addition, previous studies suggested that dystrobrevin interacts with the sarcoglycan complex (Crawford et al., 2000; Yoshida et al., 2000). Interestingly, α-dystrobrevin knock-out mice developed a mild myopathy, that is not due to mechanical failure of the sarcolemma (Grady et al., 1999). These mice displayed impaired nNOS signaling and abnormal maturation of postsynaptic membranes, suggesting a signaling role for dystrobrevin (Grady et al., 1999; Grady et al., 2000). No patient mutations have been found in the coding regions of syntrophin or dystrobrevin, however patients were characterized with a deficiency in these proteins and a severe congenital muscular dystrophy (CMD) (Jones et al., 2003).

Taken together, the absence or altered expression of dystrophin and/or various DGC members results in a number of different forms of muscular dystrophy, which vividly illustrates the importance of the complex for maintaining normal muscle stability and function.

3.5. The function of dystrophin and the DGC

The complete function of dystrophin is not yet fully understood. Dystrophin is thought to play a structural role in providing a link between the intracellular cytoskeleton and the extracellular matrix *via* its interaction with actin and the DGC (Ervasti and Campbell, 1993). This link dissipates the contractile force produced in the intracellular cytoskeleton to the extracellular connective tissue and protects muscle fibers from mechanical injury (Brooks and Faulkner, 1988; Cox et al., 1993b; Petrof et al., 1993). The absence of dystrophin leads to a disruption of this linkage and very low levels of the DGC, resulting in membrane instability and high susceptibility of the sarcolemma to mechanical injury. Dystrophin shows high similarity to the structural proteins α-actinin and spectrin, further supporting the idea of its structural role in muscle fibers.

In addition to a structural role, several members of the DGC have been implicated in cell signaling. However, the contribution of cell signaling to muscle function remains unclear. Cell signaling may play an important function in adapting DGC members to mechanical and metabolic changes in muscle. Several core components of the DGC, such as sarcoglycan, syntrophin and dystrobrevin have a number of characteristics suggestive of a signaling role in muscle and may connect the DGC to important signaling pathways (Adams et al., 2000; Grady et al., 1999; Hack et al., 1998; Yoshida et al., 2000). In addition, a variety of proteins loosely associated with the complex, such as Grb2, calmodulin, nNOS, caveolin-3, the voltage gated sodium channels, serine/threonine kinases are known cell signaling molecules, although their function in relation to specific roles of the DGC is not clear (Crosbie et al., 1998b; Gee et al., 1998; Hasegawa et al., 1999; Lumeng et al., 1999; Schultz et al., 1998; Song et al., 1996; Thomas et al., 1998; Yang et al., 1995a).

Studies of patients with dystrophin gene deletions have indicated that small in-frame deletions in almost all parts of the gene, except the WW and cystein-rich domain, lead to the milder BMD phenotype. Remarkably, large in-frame deletions of the central rod domain, removing up to two thirds of the dystrophin coding region, can result in a mild course of the disease (England et al., 1990). In contrast, deletions of the WW or cysteine-rich domain or frame-shifting deletions that prevent expression of C-terminal portions of dystrophin generally lead to unstable proteins and result in a severe DMD phenotype. A variety of

transgenic animal studies have provided a better understanding of the functional domains of dystrophin, necessary for the assembly of the DGC and maintenance of normal muscle physiology and stability (Cox et al., 1994; Crawford et al., 2000; Greenberg et al., 1994; Phelps et al., 1995; Rafael et al., 1996; Warner et al., 2002). Transgenic *mdx* mice have been generated that expressed a variety of truncated forms of dystrophin that either lack DGC member binding sites, actin binding sites or portions of the central rod domain (figure 3). These animals have provided an excellent *in vivo* model to study the localization, assembly and function of the DGC complex.

3.5.1. Structure/function analysis of dystrophin domains

Transgenic *mdx* animals that expressed a truncated dystrophin molecule (ΔCR, figure 3) lacking the dystroglycan binding site (cysteine-rich domain encoded by exons 68-70), displayed a severe dystrophic phenotype (Rafael et al., 1996). Analysis of DGC complex members showed less dystroglycan and sarcoglycan expression in ΔCR muscles than in *mdx* muscles. While utrophin partially compensates for the absence of dystrophin in *mdx* muscle by maintaining low levels of dystroglycan and sarcoglycan at the sarcolemma, the ΔCR truncated dystrophin protein displaces utrophin, resulting in a complete loss of dystroglycan and sarcoglycan from the sarcolemma and a slightly worse *mdx* phenotype. Similar results were observed in transgenic *mdx* mice that expressed dystrophin deleted for two other regions of the cysteine-rich domain (encoded by exons 64-67, and exons 65-66) (Rafael et al., 1996). Thus, the cysteine-rich domain of dystrophin is responsible for the interaction with β-dystroglycan and is indispensable for normal muscle function.

In contrast, transgenic *mdx* animals that expressed a truncated dystrophin molecule deleted for either the syntrophin binding site (alternatively-spliced domain encoded by exons 71-74), the dystrobrevin binding site, (coiled-coil domain encoded by exon 75-78) or both, (exon 71-78, ΔCT, figure 3) displayed no signs of dystrophic pathology (Crawford et al., 2000; Rafael et al., 1996). The only exceptions were older animals that demonstrated a slightly higher level of regeneration and altered ratios of the syntrophin and dystrobrevin

isoforms. *In vitro* studies suggested that syntrophin and dystrobrevin bind each other, so that the deletion of the binding site for either protein would have no effect on expression and localization of both proteins (Rafael et al., 1996; Yang et al., 1995b). Surprisingly, the deletion of both binding sites (ΔCT) also retained normal syntrophin and dystrobrevin expression levels and localization (Crawford et al., 2000). Thus, syntrophin and dystrobrevin localization to the sarcolemma is not solely dependent on the interaction with dystrophin, suggesting an alternative interaction within the DGC complex. A potential candidate is the SG complex, which has been shown to interact with dystrobrevin using *in vitro* binding assays (Yoshida et al., 2000). In summary, these transgenic ΔCT *mdx* mice, lacking the syntrophin and dystrobrevin binding sites on dystrophin, demonstrated that the extreme C-terminus is not crucial for dystrophin function.

Transgenic *mdx* mice that expressed the Dp71 dystrophin isoform (figure 3) developed a severe dystrophic phenotype (Cox et al., 1994; Greenberg et al., 1994). Dp71 is the major dystrophin isoform in non-muscle tissues and lacks the N-terminal and rod domain. Although transgenic Dp71 localized to the sarcolemma and assembled the entire DGC complex, the muscles displayed extensive sarcolemmal damage, which is comparable or worse than in *mdx* muscles. Thus, full dystrophin function requires not only an ability to restore expression of the DGC, but also an ability to establish a link to the intracellular cytoskeleton. Several actin-binding sites in dystrophin have been identified using *in vitro* binding assays (Jarrett and Foster, 1995). These actin-binding sites have been located to the N-terminus and the rod-domain of the dystrophin molecule. *In vivo* studies indicated that the N-terminal actin-binding domain (ABD) is the most important. Transgenic mice that expressed a dystrophin molecule lacking (1) the N-terminal ABD (ΔABD1, figure 3) or (2) the N-terminal ABD and a significant portion of the rod domain (Dp260, figure 3), but both retaining the internal ABD, displayed a mild dystrophic phenotype (Corrado et al., 1994; Corrado et al., 1996; Warner et al., 2002). Both deletions have no impact on DGC expression and showed a partial protection from contraction-induced injury. In addition, Dp260 muscles displayed an elevated level of muscle fiber degeneration and regeneration. In contrast, deletion of the internal ABD (ΔABD2) does not affect the function of dystrophin in transgenic mice or in humans (see below; England et al., 1990; Harper et al., 2002b; Phelps et al., 1995). In summary, the N-

terminal ABD is indispensable for muscle stability and function, however the internal ABD domains are partially able to compensate and maintain the interaction with actin.

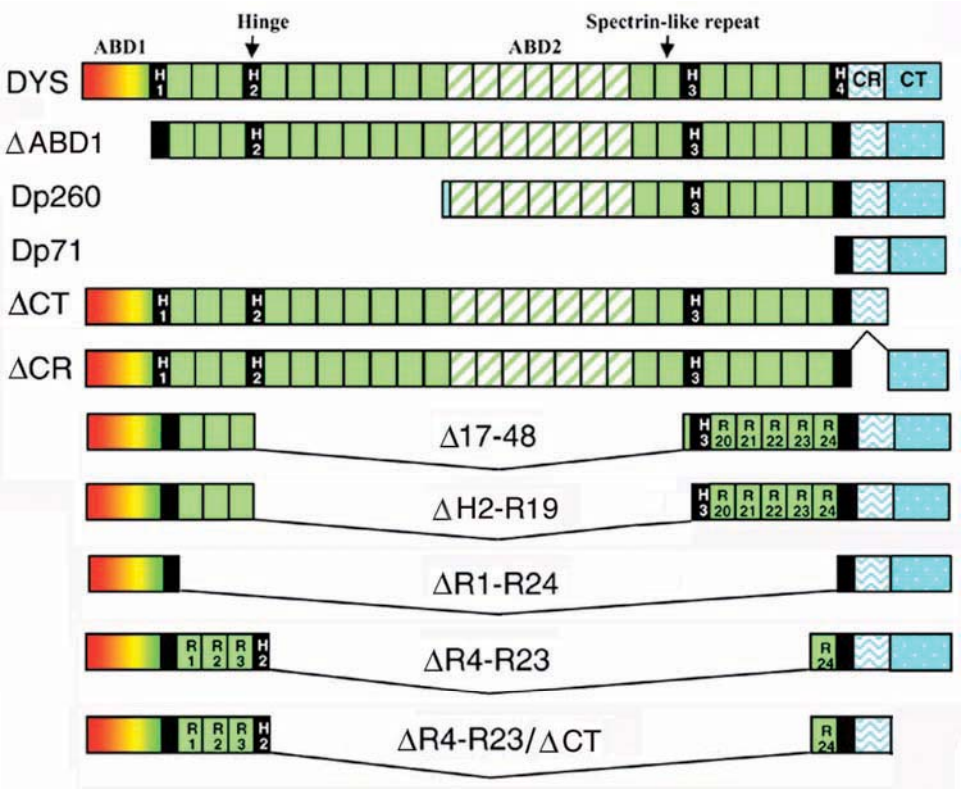

Figure 3. Domain structure of full-length and truncated dystrophins. Full-length dystrophin consists of the N-terminal domain (ABD), the 24 spectrin-like repeats (R) that are interrupted by four 'hinge' regions (H), the cystein-rich domain (CR), and the C-terminal domain (CT). Also shown are the Dp260 and the Dp71 isoforms and various truncated versions of dystrophin that have been tested in animal models for DMD.

The central rod domain spans more than half of the dystrophin molecule and consists of 24 'spectrin-like' repeats interrupted by a few proline-rich spacer regions. The rod domain folds into a coiled-coil, composed of triple-helical repeats with alternating long and short sections (Kahana and Gratzer, 1995; Kahana et al., 1994; Koenig and Kunkel, 1990). Each repeat covers approximately 109 amino acids in length and spans about two exons. Transgenic *mdx* mice lacking the entire rod domain (ΔR1-R24, figure 3) displayed a dystrophic phenotype

(Harper et al., 2002b). However, a BMD patient with a deletion of 16 spectrin-like repeats (exons 17-48) was found to be mildly affected. Despite lacking 2/3 of the rod domain and 46% of the dystrophin protein, this patient was still walking in his late seventieth (England et al., 1990). Based on that observation, a variety of truncated dystrophin molecules (figure 3) were tested in transgenic mice and confirmed that large portions of the dystrophin rod domain could be deleted without any major impact on the phenotype. Muscles from transgenic *mdx* animals that expressed the same deletion as observed in the patient with a deletion of exons 17-48, displayed correct expression and localization of the DGC and generated 95% of the specific force as did control muscles (Phelps et al., 1995). Additional slight modifications to this deletion, which not only preserved the reading frame of the mRNA, but also the phasing of the repeat units, resulted in a mini-dystrophin protein with full function (ΔH2-R19) (Harper et al., 2002b). In order to identify the minimal portion of the rod domain needed to maintain muscle function, additional deletion constructs with either four, five, or six spectrin-like repeats were tested in *mdx* animals (Harper et al., 2002b; Sakamoto et al., 2002; Wang et al., 2000). Remarkably, these micro-dystrophin constructs resulted in highly functional proteins, although individual constructs differed in their effectiveness. The most functional micro-dystrophin construct (ΔR4-23) displayed normal morphology and showed full protection from contraction-induced injury, however muscles were slightly weaker and produced less force (Harper et al., 2002b; Sakamoto et al., 2002). Overall, constructs that maintained the natural phasing of the repeats and hinges were more functional than constructs that had an odd number of repeats or which had repeats and hinges joined in ways that differed significantly from the natural pattern of these units in dystrophin (Harper et al., 2002b). Furthermore, some studies suggested that the rod domain interacts with signaling molecules such as aquaporin-4 and nNOS, which may explain the fact that some repeats are more important than others (Crosbie et al., 2002b; Wells et al., 2003). Taken together, large in frame deletion of the dystrophin rod domain are well tolerated and do not disrupt normal muscle stability and function. Nevertheless, the rod domain cannot be fully deleted or interchanged with homologous domains from other proteins (Harper et al., 2002a). These data support the idea that the rod domain confers an essential function to dystrophin, perhaps acting as a shock absorber and/or force and/or signal transducer.

Structure-function analysis of the different dystrophin domains showed that dystrophin maintains a crucial function in providing a link between the intracellular cytoskeleton and the extracellular matrix *via* its interaction with actin and dystroglycan. A mild dystrophic phenotype may result from partially maintaining this linkage and/or from altered signaling pathways associated with sub-portions of the DGC. The next section of this chapter summarizes in greater detail the evidence that dystrophin and the DGC may play a role in cell signaling.

3.5.2. Signaling roles of dystrophin and the DGC

Several DGC core components and various accessory proteins that loosely interact with the complex have been implicated in cell signaling. Core components of the DGC, such as the sarcoglycans, syntrophins and dystrobrevin have properties suggestive of a signaling function and they may link important signaling pathways throughout the sarcolemma. Accessory proteins, such as nNOS, serine/threonine kinases, calmodulin, caveolin-3, Grb2, aquaporin-4 and voltage gated sodium channels are known cell signaling molecules and may transduce important signals to other DGC members. Several DGC members, including dystrophin, are phosphorylated *in vivo*, however the reason of such phosphorylation remains unknown (Campbell, 1995; Cox et al., 1994; Hasegawa et al., 1999; James et al., 2000; Madhavan and Jarrett, 1994; Ozawa et al., 1995). Phosphorylation by other DGC-associated signal transducers may modulate the conformation of dystrophin and the DGC in response to exercise, or stress, or may help to adapt muscle fibers to altered mechanical or metabolic changes.

Mutational analysis of single members of the sarcoglycan complex revealed that the absence of either α, β and δ-sarcoglycan leads to the secondary loss of the full sarcoglycan complex and mechanical injury of the sarcolemma (Bönnemann et al., 1995; Duclos et al., 1998; Nigro et al., 1996). In contrast, the absence of γ-sarcoglycan leads to an incomplete loss of α, β or δ-sarcoglycan and does not affect dystrophin, dystroglycan or laminin expression (Hack et al., 1999; Hack et al., 1998). Despite maintaining the mechanical link

between intracellular actin and the extracellular matrix, γ-sarcoglycan deficiency causes a dystrophic phenotype (Hack et al., 1999; Hack et al., 1998). Thus, it is thought that this form of LGMD may result from alterations in signaling rather than a structural or mechanical failure of the sarcolemma (Hack et al., 1999; Hack et al., 1998). Nonetheless, the types of signaling pathways that might be perturbed in the absence of γ-sarcoglycan remain obscure.

Mutations in the α-dystrobrevin gene resulted in a mild dystrophic phenotype, which was not associated with contraction-induced injury and was proposed to be the result of altered signaling possibly by disrupting the normal expression and localization of nNOS. These mice displayed physiological abnormalities, such as a reduced vasodilation during muscle exercise, resulting into hypoxic muscles (see below; Grady et al., 1999). Mutations in the α1-syntrophin gene did not lead to muscle weakness, however mutant mouse muscles failed to express utophin and displayed abnormal NMJ, suggestive of a possible linkage to signaling pathways affecting utrophin transcription or post-translational processing (Adams et al., 2000). Further evidence for a signaling role of syntrophin and dystrobrevin was given by transgenic ΔCT *mdx* mouse studies (Crawford et al., 2000). While α-dystrobrevin and α1-syntrophin were dislocated from the sarcolemma in the absence of dystrophin, they were retained at the sarcolemma in the presence of a truncated dystrophin ΔCT that lacked their binding sites (Crawford et al., 2000). These ΔCT transgenic mice displayed normal muscle structure and function despite the lack of a direct association between dystrophin and either syntrophin or dystrobrevin. These data strongly suggest that the latter two proteins are not likely to participate in a mechanical role with dystrophin, since they can function fully without binding to dystrophin. Nonetheless, since syntrophin and dystrobrevin are not required for normal muscle function, these data suggest a more subtle signaling role (Crawford et al., 2000). In addition, it has been shown that α-dystrobrevin interacts with the sarcoglycan complex, providing a connection between core DGC members implicated in cell signaling (Yoshida et al., 2000).

Several proteins have been described that are loosely associated with the DGC and which have been implicated in cell signaling: (1) nNOS, a signaling component of the DGC, binds to syntrophin *via* the syntrophin PDZ domain (Adams et al., 2001). Primary mutations in various DGC members, such as the sarcoglycans, α-syntrophin, α-dystrobrevin and dystrophin have shown to lead to the seconday loss of nNOS from the sarcolemma (Brenman

et al., 1995; Crosbie et al., 1998a; Grady et al., 1999; Kameya et al., 1999). Altered nNOS signaling may provide a major contribution to muscle pathology in different types of muscular dystrophy (Chao et al., 1998; Crosbie et al., 1998a). For example, dystrophin-deficient muscles in mice and humans were shown to generate insufficient amounts of NO, resulting in impaired metabolic modulation of α-adrenergic vasoconstriction and functional ischemia (Sander et al., 2000; Thomas et al., 1998). These data suggest that NOS plays an important role in modulating blood flow to exercising muscles by regulating vascular blood flow. (2) SAPK3 is a member of the mitogen-activated protein kinase (MAPK) family and binds to the PDZ domain of α-syntrophin (Hasegawa et al., 1999). SAPK3 phosphorylates α-syntrophin, whereby this phosphorylation has been shown to be dependent on SAPK3-binding to the PDZ domain. SAPKs are activated by cellular stress and are connected to the SAPK/JNK pathway (Hasegawa et al., 1999). These data suggest that SAPK and perhaps other protein kinases may directly phosphorylate components of the DGC to modulate the function of this complex in response to exercise, mechanical stress and metabolic alterations. (3) Ca^{2+}-calmodulin binds to the C-terminus of dystrophin and to syntrophin and activates calcium-dependant protein kinases (Anderson et al., 1996; Madhavan et al., 1992). Ca^{2+}-signaling may play an important role in modulating DGC function by regulating DGC interaction (4) Caveolin-3 is predominantly expressed in muscle tissue and is an important regulatory component of the sarcolemma. Oligomeres of calveolin bind cholesterol and form calveolae pockets, which provide a scaffold to concentrate a variety of signaling proteins. Caveolin-3 is localized to the sarcolemma and *in vitro* studies suggested its association with dystrophin (Crosbie et al., 1998b; Okamoto et al., 1998; Song et al., 1996). Mutations in the caveolin-3 gene causes LGMD with mild clinical symptoms (Hagiwara et al., 2000; Minetti et al., 1998) (5) Grb2 is an accessory protein of the DGC that interacts with β-dystroglycan and syntrophin (Oak et al., 2001; Yang et al., 1995a). Grb2 contains a SH2/SH3 domain, which is a common motif shared by a number of signaling proteins. The SH2/SH3 domain links tyrosine kinases to small GTP-binding proteins in a variety of signal transduction pathways. Dystroglycan contains phosphotyrosine and P-rich regions, which could interact with Grb2 and function to transduce extracellular signals into the cell (Yang et al., 1995a). Recently, *in vitro* studies suggested that signaling *via* dystroglycan, syntrophin and Grb2 provides a connection from laminin in the extracellular matrix to the intracellular JNK signaling pathway (Oak et al.,

2003) (6) Aquaporin-4 is a member of the water channel protein family and binds to the PDZ domain of α-syntrophin (Adams et al., 2001; Neely et al., 2001). In addition, it was suggested that Aquaporin-4 interacts with the rod domain (Crosbie et al., 2002b). Aquaporins play a role in regulating water membrane permeability and may be essential in adapting muscle tissue to volume changes during contraction. The absence of α-syntrophin leads to the absence of aquaporin-4 from the sarcolemma (Adams et al., 2001; Crosbie et al., 2002b; Neely et al., 2001).

Analysis of dystrophin/utrophin double knock-out (*dko*) mice also supported the idea that dystrophin and the DGC play a role in cell signaling. These mice displayed a much more severe dystrophic pathology than *mdx* mice, because neither dystrophin nor utrophin are able to partially compensate for the absence of each other's function. However, transgenic *dko* mice expressing the ΔCR truncated dystrophin construct, showed an amelioration of post-synaptic membrane abnormalities and fiber-type abnormalities despite not having an effect on the primary dystrophic pathology (Rafael et al., 2000). Since ΔCR is not able to rescue mechanical function, the amelioration of the post-synaptic membrane and fiber-type abnormalities is likely the result of restoring signaling networks, whose identity is not clear (Rafael et al., 1996; Rafael et al., 2000).

In summary, there is growing evidence that dystrophin and the DGC are implicated in signal transduction pathways. Developing a better understanding of the connection between these signaling centers and their role in regulating the DGC and muscle function will be important to further understand the complete role of dystrophin and the DGC.

3.6. Pathophysiology of muscular dystrophy

The relationship between the absence of dystrophin and the pathological mechanisms of dystrophy are poorly understood. Multiple functions of dystrophin and the DGC make it difficult to determine if the initiating event that leads to cell death is a consequence of mechanical or signaling failure or both. Dystrophic muscle displays a variety of pathological features such as loss of membrane integrity, elevated Ca^{2+} levels, increased susceptibility to oxidative stress, functional ischemia, altered mitochondrial function and extensive infiltration

of immune cells (Arahata and Engel, 1988; Chen et al., 2000; Franco and Lansman, 1990; Rando et al., 1998; Spencer et al., 2001; Thomas et al., 1998).

Mechanical failure may cause an accumulation of tears in the sarcolemma and a gradual loss of membrane integrity, followed by an increased calcium influx (Carpenter and Karpati, 1979). Then, elevated intracellular Ca^{2+} levels may activate calcium dependant proteases (calpains), which are capable of widespread proteolysis of intracellular proteins, and of initiating cell death (Turner et al., 1993). In contrast, signaling failure may increase the susceptibility of muscle fibers to secondary triggers, such as functional ischemia and oxidative stress (Disatnik et al., 2000; Disatnik et al., 1998; Rando et al., 1998; Sander et al., 2000; Thomas et al., 1998). Dystrophic muscles show an impaired metabolic modulation of α-adrenergic vasoconstriction and functional ischemia. Furthermore, *mdx* muscles demonstrate an increased susceptibility to oxidative stress compared to normal muscles (Disatnik et al., 1998; Rando et al., 1998).

The progressive nature of the disease reinforces the idea that muscle cell death is a dynamic process and may reflect the increased susceptibility of myofibers to damage leading to active, apoptotic and/or passive, necrotic cell death. However, it remains unclear if muscle fiber breakdown occurs primarily through apoptotic or necrotic processes. Recent studies suggested that cell death in dystrophic muscle may be initiated by apoptosis and followed by necrotic processes (Tidball et al., 1995). Tissue sections of dystrophic muscle demonstrated apoptotic myonuclei and activated caspases in degenerating muscle fibers (Abmayr et al., 2004; Matsuda et al., 1995; Sandri et al., 1998; Sandri et al., 1997; Tews and Goebel, 1997a). Although apoptosis and necrosis represent different mechanism of cell death, both may be intertwined. The ultimate fate of a cell may depend on the nature of the trigger and the energy status of the cell. The intensity of the signal, such as intracellular ATP levels, Ca^{2+}-levels, hypoxia and/or reactive oxygen species may dictate whether a cell dies by a primarily necrotic, or an apoptotic, pathway (Bonfoco et al., 1995; Eguchi et al., 1997; Higuchi et al., 1998).

It remains unclear whether infiltrating immune cells actively contribute to muscle cell death as a primary cause of the disease, or whether their activity is a secondary consequence of myofiber breakdown. Previous studies demonstrated that depletion of $CD4^+$ and $CD8^+$ T-lymphocytes reduces dystrophic pathology. In addition it was shown that T-lymphocytes

were able to stimulate apoptotic cell death through perforin-mediated cytotoxicity. Overall these data suggested that immune cells actively contribute to dystrophic pathology (Spencer et al., 2001; Spencer et al., 1997).

An additional aspect that may play a major part in the progression of dystrophic pathology is the gradual exhaustion of satellite cells. Satellite cells are the primary contribution to muscle regeneration. Following myofiber injury, satellite cells are activated, begin proliferating and fuse into damaged, or new myofibers to initiate repair of the injury (Bischoff, 1975). Dystrophic muscle progressively looses its self-renewal potential, leading to severe fibrosis, adipose tissue replacement and abnormal muscle architecture. Thus, an impaired repair mechanism may provide a major contribution to muscle pathogenesis. This hypothesis is supported by a previous study showing that conditional knock-out mice with a disruption of dystroglycan, exclusively in mature muscle fibers, demonstrated a mild phenotype (Cohn et al., 2002). This observation stands in surprising contrast to the severe phenotype reported in chimeric dystroglycan knock-out mice (Côté et al., 1999). Since the conditional knock-out mice expressed dystroglycan in satellite cells, it is thought that the mild phenotype is due to the constant activation of satellite cells and subsequent muscle regeneration. In contrast, satellite cells in chimeric dystroglycan null mice as well as in *mdx* mice displayed abnormal expression of DGC members that may be responsible for impaired satellite cell function in conjunction with a loss of muscle self-renewal potential.

In summary, dystrophic pathology may be an accumulation of malfunctions, which together contribute to muscle degeneration. The balance of muscle fiber degeneration and renewal may be maintained in young patients by cellular repair mechanism and continious activation of satellite cells. However, insufficient survival stimuli and an impaired regenerative potential may lead to a gradual replacement of muscle fibers by fibrotic and adipose tissue, resulting in a loss of muscle mass and the devastating course of the disease.

3.7. Therapy of DMD

3.7.1. Gene replacement

No cure for muscular dystrophy exists at this time. However, progress over the last years in understanding muscle function and dystrophic pathology have encouraged the development of various therapeutic approaches. Since DMD is recessively inherited and arises from a single gene mutation, gene replacement appears as a promising treatment (Chamberlain, 2002). It was demonstrated that expression of dystrophin in transgenic *mdx* mice at levels that reached >20% of wild-type dystrophin levels prevented dystrophic pathology (Cox et al., 1993a; Phelps et al., 1995). In addition, viral gene delivery of full-length or truncated dystrophin molecules (figure 4) showed that gene replacement can almost fully prevent and partially reverse muscular dystrophy (Chen et al., 1997; DelloRusso et al., 2002; Gilbert et al., 2001; Harper et al., 2002b; Sakamoto et al., 2002; Wang et al., 2000). Current research focuses on testing different vector systems for their ability to transduce and persist in muscle and whether they trigger immunological reactions that may be harmful and cause more damage than benefit.

3.7.2. Vectors for muscle gene therapy

Various vectors, including adenovirus (Ad), adeno-associated virus (AAV), retroviruses and plasmids are promising candidates to deliver dystrophin to muscle. Research has been focused on evaluating each vector in terms of packaging size, vector production efficiency, immunogenicity and transfer efficiency for DMD gene therapy.

Ad vectors have been widely studied for DMD gene therapy as they can be grown to very high titers and have a relatively large cloning capacity (Graham and Prevec, 1991). These vectors further enable transfer of highly functional mini-dystrophin constructs. Animal studies demonstrated that Ad vectors transduce muscle extremely well and prevent dystrophic pathology in expressing fibers (Deconinck et al., 1996; Ragot et al., 1993; Vincent et al., 1993; Yang et al., 1998). However, most studies have been performed in immune-

compromised animals since conventional, first generation adenoviruses elicit a substantial immune response (Yang et al., 1994). Despite the fact that first generation adenoviruses are deleted for the E1 and E3 genes that regulate viral replication and gene expression, the remaining viral genes may also be highly immunogenic. Also, a number of transgenes expressed by adenoviral vectors can be highly immunogenic, especially if they encode proteins not normally produced by host animals (Tripathy et al., 1996). In addition to muscle tissue, Ad vectors also transduce macrophages and dendritic cells that trigger a substantial immune response. Several approaches taken to reduce the immune response worked remarkably well. First, tissue-specific promoters were shown to be very effective in shutting down gene expression in macrophages and dendritic cells (Hartigan-O'Connor et al., 2001; Pastore et al., 1999). Second, "gutted" adenoviral vectors lacking all viral genes further reduced the immune response significantly. These vectors are dependant on a helper adenovirus for growth and production, however after purification they are 99% helper-free (Barjot et al., 2002; Parks et al., 1996). Since "gutted" vectors are deleted of all viral genes, they have a higher cloning capacity, allowing transfer of full-length dystrophin expression cassettes. Animal studies using "gutted" adenoviral vectors as a vehicle to express full-length dystrophin displayed efficient transduction, partial reversal of dystrophic pathology and persistent gene expression for at least six months (Chen et al., 1997; DelloRusso et al., 2002; Gilbert et al., 2001; Schiedner et al., 1998) (figure 4). Since Ad vectors are non-integrating vectors, they may not persist long-term and may have to be re-administered. Therefore, current research focuses on developing hybrid vectors between Ad and retroviruses or AAV that could enable integration and consequently higher persistence over a longer time period (Roberts et al., 2002; Shayakhmetov et al., 2002).

Retroviral vectors also have a relatively high cloning capacity (7-11 kb), which enables them to transfer highly functional mini-or micro-dystrophin constructs (Dunckley et al., 1993). However, retroviruses are very difficult to grow to high titers and they cannot be applied in the quantities that may be needed to efficiently transduce muscle. No immunological side effects have yet been reported, but again, low titers do not allow the same studies to be performed as with Ad or AAV vectors. *In vitro* studies demonstrated that lentiviruses transduce muscle stem cells very well, supporting the potential use of lentiviruses as a promising tool for *ex vivo* gene therapy (Li and Chamberlain, manuscript in preparation).

In addition, lentiviruses integrate into the host genome and enable persistent expression (Naldini et al., 1996). Current research focuses on identifying ways to control integration of the virus into the host genome for safety reasons.

Currently, AAV viruses are the most promising vectors for DMD gene therapy. These vectors can be grown to high titers, transduce muscle tissue very well and can persist for several years (Fisher et al., 1997; Xiao et al., 1996). A variety of different AAV serotypes are available that demonstrate different tissue tropism. In particular, serotype 1, 5 and 6 proved to be remarkably efficient in transducing muscle tissue (Chao et al., 2000; Hildinger et al., 2001; Scott et al., 2002) (figure 4). Despite the fact that AAV vectors have a limited cloning capacity (<5 kb), they can be used as a vehicle to express highly functional micro-dystrophin constructs (Harper et al., 2002b; Sakamoto et al., 2002; Wang et al., 2000). Studies in the *mdx* mouse model demonstrated high, persistent expression of micro-dystrophin and a partial reversal of dystrophic pathology (Harper et al., 2002b). AAV vectors integrate into the host genome with very low efficiency, however long-term persistence may be achieved by the formation of high-molecular weight concatemeres tightly associated with the host genomic DNA (Vincent-Lacaze et al., 1999). AAV vectors lack all viral coding sequences, which prevents a potential immune response against viral gene expression. In addition, AAV vectors transduce dendritic cells and macrophages very poorly (Zhang et al., 2000). As a result, these vectors efficiently evade the cellular immune response caused by direct antigen presentation of foreign transgenes by dentritic cells. Nevertheless, several cases have been reported where a cellular immune response cannot be completely avoided (Cordier et al., 2001; Yuasa et al., 2002). First, intracellular localization of the transgene appeared to have an effect on the immune response, since transmembrane proteins were more immunogenic than cytoplasmic proteins in the context of AAV-mediated gene delivery (Sarukhan et al., 2001b). Second, AAV-mediated delivery is far more likely to trigger a cellular immune response against the transgene in dystrophic than in healthy muscle (Cordier et al., 2001; Yuasa et al., 2002). The latter observation may be explained by the fact that dystrophic muscle displays a loss of membrane integrity, accompanied by muscle cell necrosis and massive infiltration of immune cells (Hartigan-O'Connor et al., 2001). The cellular immune response in dystrophic muscle may therefore be triggered by antigen cross presentation from necrotic fibers to dentritic cells (Sarukhan et al., 2001a; Yuasa et al., 2002; Zhang et al., 2000). Unlike the case

with Ad vectors, the cellular immune response could not always be blocked by using tissue-specific promoters. However, the expression of therapeutic genes rescues muscle fibers from degeneration, and therefore blocks the release of immune stimulating antigen in conjunction with cross presentation to dendritic cells.

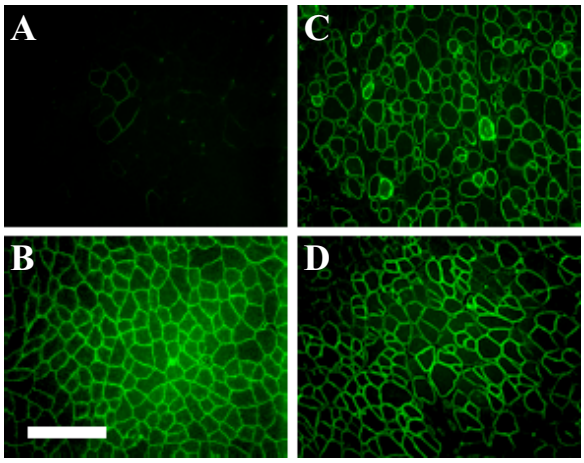

Figure 4. Transduction of *mdx* muscles by dystrophin expression vectors. The figure shows immunofluorescent staining of *tibialis anterior* muscle cross sections for dystrophin. A) *mdx* B) wild-type C) gutted Ad vectors expressing full-length human dystrophin and D) AAV vectors expressing human micro-dystrophin. Muscles of one year old mice were injected and analyzed one month post-injection. Scale bar: 100 μm.

Plasmid DNA vectors have a very large cloning capacity and can be produced inexpensively at very high quantities. These vectors have the advantage of being free of viral genes and proteins. Naked DNA may elicit an immune response against foreign transgenes, however the immune response can be widely blocked by using tissue specific promoters (Wells et al., 1997). The delivery of plasmid DNA to skeletal muscle showed persistent expression and can be safely re-administered, but the transduction efficiency is very low (Acsadi et al., 1991; Wolff et al., 1990). Current research focuses on improving the efficiency by using high-pressure injection methods in combination with DNA carriers such as liposomes, lipids,

polymers and synthetic peptides (Aihara and Miyazaki, 1998; Lu et al., 2003a; Lu et al., 2003b).

3.7.3. Gene repair

Several efforts have been made to develop strategies to correct dystrophin deficiency at the DNA or RNA level. DNA repair is based on chimeric molecules of DNA/RNA (chimeroplasts) that specifically correct point mutations or change exon splice donor or acceptor sites in the genomic DNA (Bertoni and Rando, 2002). RNA repair uses the technology of antisense oligonucleotides that bind to pre-mRNA to alter exon/intron splicing and restore a mRNA open reading frame (Mann et al., 2001; van Deutekom et al., 2001). The clear advantage of DNA/RNA repair is the fact that nucleotide sequences are expressed by the patient's own genes and are therefore not immunogenic. These methods proved to be safe, cheap and have the potential to be administered systemically, but the efficiency is very low. However, encouraging data showed that *mdx* muscle produces functional amounts of dystrophin by administration of antisense oligonucleotides in combination with a transfection enhancing reagent, such as the nonionic block copolymer F127. This polymer is thought to facilitate dissemination within tissue, penetration through cell membranes, stability and entry into the nucleus (Lu et al., 2003c).

3.7.4. Upregulation of compensatory proteins

Overexpression of the dystrophin homologue utrophin in *mdx* mice demonstrated that utrophin is able to compensate for dystrophin deficiency (Tinsley et al., 1998). The up-regulation of utrophin is of general interest for developing a treatment of DMD, since utrophin is expressed normally in DMD patients and is not expected to trigger an immune response (Ebihara et al., 2000; Gilbert et al., 1999). Rather than delivering utrophin directly to skeletal muscle, several groups are testing various drugs that might enhance endogenous

utophin gene expression. In addition, a number of approaches have been taken based on the idea of up-regulating synaptic proteins that are not affected in DMD. As a result, these proteins may up-regulate DGC complex members at the sarcolemma and therefore ameliorate the dystrophic phenotype. For example, the over-expression of the synaptic cytotoxic T-cell GalNAc transferase inhibited muscular dystrophy in *mdx* mice by up-regulating expression of utrophin and several DGC members (Nguyen et al., 2002). This observation may be explained by the fact that GalNAc modifies the glycosylation pattern of α-dystroglycan which appears to facilitate utrophin binding. Since GalNAc transferase is an enzyme, minor changes in its activity may have a major impact on its function. Additional synaptic proteins which have been shown to be beneficial in ameliorating muscular dystrophy include α7β-integrin and agrin (Burkin et al., 2001).

3.7.5. Systemic delivery of genes to muscle tissue

Progress has been made in optimizing vector systems and creating mini- and micro- versions of dystrophin; however, it remains a challenging goal to deliver dystrophin to every muscle of the body. Since capillaries surround all muscle fibers, intravascular injections are a promising way to deliver genes systemically. Efforts have been focused on finding ways to enhance the permeability of capillary walls to allow penetration of vectors. It was shown that the administration of vasodilators, such as histamine and papaverine, as well as injection of vectors under high pressure, can significantly increase the efficiency of vascular delivery to muscle (Cho et al., 2000; Greelish et al., 1999). However, these methods are not safe enough to be applied in the clinic. In addition, viral mediated systemic delivery may target not only the tissue of choice, but also other organs, such as the liver. Several groups are optimizing vector systems to change their natural tropism, so that they selectively transduce muscle fibers (Bouri et al., 1999; Douglas et al., 1996; Wickham, 2000). AAV6 appeared to have a natural tropism for muscle tissue, rendering it a promising vector for the systemic delivery of genes (Scott et al., 2002).

An alternative approach is based on the systemic delivery of cells to rescue dystrophin expression. A tremendous amount of work has been put into identifying and characterizing stem cells and testing them for their potential to migrate out of blood vessels into muscle tissue. It was previously shown that stem cells from muscle and bone marrow were able to migrate into muscle tissue and form myofibers, when delivered by bone marrow transplantation. However, the efficiency is very low (Ferrari et al., 1998; Gussoni et al., 1999). Although recently, Samaolesi *et al.* demonstrated the potential of mesoangioblasts, vessel-associated fetal stem cells, to migrate out of the capillary in the presence of inflammation (Sampaolesi et al., 2003). Intra-arterial delivery of wild-type mesoangioblasts to α-sarcoglycan null mice demonstrated a morphological and functional rescue of the dystrophic phenotype. However, further research in basic stem cell biology is required to evaluate the potential of stem cells for therapy. The ultimate goal of cell therapy is to isolate stem cells from a patient, transduce the cells *ex vivo* with an integrating, dystrophin expressing virus and return the cells to the patient through intravascular administration.

3.7.6. Treatment of secondary symptoms of DMD

Gene replacement therapy and reassembly of the DGC complex may rescue any remaining muscle fibers from breakdown; however, it does not seem likely that previous damage, such as altered muscle architecture, fibrotic changes and fat accumulation, would be reversed. A major contribution to dystrophic pathology may be the result of activated immune cells and altered signaling pathways, which may not be easily turned off once activated. Consequently, a combination of treatments that replace the gene and in addition target immunological and signaling dysfunction may be the therapy of choice. The application of drugs that treat secondary symptoms of DMD/BMD are very valuable for their potential to be administered systemically.

Several immuno-suppressant drugs have been successfully used to reduce inflammation in DMD patients. Steroid-based drugs such as prednisone and deflazacort proved to have a broad anti-inflammatory effect by blocking the production of cytokines,

prostaglandins and histamines and halting the proliferation of lymphocytes (Bonifati et al., 2000; Merlini et al., 2003). Prolonged steroid treatment was shown to slow down the progression of dystrophic pathology by stabilizing muscle strength and preserving respiratory function. In addition, it was demonstrated that the depletion of $CD4^+$ and $CD8^+$ T-lymphocytes reduces dystrophic pathology in *mdx* mice (Spencer et al., 2001).

Altering or restoring signaling pathways remains a more challenging goal. Signaling failure is thought to play a role in dystrophic pathology, however not much is known about the mechanisms that are responsible for this mis-regulation. The consequences are described as an increased susceptibility of muscle fibers to elevated Ca^{2+} concentrations, oxidative stress and functional ischemia, resulting in apoptotic and/or necrotic cell death. nNOS, which is absent from the sarcolemma in dystrophic muscle, is thought to have an important signaling function by regulating blood flow to exercising muscle. The absence of nNOS results in impaired metabolic modulation of α-adrenergic vasoconstriction and functional ischemia in dystrophic muscle. Likewise, it was shown that over-expression of nNOS in *mdx* muscle ameliorates the dystrophic phenotype (Nguyen and Tidball, 2003). An alternative approach demonstrated that creatine treatment of *mdx* myoblasts lowered intracellular Ca^{2+} concentrations by stimulating sarcoplasmatic reticulum Ca^{2+}-ATPase (Pulido et al., 1998). Based on that observation, a clinical study supplementing the diet of DMD patients with creatine was found to slow the progression of joint stiffness, improve strength and increase resistence to fatigue (Louis et al., 2003). These approaches clearly show that understanding signaling pathways in DMD will be helpful in designing treatments to rescue muscle fibers from cell death and ameliorate the dystrophic phenotype.

Another promising approach centers around the idea of activating satellite cells and maintaining their regenerative potential in muscular dystrophy. It was demonstrated in previous studies that muscle pathology can be ameliorated by the activation of satellite cells in conjunction with an efficient replacement of degenerating myofibers throughout life (Cohn et al., 2002). Furthermore, insulin-like growth factor (Igf-I), which activates satellite cells and promotes cell growth and differentiation, was shown to ameliorate dystrophic pathology by maintaining muscle mass and function in old and dystrophic animals (Barton et al., 2002; Barton-Davis et al., 1998; Gregorevic et al., 2002; Lynch et al., 2001a). Igf-I treated animals displayed an increase in muscle mass, fiber size, fiber number and absolute muscle strength

along with a significant decrease in muscle degeneration. Similarly, neutralizing antibodies to myostatin, which is an inhibitor of Igf-I induced pathways, were also able to ameliorate dystrophic pathology (Bogdanovich et al., 2002).

3.8. Scope of this dissertation

This work focuses on studying the role of proteins that repress apoptosis and/or enhance muscle regeneration to determine whether they have potential to modulate dystrophic pathology. Since several malfunctions such as mechanical, signaling and regeneration may contribute to muscular dystrophy, we sought to study a number of treatments and their relative and combined potential for reversing the dystrophic pathology of the *mdx* mouse. The first part of the work centers around the characterization of ARC, apoptosis repressor interacting with caspase-recruitment domain (CARD), in normal and dystrophic *mdx* muscle and its potential to ameliorate muscular dystrophy. The second part focuses on the delivery of Igf-I to *mdx* muscle without and in conjunction with gene replacement therapy to assess if the beneficial effect of Igf-I is synergistic with the protective effect of dystrophin in restoring muscle strength and function in muscular dystrophy.

The potential contribution of ischemia, oxidative stress and inducers of apoptosis to the dystrophic process are of interest in view of the recent identification of ARC. ARC expression in humans is restricted primarily to striated muscles, tissues that do not normally undergo rapid cell turnover or apoptosis. This high level expression of an apoptosis inhibitor in long-lived cell types raises the possibility that ARC could help protect muscle fibers from apoptotic death resulting from mechanical stress or oxidative damage. ARC was identified in the GenBank database using a screen for proteins with homology to the CARD of caspase-9, a key initiator of apoptosis in many cell types (Koseki et al., 1998). The CARD domain is conserved in numerous proteins and mediates binding to, and regulation of, various caspases (Deveraux et al., 1998; Hofmann et al., 1997; Li et al., 1997). ARC was shown to interact selectively with caspase-2 and caspase-8 *via* its CARD and to inhibit caspase-8 induced apoptosis (Koseki et al., 1998). ARC has also been shown to inhibit both hypoxia induced and hydrogen peroxidase mediated cell death in cardiac H9C2 cells (Ekhterae et al., 1999;

Neuss et al., 2001). Since myofiber death in dystrophic muscles has been linked to increased oxidative stress and functional ischemia, we sought to study the expression of ARC in *mdx* mice. We cloned and characterized murine ARC in normal and *mdx* muscle. In addition we generated ARC transgenic mice to assess the potential of forced overexpression to ameliorate the dystrophic phenotype.

In a complementary approach, we examined the role of Igf-I in muscle tissue to evaluate its ability to modulate the *mdx* muscle pathology. Igf-I has been widely studied in various cell types and tissues and has been shown to play an important role in regulating tissue growth and differentiation (Florini et al., 1991; Lund, 1994; Stewart and Rotwein, 1996). Igf-I, a peptide growth factor that is structurally related to proinsulin, is primarily synthesized by the liver in response to growth hormone secretion and mediates endocrine effects on various tissues, in particular during growth and development (Rinderknecht and Humbel, 1978; Stewart and Rotwein, 1996). In addition, Igf-I is produced locally in several tissues, where it exerts autocrine and paracrine effects (D'Ercole et al., 1984; LeRoith and Roberts, 1991; Sjogren et al., 1999). Igf-I binds to the Igf-I receptor and mediates its cellular effects mainly *via* the phosphatidylinositol 3-kinase (PI3K) and the mitogen activated protein kinase (MAPK) pathway, respectively (Singleton and Feldman, 1999). The MAPK pathway triggers proliferation, whereas PI3K signaling induces differentiation in conjunction with anti-apoptotic pathways. In skeletal muscle, overexpression of Igf-I was found to enhance muscle repair mechanism and to maintain muscle mass and function in old and dystrophic *mdx* animals (Barton et al., 2002; Barton-Davis et al., 1998). We have cloned and characterized the isoforms of Igf-I that are expressed in normal and dystrophic mouse muscle. Based on this information, we have tested virally mediated overexpression of Igf-I *in vitro* and *in vivo* in dystrophic muscle and established quantitative PCR and morphological and functional assays to assess expression and effects of Igf-I. Additionally, we have co-treated dystrophic muscle with Igf-I and dystrophin to determine if the protective effect of Igf-I is synergistic with the beneficial effects of dystrophin in ameliorating the *mdx* phenotype.

4. RESULTS

4.1. Characterization of ARC in normal and dystrophic *mdx* muscle

4.1.1. Isolation of mouse ARC cDNA

The full-length mouse ARC cDNA was isolated by direct PCR amplification from a muscle cDNA library (Lumeng et al., 1999) using primers derived from an EST clone (accession number AA596110) and vector specific primers. Direct sequencing of PCR products revealed that the longest open reading frame encoded a protein of 220 amino acids with a predicted molecular mass of 24.5 kDa (GenBank accession no. AY459322). The protein sequence displayed 80% identity to the previously identified human ARC (Koseki et al., 1998) and 91% identity to the rat ortholog (figure 5). Alignment analysis confirmed that mouse ARC contains a N-terminal CARD and a C-terminal proline/glutamic acid-rich (P/E) domain. The CARD domain of ARC has significant amino acid similarity to the CARD domains from caspase-2, caspase-9, RAIDD and APAF-1 (Koseki et al., 1998) and is structurally related to the death effector domain (DED) shared by effector caspases (Hofmann et al., 1997).

Figure 5. Alignment of mouse, rat and human ARC protein sequence. Mouse ARC displays 80% identity to human ARC and 91% identity to the rat ARC protein sequence. The identical residues in mouse, rat and human ARC are indicated as black boxes. ARC contains a N-terminal CARD domain (1-97 AA) and a C-terminal P/E rich-domain.

The human ARC gene has been reported to encode two proteins that differ by alternative RNA splicing. The alternative product has been named nucleolar protein Nop30 and has been shown to interact with the splicing factor SRp30c (Stoss et al., 1999). Nop30 contains a 10 bp deletion that leads to a frame shift between amino acids 95 and 96, resulting in a different C-terminal domain consisting of 124 amino acids (Stoss et al., 1999). To determine whether the mouse ARC gene also encoded a Nop30 like protein we amplified ARC from a mouse muscle cDNA library and subcloned the PCR product. Ten independent clones were sequenced and all encoded the normal, full-length ARC. Furthermore, we digested the PCR product with PmlI, which cuts within the 10 bp deletion of the potential Nop30 cDNA and would distinguish between ARC and Nop30. We were able to detect the ARC cDNA, but less than 5% of the product remained undigested (data not shown). However, analysis of the amino acid sequence demonstrated that the 10 bp deletion observed in the human alternative transcript would only yield a 56 amino acid C- terminal domain, compared to the 124 amino acids in human Nop30. These data indicate that in mouse skeletal muscle, the ARC gene does not encode a Nop30-related protein.

4.1.2. Chromosomal localization of mouse ARC

The mouse ARC gene was mapped to chromosome 8 by typing a backcross panel (kindly provided by the Jackson Laboratories). The loci was named Nol3, nucleolar protein 3, in correspondence with the previously mapped human ARC gene product Nop30 (Stoss et al., 1999). The mouse loci on chromosome 8 corresponds to human chromosome 16q22.1 and agrees with the mapping data of human ARC. ARC cosegregates with Psmb10 and Sntb2 (figure 6).

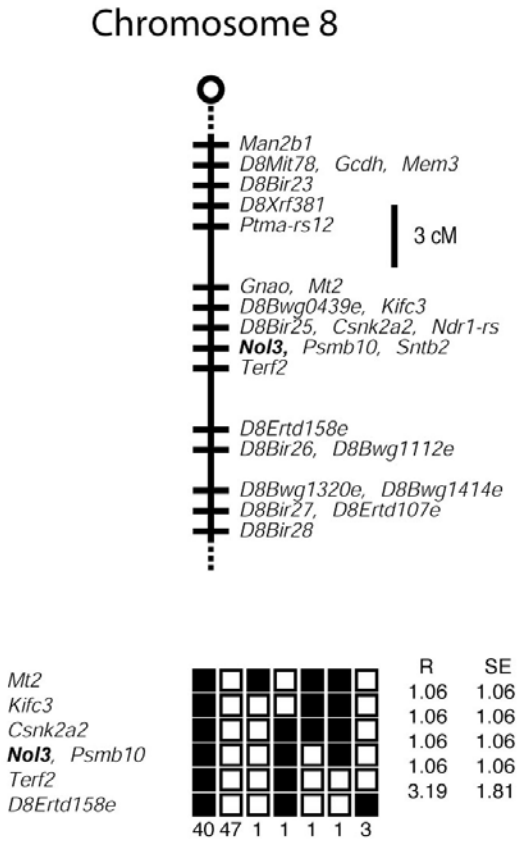

Figure 6. **Chromosomal localization of the mouse ARC gene**. Figures from the TJL BSS backcross showing part of Chromosome 8 with loci linked to *Nol3*. The map is depicted with the centromere toward the top. A 3 cM scale bar is shown to the right of the figure. Loci mapping to the same position are listed in alphabetical order. In the haplotype figure loci are listed in order with the most proximal at the top. The black boxes represent the C57BL6/JEi allele and the white boxes the SPRET/Ei allele. The number of animals with each haplotype is given at the bottom of each column of boxes. The percent recombination (R) between adjacent loci is given to the right of the figure, with the standard error (SE) for each R. Missing typings were inferred from surrounding data where assignment was unambiguous. Raw data from the Jackson Laboratory were obtained from http://www.jax.org/resources/documents/cmdata.

4.1.3. ARC expression in mice

To examine ARC gene expression in mice we initially probed a multiple tissue northern blot. Mouse ARC was highly expressed in heart, and at a slightly lower level in skeletal muscle (figure 7). Some ARC expression was detected in brain and testis, with very low levels in kidney and lung. No ARC expression was detected in liver or spleen. Interestingly, in testis ARC mRNA was expressed as a longer transcript than in other tissues possibly due to an alternative polyadenylation site as seen in human tissue (Stoss et al., 1999). The nature of the larger transcript in heart is unclear and could be the result of alternative splicing or polyadenylation site usage. This expression agrees with the reported ARC mRNA expression pattern in human and rat tissues (Geertman et al., 1996; Koseki et al., 1998). As the *mdx* mouse represents a good model for myofiber breakdown and turnover, we asked if ARC displayed a different expression pattern in dystrophic muscle. We compared ARC protein levels in wild-type (C57BL/10J) and *mdx* mouse skeletal muscles at two and six months of age *via* western blotting. ARC was found to be expressed at essentially the same levels in wild-type and *mdx* muscles at both ages (figure 8A).

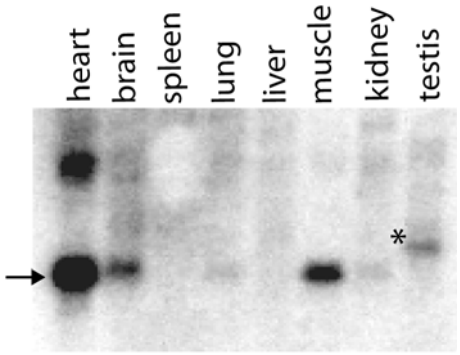

Figure 7. Northern blot analysis of mouse ARC expression. mRNAs from various mouse tissues were hybridized with a cDNA for the full-length coding region of mouse ARC. The arrow indicates the 1.0 kb transcript characterized in this study, which is expressed in skeletal muscle and heart, and at a lower level in brain. The nature of the larger transcripts observed in heart and testis (asterix) is unclear.

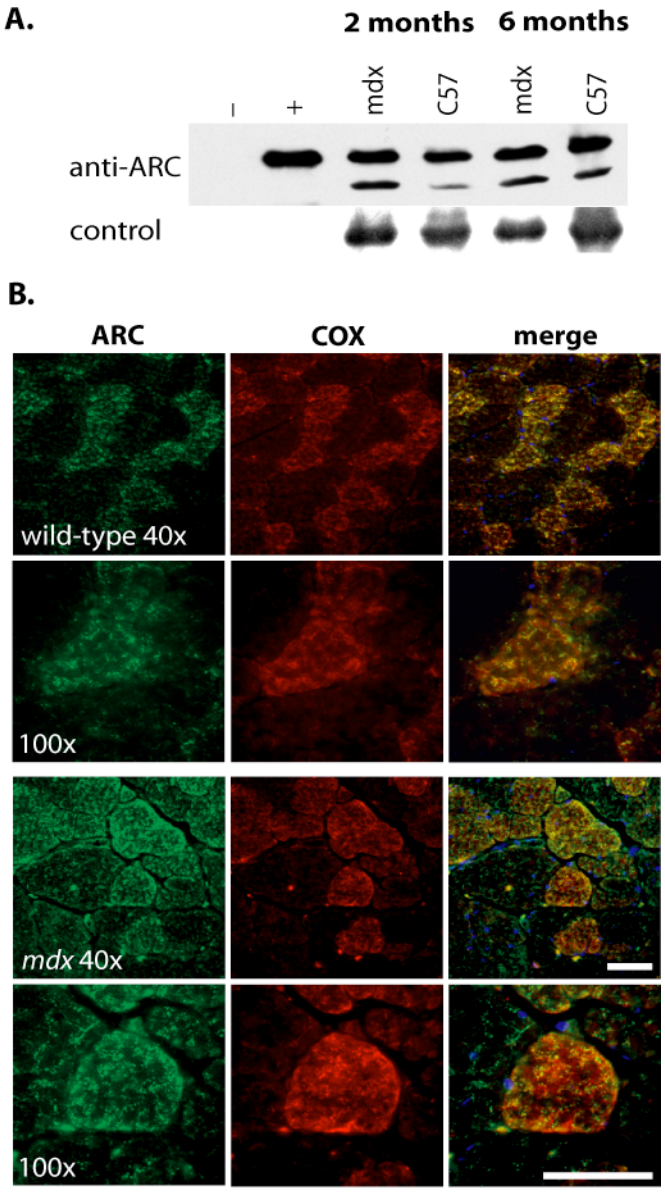

Figure 8. Expression and localization of endogenous mouse ARC in muscle tissue. A) Immunoblot staining of quadriceps muscle extracts from 2 and 6 months old C57Bl/10J and mdx mice using an anti-ARC antibody. The positive control represents 293T cells transfected with a human ARC FLAG expression cassette. **B)** Immunofluorescent staining of quadriceps muscle sections for endogenous mouse ARC and for the mitochondrial marker COX (cytochrome oxidase subunit V). ARC shows a fiber-type specific expression pattern and co-localizes with COX. Scale bar: 50 mm.

4.1.4. Co-localization of ARC with mitochondria

To examine the localization of ARC in muscle fibers, we immuno-stained serial frozen sections of C57BL/10J and *mdx* mice for ARC (figure 8B). ARC staining showed a non-uniform expression pattern across the muscle section, suggesting that ARC was expressed in a fiber-type specific manner. This pattern was observed in diaphragm, quadriceps and tibialis anterior muscles, while the expression in heart showed a uniform expression pattern (figure 8B, figure 11C and data not shown). ARC was expressed at similar levels in wild-type and *mdx* animals in these muscle types and appeared to be predominantly cytoplasmic. Hypercontracted myofibers in *mdx* muscle demonstrated a shift of ARC to the sarcolemma (data not shown). ARC expression in wild-type muscle showed a distinct regular pattern of ARC positive and negative fibers, while ARC expression in the *mdx* background appeared as a less distinct and more irregular pattern. To determine if ARC expression is fiber type specific, we co-stained for ARC and for the mitochondrial-specific protein cytochrome oxidase. Cytochrome oxidase is mainly restricted to oxidative fibers, which display an oxidative metabolism and contain numerous mitochondria (Schiaffino and Reggiani, 1994). ARC co-localized with cytochrome oxidase, showing that ARC is expressed mainly in oxidative fibers and that it is co-localized with mitochondria within the muscle fiber (figure 8B).

4.2. Overexpression of ARC in dystrophic *mdx* muscle

4.2.1. Transgenic ARC expression and localization

We generated transgenic mice in order to test the hypothesis that forced overexpression of ARC might maintain myofiber survival and alleviate the dystrophic muscle pathology of *mdx* mice (figure 9A). Transgenic ARC expression was analyzed in wild-type and *mdx* mice and expression levels were compared with endogenous ARC levels (figure 9B).

Western analysis showed that the transgene was highly expressed in quadriceps and diaphragm muscle on both the C57Bl/10J and the *mdx* background. Immunohistochemical

analysis revealed that the transgene was uniformly expressed in quadriceps and diaphragm muscle and that it localized predominantly to the sarcoplasm in C57BL/10J muscle and shifted towards the sarcolemma in the mutant *mdx* background (figure 10A). Immunohistochemical analysis of soleus and heart muscle showed a mosaic overexpression pattern in soleus, while expression in heart muscle was observed only in rare myocytes (figure 11C). This latter observation is consistent with our previous results showing that the human α-skeletal actin promoter (HSA) expression cassette used in this study is generally not active in cardiac muscle (Crawford et al., 2000; Warner et al., 2002).

To examine whether transgenic ARC co-localized with mitochondria, we co-stained transgenic quadriceps muscle sections for ARC and for the mitochondrial marker cytochrome oxidase (figure 10B). Transgenic ARC was expressed much more uniformly in all fiber types from the HSA promoter in both normal and *mdx* muscle, compared with the endogenous ARC gene. However, transgenic ARC co-localized with cytochrome oxidase in oxidative fibers.

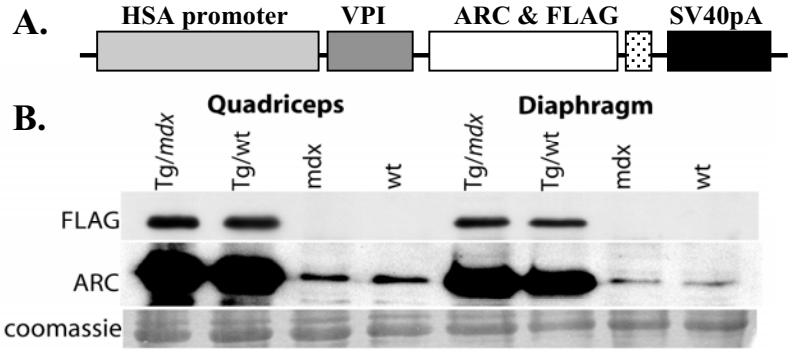

Figure 9. Overexpression of human ARC in mouse muscle tissue. A) Schematic illustration of the expression cassette used to generate transgenic mice. A human ARC cDNA with a FLAG tag epitope was driven by the human skeletal α-actin promoter. In addition, the expression cassette included the SV40 VP1 intron and the SV40 polyA adenylation site. **B)** Western analysis of transgenic and endogenous ARC expression. Quadriceps and diaphragm muscle extracts from six week old transgenic ARC/*mdx*, transgenic ARC/C57BL/10J, *mdx* and C57BL/10J mice were probed with anti-ARC and anti-FLAG antibodies

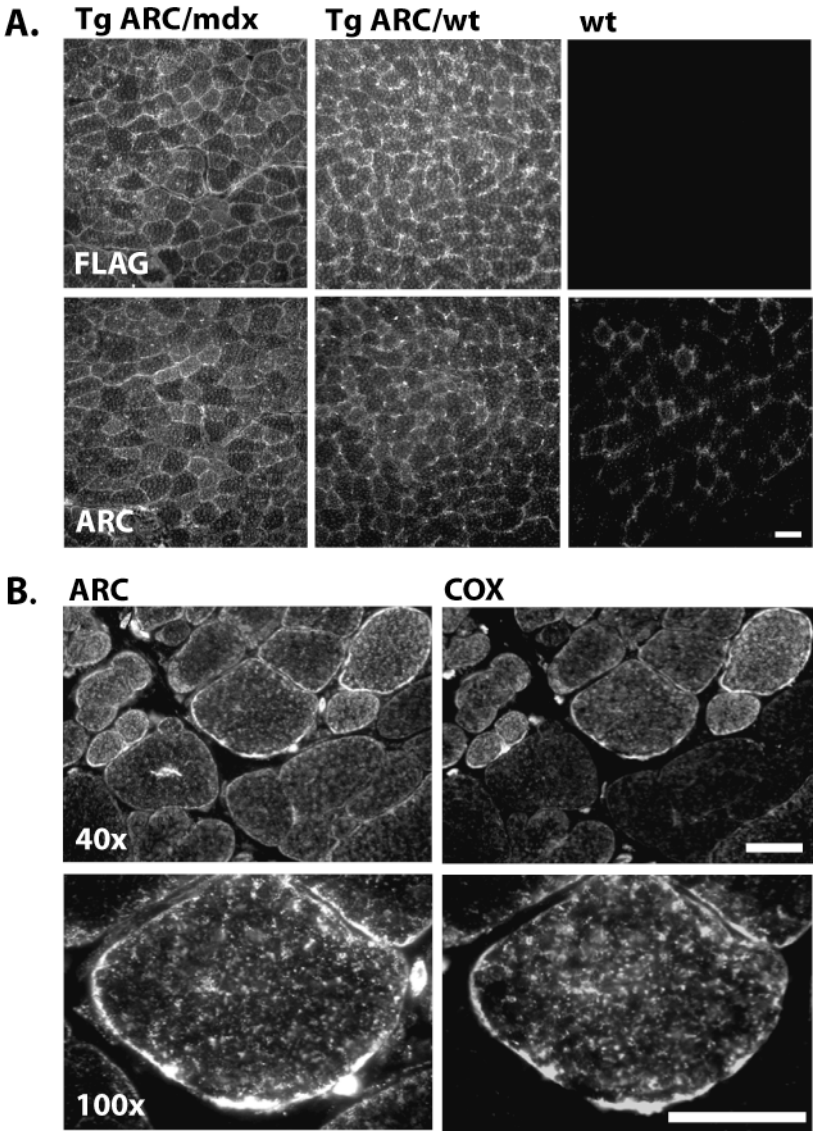

Figure 10. Overexpression and localization of human ARC in mouse muscle tissue. A) Immunofluorescence analysis of ARC and FLAG expression in quadriceps muscle sections from six week-old transgenic ARC/mdx, transgenic ARC/wild-type and wild-type mice. Muscle sections demonstrate a uniform expression pattern of the transgene. **B)** Immunofluorescent staining of transgenic ARC/mdx quadriceps muscle section for ARC and for the mitochondrial marker COX. Transgenic ARC co-localized with COX in oxidative fibers. Scale bar: 50 mm.

4.2.2. Morphological analysis of transgenic ARC/*mdx* mice

Morphological studies were performed on tissue sections of different age groups to examine the effect of ARC overexpression on the histopathology of dystrophic *mdx* skeletal muscle fibers. Hematoxylin and eosin staining of transgenic/*mdx* mice confirmed the presence of a clear pattern of dystrophic muscle pathology including mononuclear cell infiltration, fibrosis, centrally located nuclei and necrotic fibers in quadriceps, diaphragm and soleus of six week, six month, 18 month and two-year old mice (figure 11 and data not shown). To estimate myofiber degeneration and regeneration we counted centrally nucleated myofibers in quadriceps muscles of six week-old transgenic ARC/*mdx*, transgenic ARC/C57BL/10J, C57BL/10J and *mdx* littermates. At this age, quadriceps muscles from *mdx* mice, as well as transgenic ARC/*mdx* mice, displayed a high degree of central nucleation, 76% in *mdx* and 77% in Tg/*mdx*. Wild-type and transgenic ARC/wild-type mice both displayed less than 1% centrally nucleated myofibers (figure 11A).

To evaluate the potential benefit of ARC overexpression in old *mdx* mice, we analyzed the morphology of two year-old transgenic ARC/*mdx* and *mdx* quadriceps and diaphragm muscles (figure 11B). Both *mdx* and transgenic ARC/*mdx* muscles demonstrated an advanced state of muscle degeneration characterized by substantial fat accumulation and fibrotic tissue. No obvious sign of phenotype amelioration was observed in *mdx* muscles overexpressing the ARC protein.

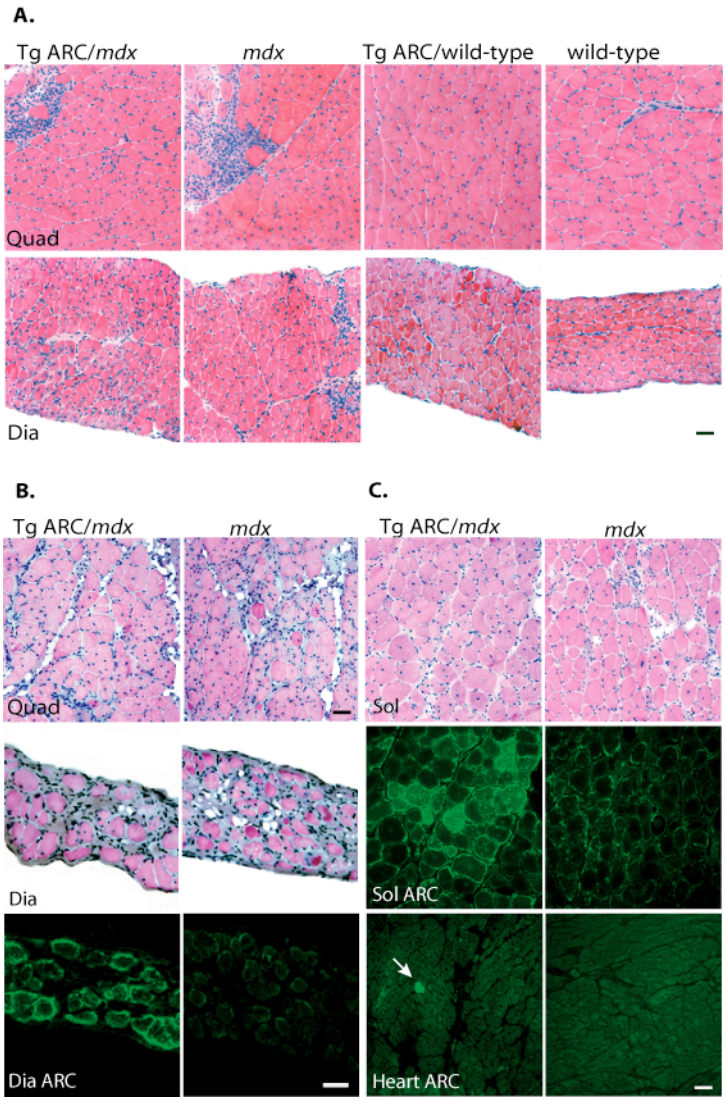

Figure 11. Morphological analysis of muscle tissue from transgenic mice. A) Hematoxylin and eosin (H&E) staining of quadriceps and diaphragm muscle sections of six week old transgenic ARC/mdx, transgenic ARC/wild-type, mdx and wild-type mice. Transgenic ARC/mdx and mdx sections display a characteristic mdx pathology including centrally located nuclei, variation in fiber size, infiltrating immune cells and fibrosis. Transgenic ARC/wild-type sections were not different from wild-type sections. **B)** Morphology of quadriceps and diaphragm muscle of age-matched two year-old transgenic ARC/mdx and mdx mice demonstrates a dystrophic pathology despite ARC overexpression (bottom). **C)** Immunofluorescent staining of age-matched 18 months old transgenic ARC/mdx and mdx soleus sections display a mosaic overexpression of ARC in the transgenic animals. H&E staining of transgenic ARC/mdx muscle sections show no morphological difference with mdx muscle sections. Expression of the transgene in heart was observed only in a few isolated myocytes (arrow). Scale bar: 50 mm.

4.2.3. Caspase-3 activity and membrane permeability in transgenic ARC/*mdx* mice

ARC has been suggested to act as an inhibitor of apoptotic cell death by preventing activation of caspase-8 and caspase-2 (Koseki et al., 1998). To compare the level of apoptosis in wild-type, *mdx* and transgenic ARC/*mdx* muscle we analyzed active caspase-3 expression by immunofluorescence (figure 12). Caspase-3 represents the key effector caspase and is therefore a good indicator for cells undergoing apoptosis. Previously, TUNEL positive fibers were detected in *mdx* mice by several groups, suggesting the presence of a low level of apoptosis (Matsuda et al., 1995; Sandri et al., 1997; Tidball et al., 1995). *mdx* and transgenic/*mdx* muscle showed a number of caspase-3 positive fibers, the vast majority of which appeared necrotic by hematoxylin and eosin staining. No obvious differences could be detected between *mdx* and transgenic/*mdx* skeletal muscles. No active caspase-3 staining was observed in wild-type muscles.

Evans blue dye is commonly used as a marker to distinguish degenerating and intact muscle fibers (Straub et al., 1997). Consequently, we analyzed Evans blue uptake in *mdx* and transgenic ARC/*mdx* mice. *mdx* as well as transgenic ARC/*mdx* mice displayed a large and variable number of Evans blue positive myofibers, the majority of which appeared to be necrotic. We did not observe an obvious difference in Evans blue uptake between *mdx* and transgenic ARC/*mdx* muscle (figure 12). We compared Evans blue localization with active caspase-3 localization to address the possibility that caspase-3 activation might be a consequence of membrane damage. Interestingly, all active caspase-3 positive fibers were also positive for Evans blue, but not all Evans blue positive fibers stained positively for activated caspase-3 (figure 12). Muscle fibers that showed co-localization of Evans blue and caspase-3, however, showed different distribution patterns and intensity levels of Evans blue and caspase-3 immunoreactivity. Fibers with intense Evans blue stain demonstrated weak caspase-3 staining and *vice versa*. This difference may correspond to the stage of apoptosis and/or necrosis in each muscle fiber.

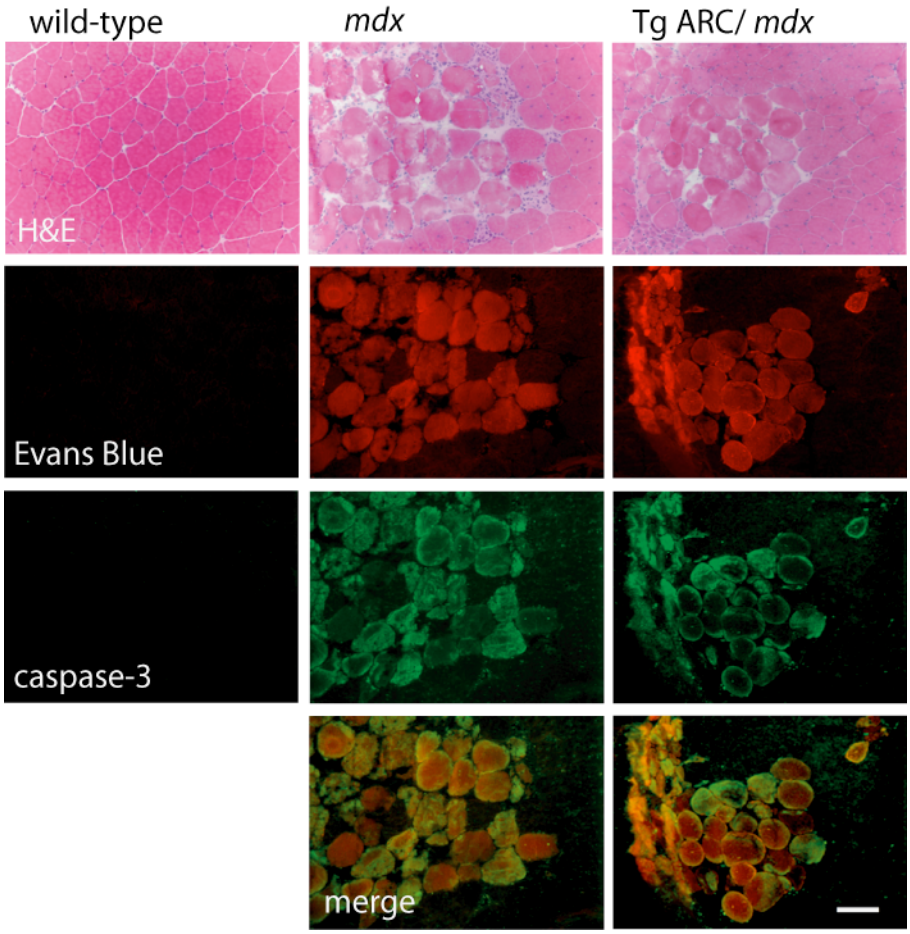

Figure 12. Evans blue dye uptake and caspase-3 expression in mdx and ARC transgenic/mdx mice. H&E staining of quadriceps muscle sections of eight week old exercised mice demonstrate necrotic lesions in mdx and ARC transgenic/mdx characteristic of the mdx phenotype. Necrotic fibers take up Evans blue dye and express active caspase-3. The merged images show that the intensity levels and distribution of Evans blue dye in muscle fibers varies relative to the active caspase-3 staining, which may be due to the stage of fiber breakdown. Scale bar: 50 mm.

4.2.4. Localization of caspase-3 and ARC in transgenic ARC/*mdx* mice

We co-stained serial sections from quadriceps muscle of transgenic ARC/*mdx* mice for active caspase-3 and ARC to compare their expression and localization pattern in muscle fibers (figure 13). Interestingly, caspase-3 positive fibers displayed faint or no ARC staining, suggesting that ARC is downregulated or degraded in these fibers. Downregulation could be a consequence of altered signaling and apoptosis in *mdx* muscle, while degradation could be a consequence of muscle fiber necrosis.

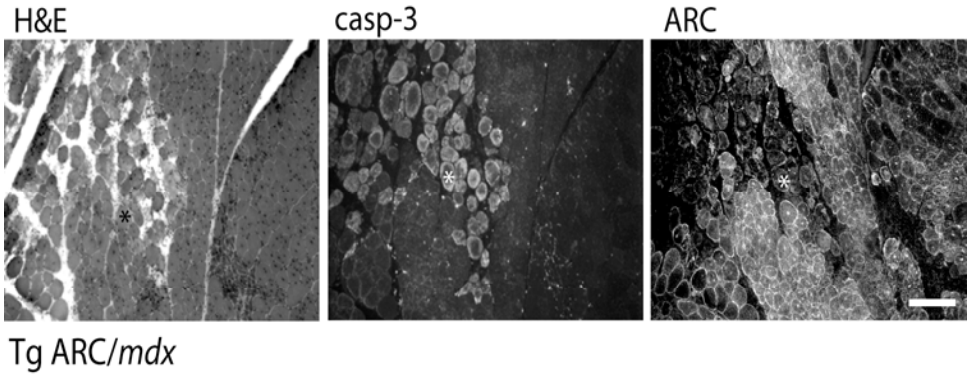

Figure 13. Localization of ARC and active caspase-3 in transgenic ARC/*mdx* muscle sections. H&E staining of quadriceps muscle sections from six week-old transgenic ARC/*mdx* mice demonstrates typical morphological characteristics of dystrophy. Serial sections were stained with ARC and caspase-3 antibodies, showing that muscle fibers expressing active caspase-3 display diminished ARC expression. Asterix indicates orientation. Scale bar: 200 μm.

4.3. Cloning and characterization of Igf-I in skeletal muscle

4.3.1. Isolation of two Igf-I muscle specific isoforms

In order to clone the cDNA for the muscle specific Igf-I isoform, we performed direct PCR amplification from a mouse muscle cDNA library (Lumeng et al., 1999). Primers were designed based on the Igf-I exon 3 sequence of NCBI locus MUSIGF-I (accession number M28139) and vector specific primers. Direct sequencing of PCR products showed that we cloned two alternative splice products of Igf-I, Ea and Eb (figure 14). Igf-I Eb contains exons 1,3,4,5,6 while the other isoform (Igf-I Ea) contains only exons 1,3,4,6 (Bell et al., 1986; Jansen et al., 1983; Rotwein, 1986; Rotwein et al., 1986; Yang et al., 1996). Igf-I Eb differs from Igf-I Ea due to the presence of an additional 52 base pairs in exon 5. Exons 1 and 2 of the Igf-I gene encode different leader peptides, Exons 3 and 4 encode the mature Igf-I peptide as well as the first 16 amino acids of the E domain and exons 5 and 6 encode the alternative extension peptides, Ea and Eb (Adamo et al., 1991; Jansen et al., 1983; Rotwein et al., 1986).

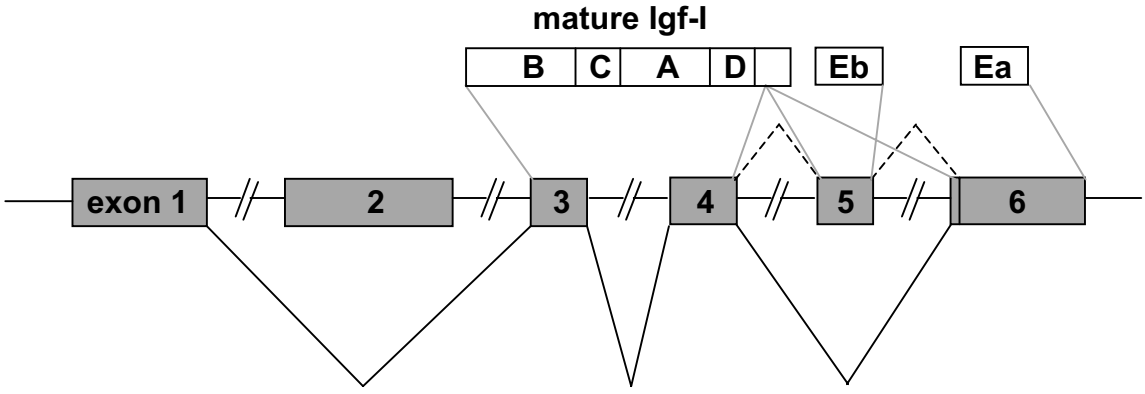

Figure 14. Alternative splicing of the mouse *Igf-I* gene in skeletal muscle. Schematic illustration of the mouse Igf-I gene and its two splice variants (Igf-I Ea and Igf-I Eb) that are expressed in skeletal muscle. Igf-I Eb contains exons 1,3,4,5,6 while Igf-I Ea contains exons 1,3,4,6. Exon 5 has an insert of 52 base pairs, leading to different carboxy termini of the peptides. Exons 1 and 2 define leader peptides, Exon 3 and 4 encode the mature Igf-I peptide as well as the first 16 amino acids of the E domain, and exons 5 and 6 define the alternative extension peptides, Ea and Eb (Janson et al., 1991, Adamo et al., 1991). The mature Igf-I peptide contains the A, B, C and D domains.

The muscle specific isoforms differ from the liver isoforms by using sequences encoded by exon 1 as a leader peptide in contrast to exon 2 (Adamo et al., 1991; Lowe et al., 1987). The mature Igf-I peptide, encoded by exons 3 and 4, contains the A, B, C and D domains, consisting of 70 amino acids with a molecular mass of 7.65 kDa. The A and B domains are homologous to the A and B chains of insulin (Rinderknecht and Humbel, 1978). The protein sequence displays 50% sequence homology to proinsulin and 70% sequence homology to Igf-II (Daughaday and Rotwein, 1989; Rinderknecht and Humbel, 1978).

4.3.2. Igf-I mRNA expression levels in normal and dystrophic *mdx* skeletal muscle

The liver is the primary site of Igf-I production. Liver Igf-I expression is growth hormone dependent, however Igf-I levels are also influenced by age, sex, nutritional status and other hormones (Landin-Wilhelmsen et al., 1994; Stewart and Rotwein, 1996). In addition, Igf-I is produced locally in various tissues, where it can exert autocrine and paracrine effects (D'Ercole et al., 1984; Daughaday and Rotwein, 1989; LeRoith and Roberts, 1991; Sjogren et al., 1999).

To characterize Igf-I expression in normal and dystrophin-deficient muscle, we developed a real-time PCR assay to measure mRNA levels of the Ea and Eb isoforms. Primer pairs were designed to uniquely detect Igf-I Eb or both Igf-I Ea and Igf-I Eb. We analyzed RNA levels in *tibialis anterior* (TA) muscles of nine month-old *mdx* and wild-type (C57BL/10J) mice and detected no significant difference in the Igf-I expression levels between *mdx* and wild-type muscles (figure 15). Wild-type animals showed a trend towards higher Igf-I mRNA expression levels than *mdx* animals, however total Igf-I levels varied significantly between tested animals. The Igf-I Ea isoform was the most abundant isoform and showed an average of six to seven fold higher expression than the Igf-I Eb isoform in our tested age group. This data is in accordance with previous publications, although these studies did not detect any Igf-I Eb levels in *mdx* muscles (McKoy et al., 1999).

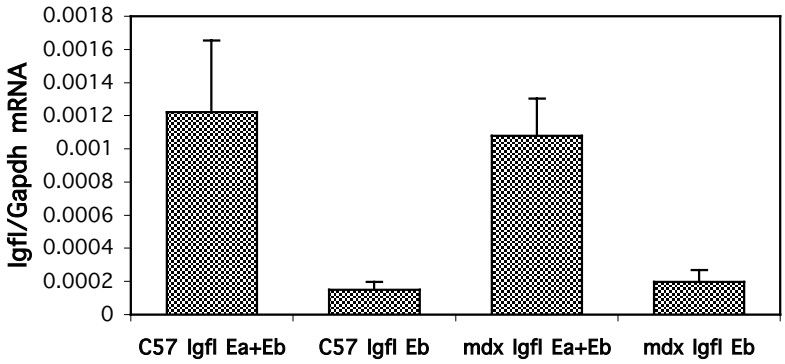

Figure 15. Quantitation of Igf-I mRNA levels in C57BL/10J and *mdx* mice. mRNA expression of Igf-I isoforms in nine month old animals is shown relative to GAPDH mRNA expression. Two different primer pairs were used to uniquely detect Igf-I Eb or both isoforms, Igf-I Ea and Igf-I Eb. Values are presented as the mean ± s.d., n=4 muscles per group.

4.3.3. Overexpression of Igf-I isoforms *in vitro*

To determine if the Igf-I cDNAs encode functional proteins, we generated replication defective adenoviral vectors deleted for E1, E3 and the adenovirus (Ad) DNA polymerase gene (Amalfitano et al., 1996) that expressed the Ea or Eb Igf-I cDNA (Ad-Igf-I) under the control of the CMV promoter (figure 16A). We used these Ad-Igf-I vectors to efficiently infect a myogenic cell line to test the effects of Igf-I *in vitro*. Since the muscle-derived L6 cell line does not express Igf-I or significant levels of Igf-II, but it is responsive to exogenous Igf-I, this cell line is commonly used to study Igf-I overexpression *in vitro* (Engert et al., 1996; Rosen et al., 1993). Low or no serum levels in conjunction with added Igf-I advances the cells from a proliferation stage into differentiation, where myoblasts differentiate and fuse into myotubes (Ewton and Florini, 1981; Florini and Ewton, 1990; Florini and Magri, 1989).

L6 myoblasts were grown to 80% confluency in proliferation medium containing 10% fetal bovine serum (FBS), then switched to serum-free differentiation medium supplemented with 500 μg/ml bovine serum albumin (BSA) one day prior to Igf-I treatment. To allow time for viral infection, Igf-I expression and secretion, we infected L6 myoblasts with the adenoviral vectors carrying Igf-I Ea or Eb at an multiplicity of infection (MOI) of 1000 eight hours prior to adding recombinant Igf-I (25 ng/ml) to the control plates.

One day post infection, total RNA was extracted from Ad-Igf-I treated and control cultures for Igf-I mRNA expression analysis by using two different primer sets (figure 16B and 3C). The primer sets were designed to specifically detect virally delivered Igf-I and to distinguish by size between both Igf-I isoforms (figure 16B) and between mRNA and potential vector DNA contamination (figure 16C). Our results demonstrate that both virally delivered Igf-I cDNAs were transcribed into mRNA.

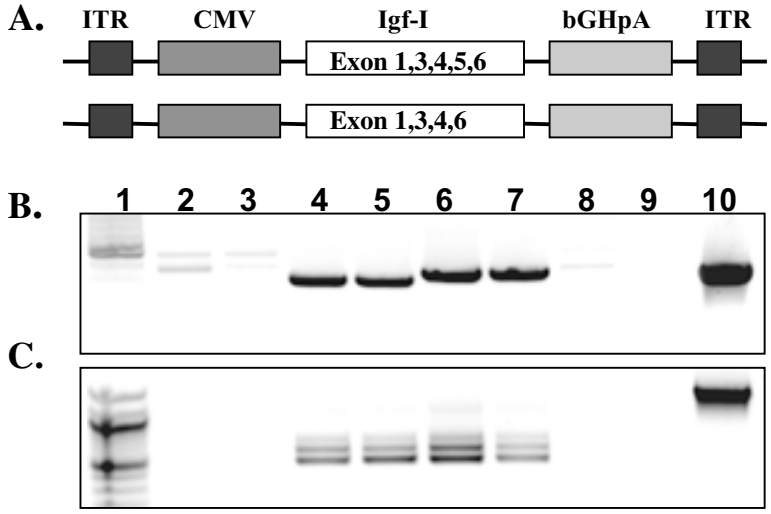

Figure 16. Overexpression of Igf-I in L6 cultures. A) Schematic illustration of the Ad-Igf-I constructs. The expression cassette includes the CMV promoter driving Igf-I expression and the bovine growth hormone polyadenylation signal (bGHpA) and Ad inverted terminal repeats (ITR). **B)** and **C)** RNA analysis of Ad-Igf-I treated and control cultures. Total RNA was isolated from infected and non-infected L6 cells and transcribed into cDNA. Igf-I mRNA expression was then analyzed by PCR using two different primer sets in order to distinguish between: **B**) isoforms **C)** amplification from RNA or DNA. 1) DNA standard 2) no virus control 3) Ad-LacZ control 4) Ad-Igf-1 (Exon 1,3,4,6) purified virus 5) Ad-Igf-1 (Exon 1,3,4,6) cell lysate 6) Ad-Igf-1 (Exon 1,3,4,5,6) purified virus 7) Igf-1 (Exon 1,3,4,5,6) cell lysate 8) total RNA from skeletal muscle 9) neg. control 10) pAd-Igf-I plasmid DNA.

Six days post infection, clear differences in cell morphology were observed in the Igf-I treated cultures. The cells were stained for myosin-heavy chain (MHC) expression, which is a marker for myocyte differentiation (Schiaffino and Reggiani, 1994). We observed the highest number of MHC expressing cells in the recombinant Igf-I treated plate; however, Ad-Igf-I

treated plates also demonstrated a high number of differentiated cells in comparison to the untreated control plates (figure 17). This result clearly shows that the Igf-I cDNAs encode functional proteins and can be used in *in vivo* studies.

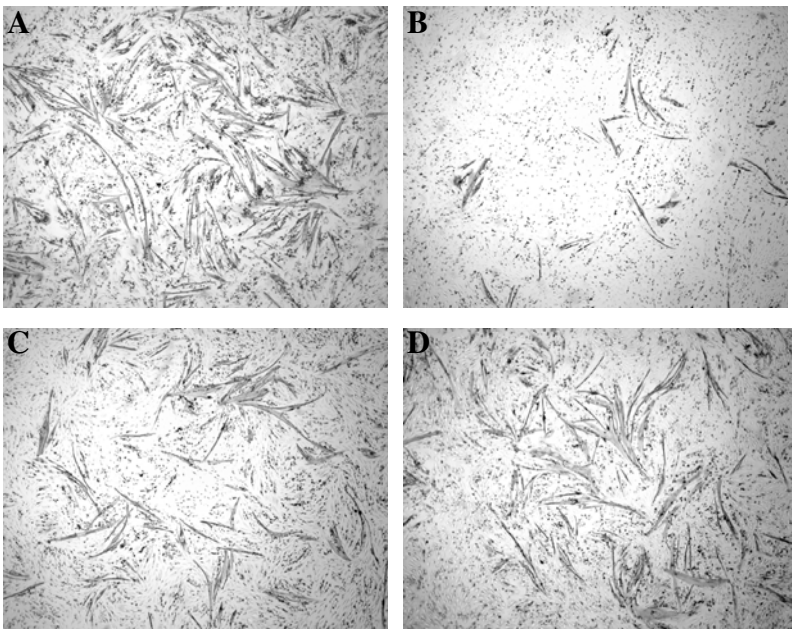

Figure 17. Ad-Igf-I enhances myogenic differentiation of L6 cells. Parallel cultures of L6 myoblasts were treated with **A**) 25 ng/ml recombinant Igf-I **B)** untreated control **C**) Ad-Igf-I (1,3,4,6) and **D**) Ad-Igf-I (1,3,4,5,6). Cells were differentiated in serum-free medium, supplemented with 500 μg/ml BSA. After six days, cells were fixed and stained with an antibody against MHC (BF-45).

Taken together, we have isolated two Igf-I cDNAs and characterized endogenous Igf-I mRNA expression in normal and dystrophic *mdx* muscles. We have further shown that both Igf-I cDNAs were functional in *in vitro* studies. Next, we studied the therapeutic potential of Igf-I for ameliorating a dystrophic pathology. For these studies, we chose to test the more abundant and more extensively studied Igf-I isoform, Ea.

4.4. Delivery of Igf-I and dystrophin to dystrophic *mdx* muscles

Gene replacement therapy using truncated versions of dystrophin (μdys) have been shown to protect dystrophic muscles from contraction-induced injury and partially reverse muscle pathology (Harper et al., 2002b; Wang et al., 2000). In addition, Igf-I overexpression in muscle has been shown to lead to an increase in muscle mass and strength and to counter muscle decline in old and dystrophic *mdx* mice (Barton et al., 2002; Barton-Davis et al., 1998; Musaro et al., 2001). Thus, we co-delivered dystrophin and Igf-I to *mdx* muscles to determine if the beneficial effect of Igf-I is synergistic with the protective effects of dystrophin in ameliorating the dystrophic phenotype.

For these studies we generated recombinant adeno-associated viral vectors pseudotyped with the serotype 6 capsid protein (AAV6), since these vectors transduce muscle tissue very well and can be persistent for several years (Scott et al., 2002). To assure muscle specific expression, these vectors carried expression cassettes in which the muscle-specific creatine kinase promoter/enhancer (CK) drove either the micro-dystrophin (ΔR4-R24/ΔCT, AAV-μdys) or the Igf-I cDNA (AAV-Igf-I) (figure 18). We injected the TA muscle of nine month old *mdx* male mice with each vector separately, together or with buffer (sham) as a control. Each muscle was treated with a total volume of 30 μl, containing either ~1.8 x 10^{10} total genomes of AAV-μdys, ~2.0 x 10^{10} total genomes of AAV-Igf-I, both or none. Four months post injection the muscles were analyzed for dystrophin expression, Igf-I mRNA transcript levels, functional properties and morphological changes.

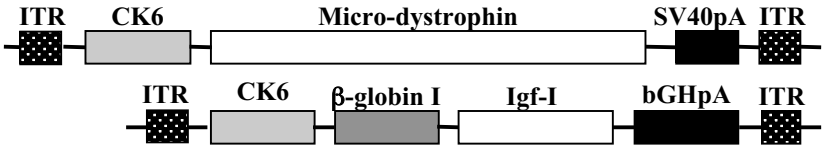

Figure 18. Schematic illustration of AAV-μdys and AAV-Igf-I constructs. The expression of both genes is driven by the CK6 promoter. In addition, AAV-μdys contains the SV40 polyadenylation signal (SV40pA), while AAV-Igf-I includes the β-globin intron and the human growth hormone polyadenylation signal (hGHpA). Both constructs contain AAV-2 ITRs.

4.4.1. Dystrophin expression in AAV-dystrophin injected *tibialis anterior* (TA) muscles

TA muscle cross-sections were immunostained for dystrophin to analyze expression levels and expression distribution throughout the muscle (figure 20). We used the ImagePro software to determine the percentage of dystrophin expressing fibers per total cross sectional area (figure 19). AAV-μdys treated and AAV-μdys & AAV-Igf-I co-treated TA muscles displayed a wide distribution of dystrophin positive fibers throughout the muscle that represented approximately 40% of the total cross sectional area. In contrast, AAV-Igf-I and untreated control muscles showed few revertant, dystrophin positive fibers, that represented less than 5% of the total cross sectional area. AAV-μdys expressing fibers showed no evidence of necrosis, while fibers that did not express dystrophin displayed features of dystrophic pathology, such as loss of membrane integrity and immune infiltration (figure 20 C-F).

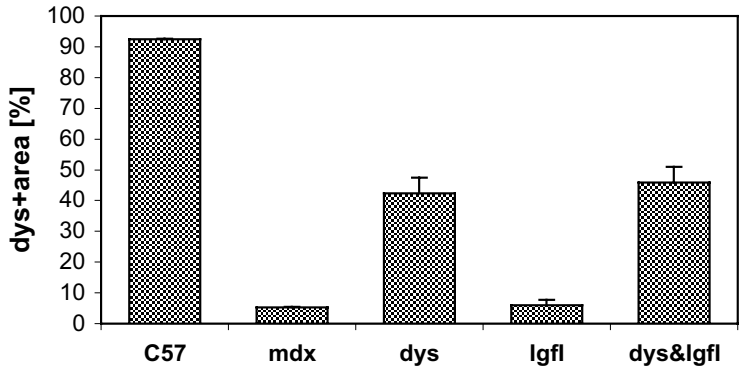

Figure 19. Quantitation of dystrophin positive area. The percentage of dystrophin positive area per total cross sectional area was determined by using the ImagePro software. AAV-μdys treated muscles and AAV-μdys and AAV-Igf-I co-treated muscles demonstrated that ~40% of the total cross sectional area was dystrophin positive. In contrast, *mdx* and AAV-Igf-I injected muscles showed dystrophin expression in only 5% of the total area. Values are presented as the mean ± SEM, n=3 muscles per group.

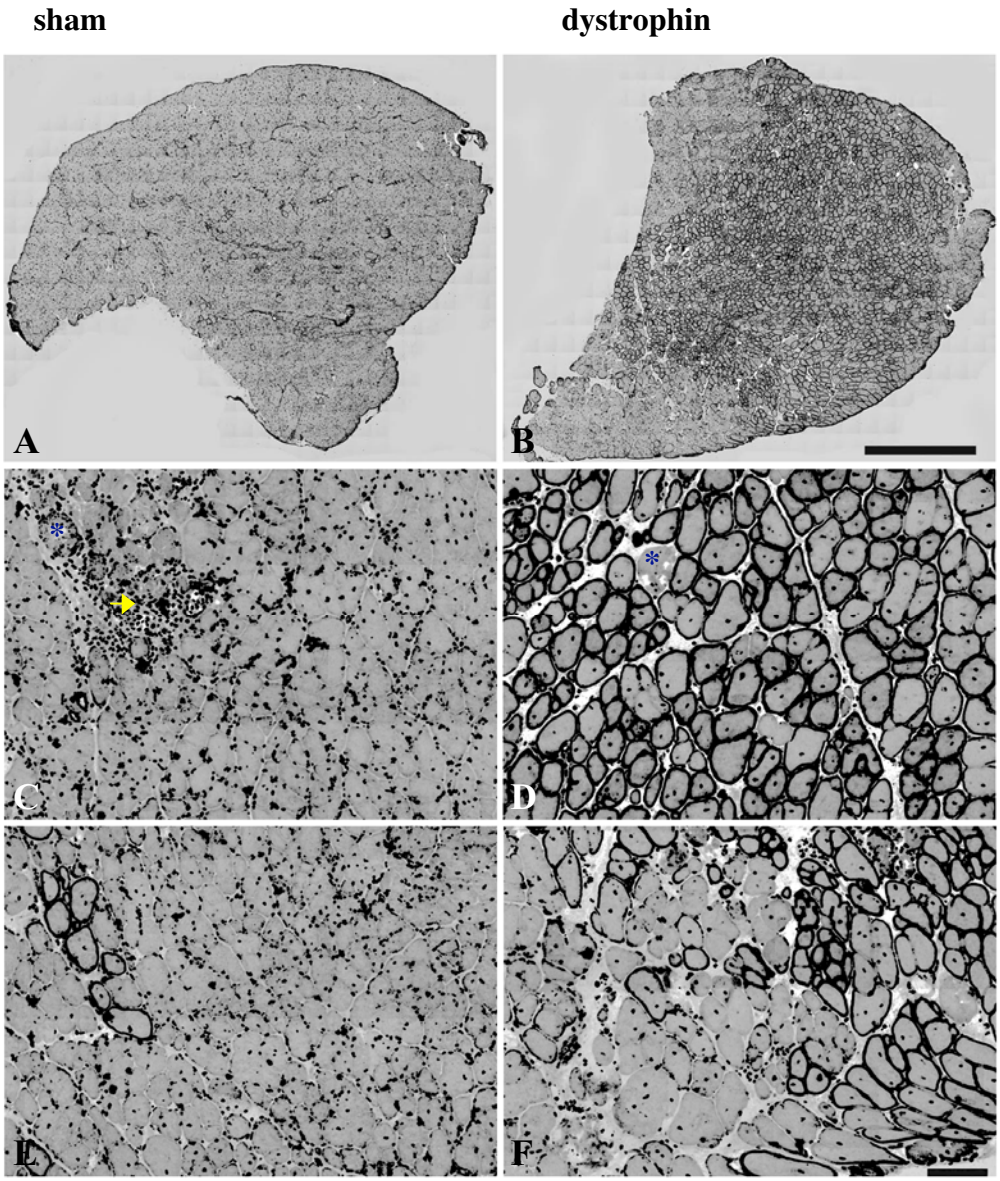

Figure 20. Expression of dystrophin in *mdx* muscle following injection with AAV6 micro-dystrophin. Shown is a montage image of the entire cross sectional area of TA muscles from 13 months old mice injected with saline (A) or AAV-μdys (2 x 10^{10} vg) (B). The results demonstrated widespread expression of dystrophin in (B) four months post-injection. (C-F) show close-ups of two regions from each of the muscles shown in A and B. (E) shows a cluster of revertant fibers in *mdx* control muscles. Asterix indicate non-dystrophin expressing, necrotic fibers. Arrow indicates immune infiltration in *mdx* control muscles. Scale bars 1 mm (A, B) and 100 μm (C-F).

4.4.2. Igf-I mRNA expression in AAV-Igf-I injected TA muscles

To examine Igf-I expression, we extracted total RNA from TA muscles of AAV-Igf-I treated and untreated *mdx*, and wild-type, animals. Two different primer pairs were designed to detect: 1) only virally delivered Igf-I to exclude potential DNA contamination; 2) total Igf-I levels in order to analyze Igf-I overexpression in treated, relative to untreated, muscles. We detected virally delivered Igf-I mRNA expression in all AAV-Igf-I injected, and AAV-μdys & AAV-Igf-I co-injected, animals (Figure 21A). Relative quantitation of Igf-I mRNA expression levels demonstrated a clear overexpression of Igf-I in treated, relative to untreated, animals (Figure 21B). Muscles co-injected with AAV-μdys & AAV-Igf-I revealed an ~200-400 fold overexpression of Igf-I mRNA relative to untreated muscles, while muscles that were only treated with AAV-Igf-I showed an overexpression of no more than 50-100 fold. The loss of Igf-I expression over time in AAV-Igf-I treated versus AAV-Igf-I & AAV-μdys co-treated animals suggests that dystrophin expression protects muscle fibers from degeneration and as a result from loss of viral vector DNA.

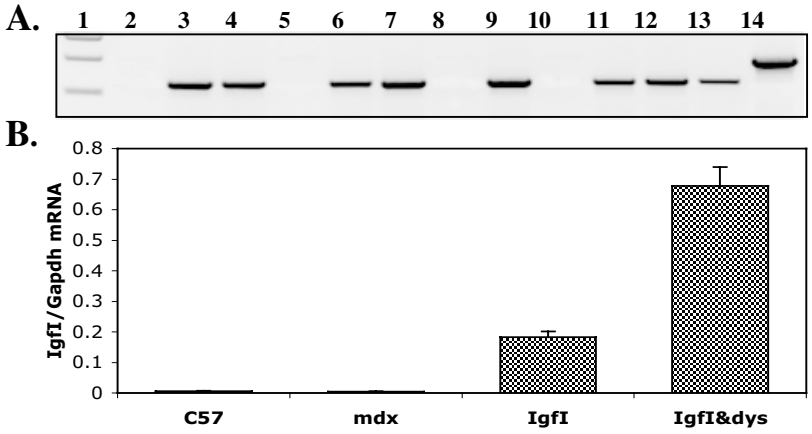

Figure 21. Igf-I mRNA expression in wild-type, *mdx* and AAV-Igf-I treated animals. A) Total RNA was extracted from TA muscles injected with AAV-Igf-I & AAV-μdys (3,4,7,9), AAV-Igf-I (6,11,12,13) and saline (2,5,8,10) and analyzed for Igf-I mRNA expression. DNA standard (1), pAAV-Igf-I plasmid DNA (14). The primer pairs were located on opposite sides of an intron in the vector, so that only virally delivered Igf-I mRNA would be expected to be amplified, and which would exclude amplification from contaminating vector DNA. **B)** Quantification of Igf-I mRNA relative to GAPDH mRNA expression. The primer pair was designed to detect virally delivered and endogenous Igf-I. Values are presented as the mean ± SEM, n=4 per group.

We also examined vector DNA persistence in AAV-Igf-I treated, and in AAV-μdys & AAV-Igf-I co-treated, animals (figure 22A). For this purpose, we designed a primer pair that amplified over part of the intron sequence, to specifically detect Igf-I vector genomes and exclude potential amplification from RNA. Quantitation by real-time PCR detected ~2.5 x 10^5 genomes/μg total DNA in AAV-μdys & AAV-Igf-I co-injected muscles, and 4-5 fold less, ~5 x 10^4 genomes/μg total DNA, in the AAV-Igf-I only injected muscles (figure 22B). This difference between AAV-Igf-I treated, and AAV-μdys & AAV-Igf-I co-treated, muscles correlated well with the observed differences in mRNA expression levels.

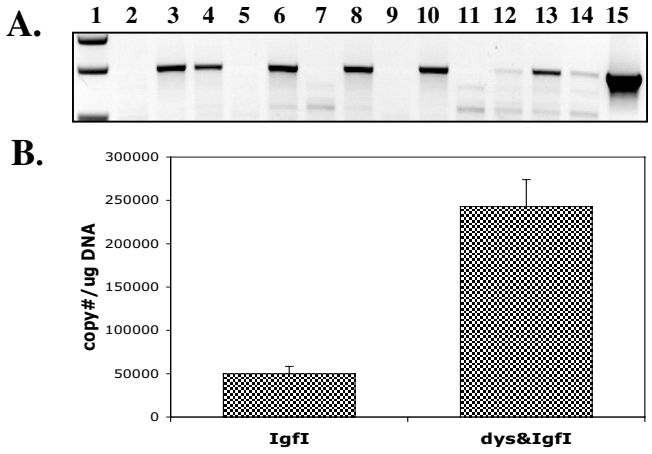

Figure 22. Igf-I vector genome persistence in AAV-Igf-I and AAV-Igf-I & AAV μdys injected muscles four months post-injection. **A)** Total DNA was extracted from TA muscles injected with AAV-Igf-I & AAV-μdys (3,6,8,10), or with AAV-Igf-I (4,12,13,14), or with saline (2,5,7,9,11) and analyzed for AAV-Igf-I vector genome persistence. One primer was designed to anneal to the intron sequence, to exclusively detect Igf-I vector genomes. Standard (1), pAAV-Igf-I plasmid DNA (15). **B)** Quantitation of vector genome persistence. Values are presented in copy number per μg total DNA as the mean ± SEM, n=4 muscles per group.

4.4.3. Functional analysis of treated *versus* untreated TA muscles

Functional properties of TA muscles from AAV-μdys, AAV-Igf-I, AAV-μdys & AAV-Igf-I and sham injected animals were analyzed four months post-injection. In addition, age-matched wild-type mice were used as controls. *Mdx* muscles displayed a ~20% increase in

muscle mass, compared to age-matched, 13 month old wild-type mice (figure 23A). Muscle mass values were normalized to body mass. In contrast, values that were not normalized to body mass did not show a significant difference in muscle mass between wild-type and *mdx* muscles. Functional analysis of contractile properties showed that *mdx* muscles generated on average 20% lower maximum isometric force values than wild-type muscles (figure 23B). Previous studies demonstrated that *mdx* TA muscles produced ~18% higher force values than wild-type muscles, however *mdx* muscles had a ~41% greater mass than wild-type muscles (DelloRusso et al., 2001). Differences in muscle masses between the animals in our study and the previous study could be due to differences in nutrition and housing conditions.

Muscle groups treated with AAV-Igf-I, and co-treated with AAV-Igf-I & AAV-μdys, showed a significant increase in muscle mass relative to untreated *mdx* animals (figure 23A). Values were normalized to whole body weight and showed a mean increase of 17% for AAV-Igf-I treated, and 19% for AAV-Igf-I & AAV-μdys, co-treated animals. In correlation with the increase in muscle mass, AAV-Igf-I & AAV-μdys co-treated animals also demonstrated a significant 20% increase in maximum isometric force generation (figure 23B). AAV-Igf-I, on the other hand, resulted in a mean increase in maximum isometric force generation of only 9% that was not significantly different from AAV-μdys and sham injected muscles.

Muscles from treated and control groups were also subjected to two lengthening contractions *in situ* (LC1 and LC2). Each muscle was analyzed by measuring force production after the injury-inducing lengthening contractions (figure 23C and D). All AAV-μdys treated animals demonstrated a significant protection from contraction-induced injury. After the first lengthening contraction, AAV-μdys injected, and AAV-μdys & AAV-Igf-I co-injected, muscles displayed force generating capacity that were ~47% and ~49% of the values before the contractions, compared to ~24% in *mdx* and ~86% in wild-type animals. AAV-Igf-I treated animals retained a ~35% force generating capacities after the first lengthening contraction, however these values were not significantly different from *mdx* animals. After the second lengthening contraction, AAV-Igf-I treated muscles were as susceptible to muscle damage as *mdx* control muscles and showed a force generating retention of only 3%. In contrast, AAV μdys treated, and AAV-μdys & AAV-Igf-I co-treated, animals demonstrated a statistically significant 10% and 13% retention of force generation, compared to 2% in *mdx* and 64% in wild-type animals.

In summary, AAV-Igf-I treatment increased muscle mass, while AAV-µdys treatment protected muscles from contraction-induced injury after one and two lengthening-contraction. In contrast, AAV-µdys & AAV-Igf-I co-treatment resulted in an increased muscle mass and strength, and protected from muscle damage. These data suggest, that the beneficial effect of AAV-Igf-I is synergistic with the protective effect of AAV-µdys in ameliorating the *mdx* phenotype.

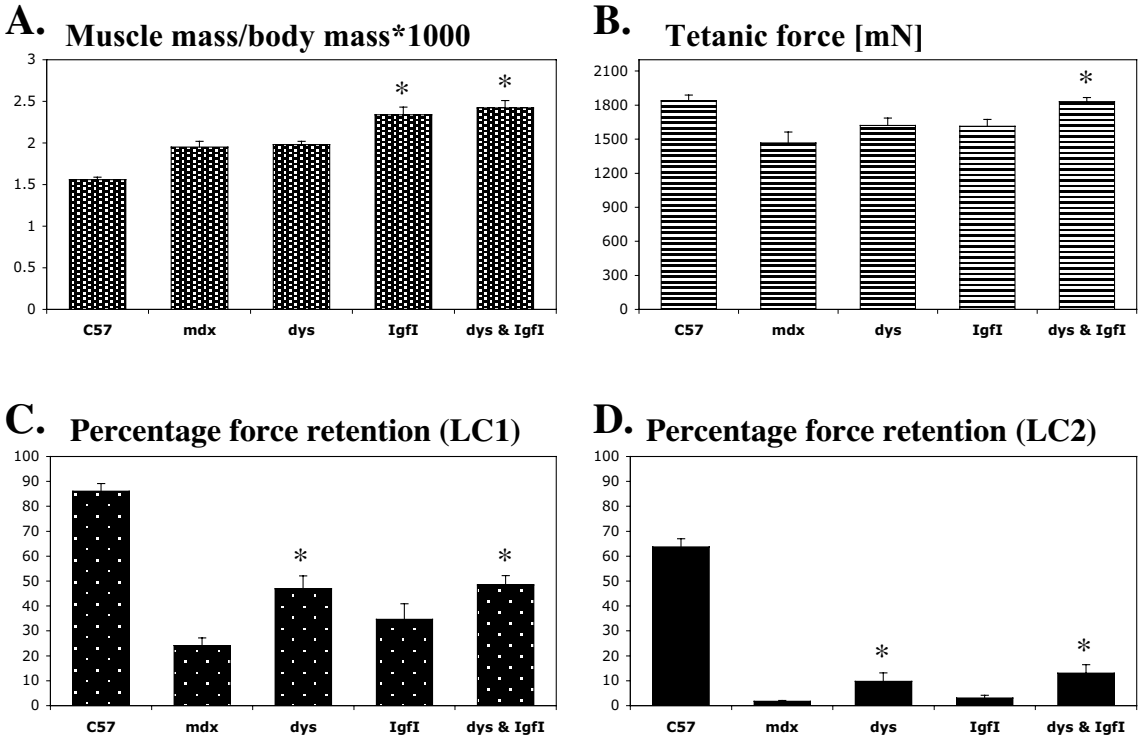

Figure 23. Effect of AAV-Igf-I and AAV-µdys treated *mdx* muscles on functional properties. TA muscles injected with AAV-µdys, AAV-Igf-I, AAV-µdys and AAV-Igf-I or saline were analyzed four months post injection. TA muscles from age-matched C57BL/10J mice served as controls. **A)** Muscle mass. Values are presented relative to body mass. **B-D)** TA muscles were analyzed *in situ* by measuring **B)** maximum force production and force after one **C)** or two **D)** lengthening contractions. The protection from contraction-induced injury is measured as the percentage of force generating capacities after each lengthening contraction. Significant differences ($P < 0.05$) by ANOVA analysis of AAV-Igf-I, AAV-µdys and AAV-Igf-I & AAV-µdys treated muscles from *mdx* muscles are as indicated (asterix). Values are presented as the mean ±SEM, n=9-12 muscles per group.

4.4.4 Histological analysis of treated versus untreated TA muscles

To examine the effect of Igf-I overexpression on muscle morphology, muscle sections were stained with hematoxylin and eosin and analyzed for total cross sectional area, centrally located nuclei and fiber number per area by using the ImagePro software. AAV-Igf-I treated, and AAV-μdys & AAV-Igf-I co-treated, animals demonstrated a ~13% increase in total cross sectional area, compared to untreated *mdx* animals. These results are in agreement with our reported increase in muscle mass (see section 4.4.3) (figure 24).

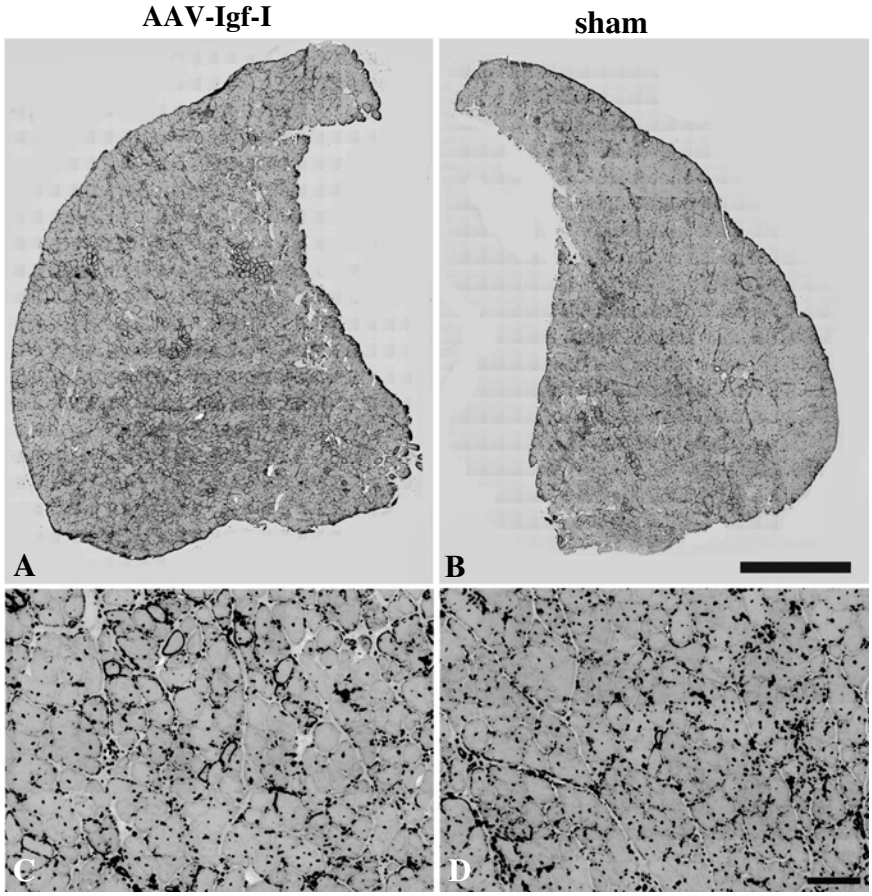

Figure 24. Effect of Igf-I expression on TA muscles. Montage of entire TA cross sectional area of AAV-Igf-I treated and sham treated animals. One TA muscle of each animal was injected with AAV-Igf-I and the contralateral muscle from the same animal served as a buffer-injected control. C and D show close-ups of two regions from each of the muscles shown in A and B. Scale bars 1 mm (A, B) and 100 μm (C, D).

Morphological analysis showed that wild-type animals were clearly distinguished from *mdx* animals by having less than 5% centrally nucleated myofibers, compared to ~50% in *mdx* (figure 25A). The number of myofibers per unit area was ~0.45 fibers/μm^2 in wild-type muscles, a value that was almost doubled in *mdx* animals (figure 25B). In addition, all treated groups revealed significant morphological changes from the *mdx* animals. Muscle fiber number per unit area measurements demonstrated a significant 15-20% reduction of fibers per area in all treated groups in comparison to *mdx* animals, probably reflecting a reduction in myofiber degeneration and thus the presence of fewer small caliber regenerating fibers (figure 25B). Central nucleation was reduced by 5% in AAV-Igf-I, by 16% in AAV-μdys and significantly by 25% in AAV-Igf-I and AAV-μdys co-treated animals relative to *mdx*, also giving evidence for the presence of fewer cycles of degeneration and regeneration in treated TA muscles (figure 25A). High variances between treated groups suggests a need to evaluate more animals per group in further studies.

In summary, treated TA muscles demonstrated a trend towards less fibers per unit area and less central nucleation compared to *mdx* muscles. These are both indications that AAV-Igf-I, AAV-μdys and AAV-Igf-I & AAV-μdys co-treatment had a protective effect and reduced muscle degeneration.

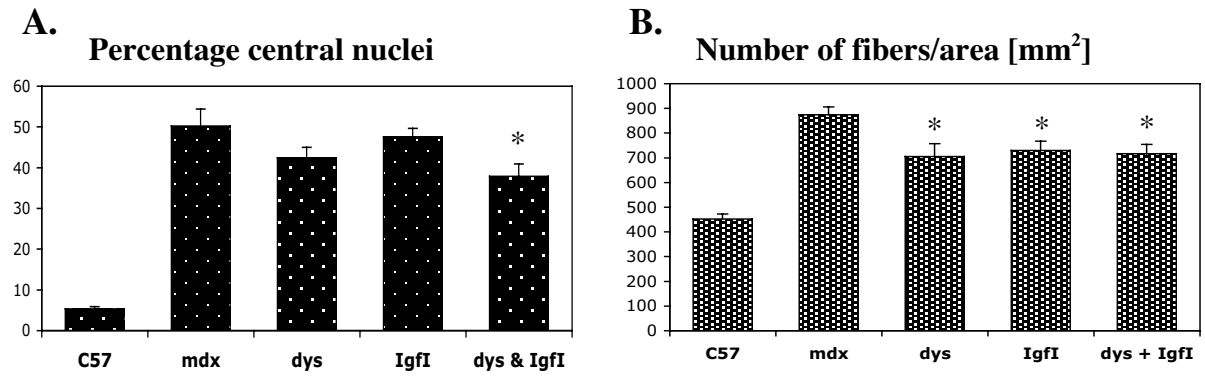

Figure 25. Morphological analysis of wild-type, *mdx*, AAV-Igf-I, AAV-μdys and AAV-Igf-I & AAV-μdys treated TA muscles. A) Percentage of central nuclei (n=1000 fibers per animal). B) Number of muscle fibers per area [mm^2] (n=4 fields per animal). ANOVA statistical analysis was performed on all data sets. Statistically significant difference ($P < 0.01$) of treated muscles from *mdx* muscles are as indicated (asterix). Values are expressed as mean ±SEM. 3-4 animals were analyzed per group.

5. DISCUSSION

5.1 Characterization of ARC in normal and dystrophic *mdx* muscle

5.1.1. ARC expression and localization in normal and dystrophic *mdx* muscle

Several groups have characterized the expression of proteins involved in apoptosis in normal and diseased skeletal muscle tissue (Sandri and Carraro, 1999; Tews and Goebel, 1997b; Veal and Jackson, 1996). Most apoptotic proteins are expressed at a low or non-detectable level in normal mice and demonstrate elevated expression only in degenerating and regenerating muscle fibers of *mdx* mice (Dominov et al., 2001; Tews and Goebel, 1997b). We cloned the mouse isoform of the anti-apoptotic protein ARC and characterized its expression pattern in mice. ARC is the only anti-apoptotic protein known to be expressed at high levels in skeletal muscle (Koseki et al., 1998). Interestingly, ARC is expressed mainly in oxidative fibers and colocalizes with the mitochondrial-specific marker cytochrome oxidase. Localization of ARC to mitochondria is regulated by phosphorylation of threonine 149 and only the phosphorylated, active form localizes to mitochondria (Li et al., 2002). Slow oxidative fibers express type I MHC and display an oxidative metabolism with a great number of mitochondria. Fast fiber types IIa and IIx are capable of both oxidative and glycolytic metabolism and fast fiber type IIb are exclusively glycolytic (Schiaffino and Reggiani, 1994). Mitochondria play a key role in responding to intracellular apoptotic signals by the release of cytochrome c followed by the activation of caspase-3 (Li et al., 1997). ARC inhibits cytochrome c release from mitochondria and protects mitochondrial function from reactive oxygen species in H9C2 cells (Ekhterae et al., 1999; Neuss et al., 2001), suggesting its anti-apoptotic role in responding to intracellular signals. In addition, ARC was shown to interact with caspase-2 and caspase-8 and to inhibit apoptosis induced by caspase-8 (Koseki et al., 1998). The inactive forms of caspase-2 and caspase-8 are located in mitochondria and are released into the cytoplasm upon stimulation (Qin et al., 2001; Susin et al., 1999). Thus, ARC may play an important role in preserving mitochondrial function and inhibiting apoptosis in skeletal muscle.

Interestingly, human ARC was shown to have an alternative splice product, named Nop30, that interacts with the splicing factor Srp30c (Stoss et al., 1999). We were not able to find any evidence that Nop30 is expressed in mouse muscle. Our data is supported by the expression profile of Srp30c, which, in contrast to human muscle, is expressed at very low levels in mouse skeletal muscle (Screaton et al., 1995). This lack of alternative splicing of the ARC gene in mouse skeletal muscle demonstrates one example of evolutionary divergence between humans and mice.

We characterized endogenous ARC expression in normal and *mdx* mice to explore the effect of a dystrophic background on ARC expression. ARC expression levels are similar in normal and *mdx* muscle. However, ARC localization is altered in the *mdx* background. Altered mitochondrial protein expression and localization could be responsible for differences in intracellular ARC localization in the C57BL/10J and *mdx* background. It was previously shown that respiratory chain-linked enzymes were downregulated in *mdx* muscle and oxidative phosphorylation was altered compared to normal muscle (Braun et al., 2001; Chen et al., 2000; Kemp et al., 1992; Kuznetsov et al., 1998).

5.1.2. Overexpression of ARC in dystrophic *mdx* muscle

To test if elevated levels of the anti-apoptotic and hypoxia-protecting protein ARC might alleviate any dystrophic phenotypic features, we generated transgenic mice that overexpressed ARC. Endogenous ARC was expressed at high levels in skeletal muscle, but mainly in oxidative fibers. We explore whether overexpression of ARC in all fiber types might protect dystrophic myofibers from apoptotic and/or necrotic cell death. Transgenic ARC was expressed uniformly in all fiber types and colocalized with mitochondria in oxidative fibers. To examine muscle fiber breakdown, we analyzed Evans blue uptake and active caspase-3 expression in transgenic ARC/*mdx* and *mdx* muscle. We found Evans blue uptake and active caspase-3 positive fibers in transgenic ARC/*mdx* and *mdx* muscle fibers, the majority of which appeared to be at various stages of necrosis. We did not observe any clear protection of myofibers in the ARC transgenic mice from the dystrophic pathology. One explanation could

be that endogenous ARC is already functionally saturated in skeletal muscle, thus overexpression does not show an additional beneficiary effect.

However, the role of ARC in the apoptotic signaling cascade in skeletal muscle is not well understood. We detected reduced ARC expression in active caspase-3 positive fibers, which could be the cause, or the consequence, of fiber breakdown. Most cells contain a very complex, tightly regulated network of pro- and anti- apoptotic triggers, the balance of which can lead to continued cell life, or death. Altered expression of one apoptosis inhibitor or effector may be compensated by the upregulation of an antagonist to maintain a balance. The overexpression of ARC could have been counterbalanced by the up-regulation of a pro-apoptotic factor and therefore might have prevented the transgene from protecting muscle fiber breakdown. Alternatively, the overexpression of ARC could have effectively inhibited one apoptotic pathway, while muscle fiber breakdown in muscular dystrophy might occur through another, ARC-independent pathway. The elimination of one apoptotic stimuli could be superceded by other signals in favor of apoptosis or necrosis.

In summary, it remains unclear whether ARC over-expression failed to inhibit apoptosis in *mdx* muscles, or whether the apoptotic pathways regulated by ARC do not contribute to the dystrophic phenotype in *mdx* mice. The multiple functions of dystrophin and the DGC make it difficult to determine the extent that signaling failures contribute to muscle fiber death in *mdx* muscles. However, it was shown that altered signaling leads to impaired modulation of α-adrenergic vasoconstriction and functional ischemia in dystrophic muscle (Thomas et al., 1998). While over-expression of ARC in the heart has been shown to protect from myocardial ischemia, over-expression of ARC in *mdx* skeletal muscles clearly did not alter the dystrophic phenotype (Chatterjee et al., 2003; Gustafsson et al., 2002). This observation could be explained by the fact that the dystrophic pathology results from alterations in multiple molecular pathways that together contribute to muscle fiber death. While the restoration of one signaling pathway may not be sufficient to ameliorate dystrophic pathology, a combination of treatments targeting mechanical, immunological and signaling pathways might be more effective (Chen et al., 2000; DelloRusso et al., 2001; Disatnik et al., 2000; Grady et al., 1999; Lynch et al., 2001b; Spencer et al., 2001; Thomas et al., 1998).

5.1.3. Apoptotic and necrotic cell death in muscular dystrophy

Much progress has been made over the last decade in understanding the genetic and biochemical features of dystrophin and the DGC. However, little is known about the pathogenic mechanisms leading to the onset of muscular dystrophy and to progression of the disease. Several members of the DGC are associated with signaling molecules that provide a link to crucial signal transduction pathways (Durbeej et al., 2000; Grady et al., 1999; Hack et al., 1999; Hack et al., 1998; Yang et al., 1995a). Disruption of these signaling cascades could alter metabolic pathways leading to increased susceptibility to oxidative stress, elevated calcium levels, altered mitochondrial function and eventually to apoptotic or necrotic cell death (Chen et al., 2000; Disatnik et al., 1998, Tidball, 1995 #2012; Franco and Lansman, 1990; Kuznetsov et al., 1998; Matsuda et al., 1995; Podhorska-Okolow et al., 1998; Rando et al., 1998). Dystrophin-deficient *mdx* muscles demonstrate oxidative injury prior to muscle pathology, and muscle cells display an increased susceptibility to oxidative stress compared to normal muscles (Disatnik et al., 1998; Rando et al., 1998). Reduced NO-mediated cell protection and increased oxidative damage might therefore contribute significantly to the pathology of muscular dystrophy. However, it remains unclear to what extent abnormal DGC-mediated signaling and/or loss of mechanical stability are responsible for the onset and the progression of the disease.

Although it has been shown in previous studies that apoptosis plays a role in dystrophic pathology, it remains unclear if apoptosis causes or is a secondary effect of muscle fiber breakdown (Matsuda et al., 1995; Spencer et al., 1997). Recent studies suggest that cell death in *mdx* muscle may be initiated by apoptosis and followed by necrotic processes (Tidball et al., 1995). Tissue sections of dystrophic muscle demonstrate apoptotic myonuclei in degenerating muscle fibers (Matsuda et al., 1995; Sandri et al., 1998; Sandri et al., 1997; Tews and Goebel, 1997b). We detected active caspase-3 in dystrophic muscle, but the majority of the fibers appeared to be necrotic and had lost their membrane integrity, which would argue in favor of apoptosis being a secondary consequence resulting from loss of muscle fiber integrity. However, not all Evans blue positive fibers displayed clear staining for active caspase-3, and the intensity level and staining pattern within individual myofibers was variable, indicating that muscle fibers were at various stages of degeneration. These

observations reinforce the idea that muscle cell death is a dynamic process and may reflect the increased susceptibility of myofibers to secondary triggers resulting from altered cell signaling, leading to active cell death. Interestingly, while we were able to detect some relatively normal appearing Evans blue dye positive myofibers that did not express caspase-3, all caspase-3 positive fibers were at least weakly positive for Evans blue dye. These observations suggest a sequence of molecular events in dystrophic muscle in which an initial membrane damaging event allows the uptake of large extracellular molecules such as Evans blue dye, which is subsequently followed by upregulation of caspase-3 and loss of ARC expression. Although apoptosis and necrosis represent different mechanism of cell death, both may be intertwined. The ultimate fate of a cell may depend on the relative intensity of the secondary triggers and the energy status of the cell (Bonfoco et al., 1995; Eguchi et al., 1997; Higuchi et al., 1998).

5.1.4. Conclusions

The aforementioned studies were carried out to characterize the role of the anti-apoptotic protein ARC and to determine whether ARC could modulate dystrophic pathology. We were able to detect ARC expression in normal and dystrophic *mdx* muscle, and showed that ARC displays an abnormal intracellular localization pattern in dystrophic muscle. We further demonstrated that over-expression of ARC in *mdx* mice failed to alleviate the dystrophic process in skeletal muscle. However, the role of the apoptotic pathway regulated by ARC in skeletal muscle remains unclear, as does the contribution of this pathway to dystrophic pathology. A detailed biochemical analysis will be needed to get further insights into ARC signaling and whether ARC signaling is linked to or independent of DGC signaling.

It is further necessary to determine if ARC plays a role in long-term cell survival. ARC is expressed at high levels in skeletal muscle, heart, testis and brain – tissues that consist of cell types distinguished by a very low cell turnover rate. The mechanism responsible for the long half-life of these cells is unknown. ARC could play an important function in providing survival stimuli to these cells. Overexpression of ARC in old animals could

therefore be beneficial by maintaining cell number and function, a possibility that could be evaluated in further long-term studies.

5.2. Characterization of Igf-I in normal and dystrophic *mdx* muscle

The expression of Igf-I has been widely studied in various cell types and tissues (Lund, 1994; Stewart and Rotwein, 1996). Igf-I has been shown to play an important role in regulating tissue growth and differentiation (Florini et al., 1991; Stewart and Rotwein, 1996). The gene encoding Igf-I has been isolated and demonstrated to display high conservation among a variety of species (Rotwein et al., 1986; Shimatsu and Rotwein, 1987; Sussenbach, 1989). Igf-I gene expression is regulated by differential promotor usage and alternative RNA splicing, generating multiple tissue-specific isoforms with variable amino-terminal signal peptides and carboxy-terminal E-peptides (Adamo et al., 1993; LeRoith and Roberts, 1991; McKoy et al., 1999). Previous studies have extensively characterized Igf-I expression in skeletal muscle; however those studies were restricted to rat, human and rabbit Igf-I muscles.

5.2.1. Cloning of murine muscle-specific Igf-I isoforms

We cloned two muscle isoforms of Igf-I from a mouse muscle cDNA libary. Both isoforms were similar to the ones characterized previously in mouse liver. However, the liver Igf-I isoforms differed from the muscle Igf-I isoforms by the presence of a different leader peptide (Adamo et al., 1991; Lowe et al., 1987; Stewart and Rotwein, 1996). This leader peptide is not part of the mature Igf-I polypeptide, but might play an important role in the regulation of Igf-I targeting (Adamo et al., 1993). The levels of the liver Igf-I isoforms are growth hormone dependent. Liver Igf-I stimulates growth in various tissues, while extrahepatic Igf-I is not growth hormone dependant and exerts mainly autocrine and paracrine functions (D'Ercole et al., 1984; Daughaday and Rotwein, 1989; Lund, 1994; Sjogren et al., 1999). In addition to tissue specific Igf-I regulation, free Igf-I is regulated by a family of six Igf-I binding proteins that control distribution, function and activity of Igf-I in various tissues (Sara and Hall, 1990).

The two muscle specific Igf-I isoforms differ in their extension peptide, resulting from alternative mRNA splicing (Bell et al., 1986; Rotwein, 1986; Yang et al., 1996). The major

muscle Igf-I isoform (Ea) has been extensively studied *in vitro* and *in vivo* and acts either through the MAPK or PI3K/AKT pathways (Singleton and Feldman, 1999). Both pathways cannot be activated simultaneously; however, *in vitro* studies demonstrated that Igf-I-Ea induces a biphasic response. This response initially stimulates cell proliferation followed later by an enhancement of myogenic differentiation (Engert et al., 1996). In contrast, the nature and function of the second muscle Igf-I isoform (Eb), also called mechanical growth factor, is not well defined. Igf-I-Eb is expressed at very low levels in normal skeletal muscle, but is up-regulated in response to muscle stretch and overload (Yang et al., 1996). This isoform is therefore thought to play an important role in adapting skeletal muscles to physical challenges (Adams, 2002; Goldspink et al., 2002).

5.2.2. Expression of muscle-specific Igf-I isoforms in normal and dystrophic *mdx* muscle

Although it was previously thought that the Eb isoform was not expressed in dystrophic muscle (Yang et al., 1996), we were able to detect Igf-I-Eb transcripts at approximately equal amounts in normal and dystrophic *mdx* muscles in nine month old mice. At this age, we detected six to seven times more Igf-I mRNA transcripts of the major Igf-I isoform (Ea) than of Igf-I-Eb in normal as well as in *mdx* mice. Overall, these results suggest that there was no significant difference in Igf-I-Ea and Igf-I-Eb mRNA expression levels between normal and dystrophic *mdx* muscles at our tested age group. However, since Igf-I levels are influenced by nutritional status, exercise and other hormones, Igf-I mRNA levels varied significantly among animals (Landin-Wilhelmsen et al., 1994; Stewart and Rotwein, 1996). Therefore, more animals need to be tested in order to determine more precise expression levels.

We performed *in vitro* analysis on both Igf-I isoforms to test their potential in enhancing myogenic differentiation. For this study, we generated adenoviral vectors expressing Igf-I-Ea or Igf-I-Eb under the control of the CMV promoter and transduced L6 myoblasts. Significantly, both Igf-I-Ea and Igf-I-Eb enhanced L6 myoblast differentiation, suggesting that both isoforms were functional and acted through the Igf-I receptor. However, a previous study demonstrated different roles for Igf-I-Ea and Igf-I-Eb in mediating myoblast

differentiation and proliferation (Yang and Goldspink, 2002). That study suggested that Igf-I-Eb mediates myoblast proliferation via a different signaling pathway. Further studies are needed to determine if both isoforms function by signaling through similar or different pathways. Since we wanted to evaluate Igf-I overexpression in dystrophic muscle, this study was performed with the major and more extensively characterized isoform, Igf-I Ea.

5.3. Delivery of Igf-I and dystrophin to dystrophic *mdx* muscle

Several groups have characterized the beneficial effects of Igf-I on muscle morphology and function. In particular, in old and dystrophic *mdx* muscles, Igf-I has been shown to counter muscle decline and to increase muscle strength. In this study, we investigated the potential of Igf-I in conjunction with gene replacement therapy to ameliorate the pathology of muscular dystrophy. In order to study the effect of Igf-I and/or dystrophin expression on dystrophic *mdx* muscles, we generated recombinant AAV vectors carrying Igf-I (AAV-Igf-I) or micro-dystrophin (AAV-μdys) under the control of the mouse muscle creatine kinase (CK6) gene regulatory element. The Igf-I vector was delivered with and without the dystrophin vector to *mdx* TA muscles of nine month old mice.

5.3.1. Overexpression of Igf-I in dystrophic *mdx* muscle

We observed Igf-I mRNA expression in AAV-Igf-I treated, and in AAV-Igf-I & AAV-μdys co-treated, muscles four months post-injection. Values ranged from 50-100 fold over-expression in AAV-Igf-I treated muscles and up to 200-400 fold over-expression in AAV-Igf-I & AAV-μdys co-treated muscles, relative to the endogenous *mdx* Igf-I mRNA levels. Thus, injection of AAV-Igf-I alone resulted in a 4-fold decline of Igf-I mRNA levels, relative to the AAV-Igf-I & AAV-μdys co-treated muscles, in the four months following injection into dystrophic *mdx* muscles. This difference in Igf-I mRNA levels is most likely due to the fact

that dystrophin expression protects fibers from degeneration and consequently from the loss of vector genomes (Harper et al., 2002b).

TA muscles that were injected with AAV-Igf-I, or co-injected with AAV-Igf-I & AAV-μdys, showed a significant increase in muscle mass of 17% and 19%, relative to saline injected, and AAV-μdys injected, muscles. Functional analysis of AAV-Igf-I & AAV-μdys co-treated animals further revealed that the increase of 19% in muscle mass translated into an increase of 20% in force generating capacity, compared to *mdx* animals. Surprisingly, we did not observe a significant increase in muscle strength in *mdx* muscles treated with AAV-Igf-I alone. The 17% increase in muscle mass of AAV-Igf-I treated muscles translated only into a 9% increase in force generating capacity, relative to *mdx* muscles. Although AAV-Igf-I treated muscles demonstrated a trend towards higher force generating capacity, the increase was not statistically different from *mdx* animals. These result suggest that the presence of dystrophin might be beneficial in mediating the effects of Igf-I overexpression; however, more extensive studies are necessary to evaluate the effect of Igf-I alone on muscle force generating capacities. Taken together, Igf-I mediated hypertrophy and increased strength could lead to a major improvement in the functionality of dystrophic muscle, in particular when co-delivered with dystrophin. Since muscular dystrophy patients become wheel-chair dependent between the age of 8-11, a 20% increase in force may extend the period during which these patients are still able to walk.

AAV-Igf-I & AAV-μdys treated muscles demonstrated an increased protection from contraction-induced injury, as was also seen with muscles treated with AAV-μdys alone. After the first lengthening contraction, AAV-Igf-I & AAV-μdys co-treated muscles showed a 49% retention of force generating capacity, whereas *mdx* control muscles demonstrated a retention of only 24%. AAV-Igf-I only treatment, in contrast, resulted in a force retention of 35%, that was not statistically different from *mdx* control muscles. Since Igf-I does not restore dystrophin expression and the DGC in dystrophic muscles, it was expected that Igf-I overexpression would not protect from contractile damage when exceeding a given threshold. However, these values were higher than *mdx* values, which could be explained by the fact that Igf-I over-expression mediates muscle hypertrophy. Therefore, a lower percentage of muscle fibers may be required to generate equivalent force, resulting in potentially reduced muscle injury and fiber degeneration (Barton et al., 2002). After the second lengthening contraction,

AAV-Igf-I only treated muscles were highly susceptible to contraction-induced injury, with levels similar to those observed in *mdx* muscles. In contrast, muscles that were injected with AAV-μdys, and co-injected with AAV-Igf-I & AAV-μdys, retained force values at an increased level that was significantly different from *mdx* muscles.

Histological analysis demonstrated that all AAV-Igf-I injected muscles were protected from muscle degeneration. Cross-sectional measurements revealed a decrease in the number of fibers per unit area and the percentage of central nucleation in AAV-Igf-I treated muscles compared with *mdx* muscles.

Igf-I promotes cell survival and muscle regeneration and differentiation through the PI3K/Akt pathway (Singleton and Feldman, 1999). Although the role of apoptosis in skeletal muscle remains unclear, we and others have demonstrated the presence of apoptotic myonuclei and activated caspases in degenerating muscle fibers (Abmayr et al., 2004; Matsuda et al., 1995). In addition to promoting cell survival, Igf-I enhances muscle regeneration by activating satellite cells (Musaro et al., 2001). Since dystrophic muscles demonstrate a progressive loss of self-renewal potential with increasing age, an impaired repair mechanism together with extensive immune infiltration may vastly contribute to the muscle pathogenesis in muscular dystrophy. Thus, Igf-I mediated activation of cell survival pathways may protect muscle fibers from degeneration. In addition, Igf-I mediated efficient regeneration may further protect muscle fibers from being gradually replaced by fibrotic and adipose tissue.

Several studies showed activation of the PI3K/Akt pathway in skeletal muscles over-expressing Igf-I and demonstrated the expression of markers of muscle differentiation and survival (Barton et al., 2002; Musaro et al., 2001). However, little is known about the role of Igf-I in promoting cell proliferation, mediated through the MAPK pathway. The induction of cell proliferation may result in an increased number of satellite cells and may play a role in maintaining the regenerative potential of old skeletal muscle. The consequences of promoting cell proliferation have to be evaluated in terms of shifting the balance of cell death and cell division, potentially leading to uncontrolled cell division and cancer. Elevated Igf-I levels were shown to be associated with tumor formation in various tissue (Baserga et al., 2003; LeRoith and Roberts, 2003; Yakar et al., 2002). However, Igf-I expression can be restricted to muscle tissue, where transgenic mouse studies did not reveal any adverse effects (Barton-

Davis et al., 1998; Musaro et al., 2001).

5.3.2. Muscle specific Igf-I expression

To assure muscle specific Igf-I expression, we used a tissue-specific promoter in conjunction with AAV6 mediated delivery, since AAV6 shows a high tropism for skeletal muscle tissue. Igf-I expression was under the control of a truncated version of the mouse muscle creatine kinase promoter/enhancer regulatory element (CK6), which was shown to drive high expression of transgenes and to restrict expression to skeletal muscle (Hauser et al., 1995). In addition, AAV6 has been demonstrated to transduce muscle tissue with great efficiency (Scott et al., 2002). This delivery system displays persistent expression of the transgene for more than one year and is not known to elicit any major cellular immune responses. We have not yet determined the minimum dose needed for the effects we observed, but injection of 1 x 10^{10} vector genomes was sufficient for dystrophin expression. In addition, we achieved an up to 400-fold over-expression of Igf-I mRNA using similar amounts of vector. It is unknown how much Igf-I over-expression is needed to exert an effect on muscle morphology and function. It is reasonable to assume that smaller amounts would be sufficient, since Igf-I is a secreted hormone and targets expressing and surrounding non-expressing cells. Further studies are needed to determine the minimal dose, that would lead to an amelioration of the dystrophic phenotype. Since these studies show that Igf-I treatment is synergistic with the protective effects of dystrophin replacement, the combination of both treatments may allow the use of a lower total virus dose. This possibility is particularly important in terms of delivering dystrophin to large muscles with a potentially lower transduction efficiency.

Previous studies have also shown that muscle-restricted Igf-I overexpression does not increase Igf-I levels in the serum (Barton-Davis et al., 1998). This is an important observation, because elevated Igf-I levels in the blood could exert adverse effects on other tissues. The mechanisms by which Igf-I is prevented from accumulating in the circulation are unknown. However, Igf-I can target other cell types within muscle tissues, such as fibroblasts and adiposites. It was previously shown that fibroblasts are responsive to Igf-I treatment and

fibrotic tissue infiltrates were detected in heart tissue of transgenic Igf-I mice (Delaughter et al., 1999; Petley et al., 1999). This result is of particular concern in the dystrophic muscle, because dystrophic pathology is characterized by the gradual replacement of muscle fibers with fibrotic and adipose tissue. Igf-I treatment may thus synergistically increase that infiltration. Nevertheless, it was shown in transgenic Igf-I/*mdx* mice that Igf-I overexpression actually decreased fibrosis (Barton et al., 2002). This observation could be explained by the fact that Igf-I decreases muscle degeneration and efficiently mediates muscle repair in *mdx* animals, creating a healthy environment where no fibrotic tissue replacement is necessary.

5.3.3. Delivery of dystrophin to dystrophic *mdx* muscle

AAV-mediated delivery of dystrophin to *mdx* muscles demonstrated persistent expression of dystrophin four months post-injection. Dystrophin expression was distributed over the entire cross sectional area and reached an average of 40% of the total area. It was reported previously that dystrophin expression of >20% of wild-type dystrophin levels is sufficient to prevent muscular dystrophy in transgenic *mdx* mice (Cox et al., 1993a; Phelps et al., 1995). In our study, we treated animals after the onset of the disease in order to test whether the dystrophic pathology could be reversed in adult *mdx* mice. We used a micro-dystrophin construct, which lacks 68% of the coding region of dystrophin and could therefore be cloned into an AAV vector backbone. Remarkably, truncated versions of dystrophin proved to be highly functional in transgenic *mdx* mouse models (Crawford et al., 2000; Harper et al., 2002b; Rafael et al., 1996). Transgenic *mdx* muscles over-expressing micro-dystrophin (ΔR4-R24) displayed normal muscle morphology and were protected from contraction-induced injury, however those muscles displayed muscle strength intermediate between *mdx* and wild-type muscles (Harper et al., 2002b).

In this study we showed that AAV-μdys and AAV-μdys & AAV-Igf-I (ΔR4-R24/ΔCT) treated muscles were protected from contraction-induced injury, demonstrating a significant recovery of force generating capacity of 47% and 49% after one, and 10% and 13% after two lengthening contractions. In contrast, *mdx* muscles recovered only up to 24%,

and 2% of their force after equivalent contractions. In addition, AAV-Igf-I & AAV-μdys co-treatment resulted in an increase of muscle mass and force generating capacities, which was not observed in AAV-μdys only treatment.

Our histological analysis demonstrated that AAV-μdys treatment protected muscle fibers from muscle degeneration. Those muscles displayed a significant trend towards less fibers per area and less centrally nucleated fibers. Central nucleation was reduced by about 20% as was the number of fibers per area in AAV-μdys treated and AAV-Igf-I & AAV-μdys co-treated muscles, compared with sham-injected *mdx* muscles. It was reported previously that AAV-mediated dystrophin expression has a more dramatic effect on muscle morphology (Harper et al., 2002b). Central nucleation was reduced by about 80% in AAV-μdys treated *mdx* muscles in comparison to sham-injected *mdx* muscles. However, it is difficult to compare the two studies, since the test animals were injected at different ages, one month in the previous study *versus* nine months in this study. One month old animals are at the beginning of the peak phase of degeneration and regeneration, which is accompanied and followed by extensive myonecrosis and immune infiltration. In contrast, nine month old *mdx* animals are beyond the peak degeneration phase and have reached a steady state of much slower myofiber turnover, showing a constant number of centrally nucleated myofibers and fewer necrotic fibers. Consequently, dystrophin treatment of one month old animals not only reverses the existing dystrophic pathology, but also prevents further muscle fiber degeneration and may also counter satellite cell exhaustion. In addition, the previous study examined muscle morphology five months post injection in contrast to a four months time point in our study, which may also account for differences in morphological features. In summary, both studies suggest that dystrophin treatment reverses histopathological features of the disease, but the extent of the effect is age dependent.

We were also able to demonstrate that dystrophin expression decreases muscle degeneration by comparing Igf-I mRNA expression levels in AAV-Igf-I treated muscles with AAV μdys & Igf-I co-treated animals, four months post injection. AAV-Igf-I treated animals demonstrated a 50-100 fold overexpression of Igf-I mRNA, in contrast to a 200-400 fold overexpression of Igf-I mRNA in AAV-μdys & AAV-Igf-I co-treated animals. The 4-5 fold higher Igf-I mRNA levels in AAV μdys & AAV-Igf-I co-treated animals relative to AAV-Igf-I treated animals clearly demonstrated that dystrophin expression protects muscle fibers from

dystrophic pathology and the associated loss of vector from necrotic fibers.

5.3.4. Gene replacement in conjunction with Igf-I treatment

In this study, we investigated a combination of gene therapy treatments for muscular dystrophy. In addition to correcting the primary defect, we delivered Igf-I to enhance muscle repair and promote cell survival. This combination is important in regards to targeting cells that did not receive, or could not be rescued by, dystrophin treatment. It still remains a challenging goal to deliver dystrophin to all the muscle cells in an animal and, depending on the size of the animal, only a subset of fibers may receive gene transfer. Igf-I is a secreted polypeptide that targets not only the expressing, but also the surrounding cells, enabling a broader treatment. Igf-I co-treatment may also be of advantage in terms of reversing muscle damage. Gene replacement therapy and reassembly of the DGC complex may rescue remaining muscle fibers from breakdown, however it does not seem likely that previous damage will be extensively reversed. In contrast, Igf-I enhances the regenerative potential of satellite cells and promotes cell survival, which may help to rescue the remaining muscle fibers and replace damaged fibers more efficiently.

Functional measurements demonstrated that AAV-μdys injected animals were partially protected from contraction-induced injury after two lengthening contractions, whereas animals injected with AAV-Igf-I alone were as susceptible as *mdx* animals to muscle damage. AAV-Igf-I treated animals, in contrast, showed an increase in muscle mass, which was not seen after AAV-μdys only treatment. Also, co-injection of AAV-Igf-I and AAV-μdys resulted in increased muscle mass and muscle strength, and in protection from contraction-induced injury.

Histological analysis of AAV-μdys, AAV-Igf-I as well as AAV-Igf-I and AAV-μdys co-treated animals revealed a protection from muscle degeneration. All the treatments demonstrated a decrease of fiber number per area and a reduction of central nucleation. However, average values varied significantly between animals and the different treatments. Thus, it needs to be evaluated in future studies if the co-treatment has an additive protective

effect on muscle morphology. Unfortunately, there do not exist reliable methods to directly visualize Igf-I expression *in vivo*, since this protein has a short half-life and is expressed at low levels. Since we were not able to determine Igf-I expressing fibers directly, we were limited to analyzing random fields, containing expressing and/or non-expressing fibers. Consequently, our analysis included both Igf-I transduced and non-transduced myofibers. Variations in the extend of transduction from one muscle to another could therefore explain the large variance we observed between the different treated muscles. Although it remains to be determined how exactly each treatment influences muscle morphology, our studies suggest that all treatments protect from muscle degeneration. Further experiments, using more animals per group, are in progress to evaluate morphological differences between AAV-Igf-I, AAV-μdys and AAV-Igf-I & AAV-μdys co-treated animals.

Taken together, AAV-Igf-I treated, as well as AAV-μdys treated, animals showed an amelioration of the dystrophic phenotype. AAV-Igf-I treatment resulted in increased muscle mass, while AAV-μdys treatment resulted in increased resistency to muscle damage. AAV-Igf-I and AAV-μdys co-treatment clearly demonstrated that the combination of both acted synergistically and was beneficial for the animal.

5.3.5. Conclusions

The studies in this chapter evaluated the relative and combined potential of gene therapy treatments for muscular dystrophy that replace dystrophin and also target signaling and regenerative dysfunction. We were able to demonstrate that the beneficial effect of Igf-I is synergistic with the protective effect of dystrophin in restoring muscle strength and function in adult *mdx* mice. Furthermore, we were able to show that each treatment protected from muscle degeneration. More extensive studies are necessary to evaluate the benefits of AAV-Igf-I and AAV-μdys co-treatment on muscle morphology. Additional delivery studies of Igf-I and dystrophin to various age groups of *mdx* mice will provide important insights into their relative and combined potential in ameliorating the dystrophic phenotype at different stages of the disease. In particular, old *mdx* mice display morphological changes more similar to the

human disease, such as significant weakness and extensive infiltration of fibrotic and adipose tissue. Studies on old *mdx* mice could therefore be valuable to determine if Igf-I and dystrophin co-delivery act synergistically in reversing dystrophic pathology at a more advanced stage of the disease such as seen in human patients.

6. EXPERIMENTAL PROCEDURES

6.1. Material & Methods for chapter 4.1 and 4.2

6.1.1. Isolation of ARC cDNA

The full-length human ARC cDNA sequence was used to screen the expressed-sequence tag (EST) database of GenBank to find related sequences from mice. A 480 bp EST clone was identified. PCR primers, 5'-CCTTGCCATCAGAGACCATTG and 5'-CTGAACTGGG TGCTTCTGGC based on this EST sequence, together with vector primers (Lumeng et al., 1999), were used to amplify the 5'- and 3'- ends of ARC directly from a mouse muscle cDNA library (Lumeng et al., 1999). The 5'- and 3'- ends of ARC were sequenced and cloned by recombinant PCR with the primers 5'-GAGTGGGACTATCCGAACGC and 5'-CACAAATAGGATTGGACAGCTAAGG to generate a full-length mouse ARC cDNA.

6.1.2. Chromosomal Localization

A 144 bp intron located between bp 475/476 of the mouse cDNA sequence was amplified from genomic C57BL/6J and *M.spretus* DNA with the primers 5'-CCTTGCCATCAGAGACCATTG and 5'-CACAAATAGGATTGGACAGCTAAGG. Direct sequence comparison of the PCR products revealed that bp 88 was different between the C57BL/6J and *M.spretus* strain, which creates an ApoI restriction fragment length polymorphism. The intron was PCR amplified from the Jackson Laboratory interspecific backcross panel (C57BL/6JEi x SPRET/Ei)F1 x SPRET/Ei, called TJL BSS, followed by an ApoI digestion, which identified different haplotypes (Rowe et al., 1994). The backcross haplotype data were analyzed by staff at the Jackson Laboratory. Raw data were obtained from http://www.jax.org/resources/documents/cmdata.

6.1.3. RNA analysis

Full-length mouse ARC cDNA was labeled with radioactive α[^{32} P]-dCTP by random priming using a commercial kit (Rediprime kit, Amersham) and hybridized to a mouse multiple tissue northern blot (Clonetech) according to the manufacturer's instructions.

6.1.4. Generation of ARC transgenic mice

The human ARC cDNA tagged at the C-terminus with a FLAG epitope (DYKDDDDK) (Koseki et al., 1998) was cloned into the NotI restriction site of pBSX (Crawford et al., 2000), which is a modified pBluescript vector (Stratagene) that contains the human α-skeletal actin promoter, a splice acceptor from the SV40 VP1 intron and tandem SV40 polyadenylation signals (Crawford et al., 2000). The human ARC expression construct was injected into SJL/J F_2 x SJL/J F_2 embryos, and positive F_0 mice were identified by PCR screening using an ARC cDNA specific 5'-GTGCATCCAATGCCTCGTACTC and a VP1 intron specific 5'-CCGTTAAGGTTCGTAGGTCATGGAC primer for the expression construct. Two positive F_0 mice were backcrossed onto the C57Bl/10J and *mdx* background. Further studies used primarily the line with the most uniform expression levels. For all studies, transgene negative/*mdx* and transgene negative/C57BL/10J littermates were used as controls.

6.1.5. Immunohistochemistry

Quadriceps and diaphragm muscle were frozen in liquid nitrogen cooled O.C.T. embedding medium (Tissue-Tek) and stored at -80^0C until use. Frozen sections were cut to a 5 μm thickness and mounted on silane-coated slides. For histochemical analysis, sections were fixed in methanol and stained with Gills #3 hematoxylin and eosin-phloxine (Fisher Scientific).

For immunostaining, sections were blocked with 1% gelatin in KPBS (20 mM K_2HPO_4, 4 mM $KHPO_4$, 160 mM NaCl) then incubated for 2 hours with the primary antibody diluted in KPBS with 0.2% gelatin and 1% donkey or goat serum. The following antibodies were

used: anti-FLAG 1:500 (Sigma), anti-ARC 1:200 (Cayman), TRITC labeled anti-cytochrome oxidase subunit V 1:500 (Molecular Probes), and anti-caspase-3 1:500 (Pharmingen). After several washes the sections were stained with a FITC- conjugated goat anti-rabbit (Alexa 488, Molecular Probes) secondary antibody for another hour, washed and mounted with Vectashield mounting media (Vector). Sections were visualized with a Nikon E1000 microscope connected to a Spot-2 CCD camera.

6.1.6. Protein analysis

Quadriceps and diaphragm muscles were frozen in liquid nitrogen and stored at -80^0C until use. Samples were homogenized (OMNI 5000) in lysis buffer (120 mM NaCl, 1mM EGTA, 1 mM EDTA, 1 mM $MgCl_2$, 1 mM Na_3V0_3, 10 mM $Na_4P_20_7$, 10 mM NaF, 1% Triton, 10% glycerol, 50 mM Tris HCl pH 8.0) plus protease inhibitor cocktail (Roche). The total amount of protein was determined using the Coomassie Plus Protein Assay Reagent (Pierce). Proteins were separated on a 15% polyacrylamide gel and immunoblotted with anti-FLAG 1/5000 (Sigma) and anti-ARC 1/2000 (Cayman) antibodies.

6.1.7. Evans blue Assay

Evans blue dye (10 mg/ml in PBS) was injected into the tail vein of six week old *mdx,* transgenic/*mdx* and C57BL/10J mice (50 µl/10 g body weight). After three hours, mice were euthanized and quadriceps muscles were frozen in liquid nitrogen cooled O.C.T. embedding media. Frozen, 5 µm thick sections were analyzed for Evans Blue uptake by fluorescence microscopy (Straub et al., 1997).

6.2. Material & Methods for chapter 4.3

6.2.1. Isolation of two Igf-I cDNAs

The 5'- and 3'-ends of the Igf-I cDNA were amplified from a mouse muscle cDNA library (Lumeng et al., 1999), using the primers 5'-GCTTCCGGAGCTGTGATCT and 5'-CTTGGGCATGTCAGTGTGG based on the published muscle Igf-I exon 3 sequence, together with vector primers (Lumeng et al., 1999). The resulting PCR products, containing the 5'- and 3'- ends of Igf-I were sequenced and the full-length mouse Igf-I cDNA was cloned by recombinant PCR (Higuchi, 1990) using primers 5'-GCGGCCGCATTGCTCTAACATCTCC and 5'-GCGGCCGCAATGTTTACTTGTAT ATTTC based on sequence data from the 5'- and 3'-amplification products. Two alternative Igf-I splice products were isolated and cloned directly into the pGEM-T vector (Promega) for sequence analysis.

6.2.2. Cloning of recombinant adenoviral (Ad) vectors

To generate Ad-Igf-I vectors, the Igf-I cDNA was cloned into the EcoRI/BamHI site of the shuttle vector pD2007 (Kirk et al., 2001), containing the cytomegalovirus (CMV) promoter and the human growth hormone polyadenylation (hGHpA) site. This shuttle vector pD2007 was created by modification of an adenoviral backbone plasmid in order to obtain the leftmost 4.8 kb and rightmost 0.7 kb of the Ad 5 genome, as well as an ampicillin resistence gene located between the inverted terminal repeats (ITR) (Hartigan-O'Connor et al., 2002). The resultant plasmid, containing the CMV Igf-I hGHpA expression cassette, was linearized and subsequently co-transformed into recombination competent E. coli BJ5183 cells with an adenoviral backbone plasmid, deleted for the adenovirus E1, E3 and the polymerase genes (Albayya and Metzger, 2003). The recombination occurred between pD2007 and the leftmost 4.8 kb and rightmost 0.7 kb of the adenoviral backbone and resulted in a complete E1, E3 and replication-deficient (E2b) adenoviral vector, containing the CMV Igf-I hGHpA expression cassette (Ad-Igf-I). Recombinants were selected for ampicillin resistance, and recombination confirmed by restriction endonuclease analyses. Prior to transfection, viral plasmids were linearized

with FseI to remove the ampicillin resistence gene between the ITRs and to facilitate transfection.

6.2.3. Production and purification of recombinant Ad vector stocks

C7 cells are modified human embryonic kidney packaging (HEK293) cells, containing expression cassettes for the adenoviral proteins E1, DNA polymerase and pre-terminal protein (Amalfitano and Chamberlain, 1997). The cells were cultured on 60-mm plates in Dulbecco's modified Eagles medium (DMEM) (Gibco/BRL), supplemented with 10% fetal bovine serum (FBS) and 5 U/ml penicillin and 5 U/ml streptomycin. At 70-90% confluency, cells were transfected with 9 μg of *Fse*I-digested viral plasmid by using the calcium phosphate-DNA precipitation method (Maniatis manual). In order to increase the transfection efficiency, the cells were subjected to a 100 mM chloroquine treatment for 4.5 hours and a 40 sec osmotic shock with 15% glycerol. When complete cytopathic effect (CPE) appeared, usually after 10-15 days, the cells and medium were harvested together and frozen in liquid nitrogen. After three rounds of freeze–thaw cycles, cell lysates containing infectious virus particles were used in subsequent passages for virus amplification. Fresh 150 mm dishes of C7 cells were infected with 2 ml cell lysate and harvested when cells displayed complete CPE, which typically occurred 2 days after infection. The lysate was serially passaged twice to yield a total of 20-30 dishes. After the second round of amplification, 0.5% NP-40 was added to the plates to dissolve all cell membranes. Cell lysates were then harvested and frozen in a dry ice-ethanol bath. Cell membranes were further disrupted by three rounds of freeze/thawing and subsequently purified according to the method of Gerard and Meidell (Glover and Hames, 1995).

The virus-containing cell lysate was centrifuged at 12,000 x g for 10 min at 4°C to remove cellular debris. The supernatant was then transferred and virus particles were precipitated by adding 0.33% PEG/NaCl solution and incubating for 1 hour on ice, followed by a centrifugation at 12,000 x g for 20 minutes at 4°C. The viral pellet was then resuspended in 3-4 ml 20 mM Tris-HCl pH 8.0, 1 mM $MgCl_2$ and treated with 50 μg/ml each of DNaseI and RNaseA (Sigma) for 30 minutes at 37ºC to remove any genomic cellular or unpackaged viral nucleic acids that were co-precipitated with the virus particles. The virus was further diluted in CsCl to a final density of 1.1 g/ml and

additional residual debris was pelleted by centrifugation at 8000 x g for 5 min at 4°C. The virus was then purified on a CsCl step gradient, containing 33% 1.4 g/ml CsCl, 33% 1.3 g/ml CsCl and 33% of the 1.1 g/ml CsCl solution with the virus particles. The gradients were centrifuged at 53,000 x *g* for 4-16 h at 4° C in a Beckman SW-28 rotor. The viral band was pulled from the gradient using a 18-gauge needle. Virus particles were then dialysed against 20 mM HEPES pH 7.4 buffer, containing 5% sucrose and 150 mM NaCl. Viral titers were determined by incubating 5 µl of virus solution in virion lysis buffer (10 mM Tris pH 7.5, 0.1% SDS, 1 mM EDTA) at 56°C for 10 min and subsequent quantitation by A_{260} spectrophotometry. Particle number per ml is equivalent to [(A_{260} x 21)/0.909] x 10^{12} P/ml (Hartigan-O'Connor et al., 2002).

6.2.4. RNA analysis

RNA isolation from cells

Cells were washed in ice-cold PBS, then transferred in ice-cold PBS to a 1.5 ml tube and pelleted at 1,000 rpm for five min. PBS was aspirated off and cells were stored at –70°C until use. Total RNA was extracted by using the RNeasy kit, according to the manufacturer's instructions (Qiagen).

RNA isolation from tissue

Tibialis anterior muscles were frozen in liquid nitrogen and stored at –80°C until use. Samples were homogenized (OMNI 5000) in lysis buffer (RNeasy, Qiagen) and then treated with proteinase K (20 mg/ml) for 10 minutes at 55°C to remove connective tissue and collagen. Residual debris was pelleted by centrifugation at 10,000 x g at room temperature and the clear supernatant was loaded on a RNA purification column and further extracted according to the manufacturer's instructions (RNeasy, Qiagen). Before washing and eluting the RNA from the columns, an on-column DNase digestion was performed to ensure complete removal of genomic and residual vector DNA (Qiagen). 500 µg total RNA of each sample was electrophoresed to confirm RNA integrity.

Reverse transcription

One µg total RNA of each sample was reverse transcribed into cDNA. Total RNA was incubated with 5 µM oligo (dT) (Invitrogen), 0.5 mM dNTPs (Promega) at 65°C for 5 minutes before adding 5 x RT buffer (Invitrogen), 5 mM DTT and 20 U RNase inhibitor (Promega). Samples were incubated at 42°C for 2 minutes, then supplemented with 200 U reverse transcriptase Superscript II (Invitrogen) and further incubated at 42°C for another 50 minutes. The enzyme was then inactivated at 70°C for 15 minutes and samples were stored at -20°C until use. The cDNA was amplified in a standard PCR reaction, using primers specific for endogenous or transgenic Igf-I (Maichele and Chamberlain, 1992). The primers used are listed in table 1.

Table 1. Primers used in regular PCR

Igf-I forward exon 3	5'-GCTTCCGGAGCTGTGATCT
hGHpA reverse	5'-AGAATCGCTTGAACCCAGG
CMV forward exon 1	5'-GGGAACGGTGCATTGGAAC
Igf-I reverse exon 3	5'-CTTGGGCATG TCAGTGTGG
Igf-I reverse exon 5	5'-GCTTCGTTTTCTTGTTTGTCG

Quantitative PCR

Igf-I mRNA transcripts were quantified by real-time PCR. Primers and fluorescence-labeled probes were chosen with the assistance of the Primer Express program (Perkin-Elmer Applied Biosystems) and are listed in table 2 under section 6.3.5. The reaction was performed in a 25 µl volume containing 0.4 µM of each primer, 0.2 µM probe, cDNA template and 2x master mix (Perkin-Elmer Applied Biosystems). cDNA templates were diluted 1:10, 1:100 and 1:1000 and each reaction was run in duplicate for Igf-I and GAPDH primer sets (Perkin-Elmer Applied Biosystems), respectively. GAPDH primer and probe were used in order to standardize the amount of cDNA added to each reaction. All samples were amplified and the fluorescence of the reporter dyes was recorded during every cycle using the Applied Biosystems 7700 sequence detection system. Results of the real-time PCR data were represented as Ct values. Ct was defined as the threshold cycle at which amplified product was first recorded as statistically significant above background, which occurred during the exponential phase of amplification (Gibson et al., 1996). Expression levels of Igf-I transcripts of injected muscles were determined relative

to uninjected muscles with the comparative method by using the arithmetric formula: $2^{-\Delta\Delta CT}$. ΔCt was the difference in the Ct values derived from Igf-I amplification and GAPDH amplification of the same sample. $\Delta\Delta$Ct represented the difference between samples derived from injected and uninjected muscles, as calculated by the formula $\Delta\Delta$Ct = ΔCt of Igf-I (injected muscle) - ΔCt of Igf-I (uninjected muscle) (Bustin, 2000; Freeman et al., 1999). Alternatively, $\Delta\Delta$Ct represented the difference between total Igf-I levels (Igf-I Ea and Eb) and Igf-I Eb levels only.

6.2.5. *In vitro* differentiation assay

The L6 myogenic cell line was generously provided by Dr. Steve Hauschka (University of Washington). L6 cells were grown and maintained as myoblasts by culturing in proliferation medium, containing DMEM supplemented with 10% FBS, 5 U/ml penicillin and 5 U/ml streptomycin, and differentiated at 80% confluency in serum-free DMEM supplemented with just antibiotics. Sixteen hours after the cells were transferred to differentiation conditions, experimental plates were infected with Ad-Igf-I purified virus at 1 x 10^4 particles per cell or Ad-Igf-I viral lysates at 1 ml per 4 ml medium. Eight hours after viral infection and 24 hours after changing to differentiation conditions, all plates were fed with fresh differentiation medium supplemented with 500 μg/ml BSA as described by Florini and Ewton (Florini and Ewton, 1990). In addition, control plates were supplemented with 25 ng/ml recombinant Igf-I (Biodesign). After 6 days without any medium change, cells were washed and fixed with AFAFIX (60% EtOH, 3% formaldehyde, 4% glacial acetic acid).

6.2.6. Immunohistochemistry

For sarcomeric myosin immunostaining, cells were fixed with AFAFIX for 2 minutes at room temperature. Then, cells were washed twice with TBS and blocked for 15 min in 2% (m/v) nonfat milk powder and 1% horse serum in TBS. After three washes, cells were stained with the monoclonal antibody MF-20 (kindly provided by Dr. Steve Hauschka) at

1:100 in TBS with 1% horse serum for 1 hour at 37ºC or alternatively overnight at 4ºC. The cells were then washed and stained with a horse anti-mouse biotinylated IgG (H+L) antibody (Vector) at 1:1000 in TBS with 1% horse serum for 30 minutes at room temperature and subsequently with HRP-conjugated streptavidine (Zymed) at 1:1000 in TBS. Finally, H_2O_2 activated (0.83 ml/ml) DAB solution (0.6 mg/ml) (Sigma) was added for 30 minutes at room temperature. Then, the plates were rinsed with water and air-dried.

6.3. Material & Methods for chapter 4.4

6.3.1. Cloning of recombinant adeno-associated viral (AAV) vectors

The Igf-I cDNAs were cloned into the EcoRI and HindIII digested pMCS-CMV plasmid (Stratagene). This step resulted in a construct that carried the Igf-I cDNA under the control of the CMV promoter and a polyadenylation site derived from bovine growth hormone (bGHpA). The CMV promoter of that resulting plasmid was removed with the restriction enzymes MluI and SacII and replaced by the muscle-specific CK6 promoter (Hauser et al., 1995). The complete expression cassette was then excised with NotI and moved into NotI digested pAAV-LacZ vector backbone (Stratagene). The final construct, pAAV-Igf-I, consists of the complete Igf-I expression cassette flanked by vector-encoded AAV2-inverted terminal repeats (ITRs), which are required for viral DNA replication.

6.3.2. Production and purification of recombinant AAV vector stocks

AAV is a naturally replication-deficient virus that requires co-infection with an unrelated helper virus, such as adenovirus, to generate AAV virions. In our system, the required helper virus genes were provided *in trans* from the helper plasmid, pADG6 (gift from Dr. David Russell) containing the adenovirus E2A, E4 and VA RNAs genes. These genes are necessary for the induction of the lytic phase of AAV. In addition, the HEK293 cell line stably expressed the adenovirus E1A and E1B genes, which are essential for packaging AAV virions (Graham and Smiley, 1977). The helper plasmid pADG6 also contains the AAV *cap* and *rep* genes that encode capsid proteins for AAV serotype 6 and DNA

replication proteins, which are required to synthesize AAV infectious virions. HEK293 cells were cultured on 100 mm plates in DMEM, supplemented with 10% FBS and antibiotics. At 60-70% confluency, cells from 50-100 plates were co-transfected with 20 μg helper plasmid pADG6 and 10 μg recombinant AAV vector by using the calcium phosphate-DNA precipitation method (Maniatis manual). 24 hours after transfection, the medium was exchanged for serum-free DMEM plus antibiotics and the plates were incubated at 37°C for an additional 48 hours. Transfected cells and medium were then harvested together and pooled from all 50-100 plates.

The harvested pool was then passed through a microfluidizer (Microfluidics, model M110S) to disrupt cell membranes and subsequently filtered through a 0.2 μM filter to generate a clear cell lysate. Virus particles were purified over a 5 ml HiTrap Heparin column (Amersham) using an AKTApurifier 10 high pressure liquid chromatography (HPLC) machine (Amersham). The virus was eluted with a linear salt gradient ranging from 200-400 mM NaCl. Fractions containing the purified virus were pooled and and dialysed against Ringer's solution (137 mM NaCl, 2.7 mM KCL (monobasic), 1.4 mM $CaCl_2$, 0.5 mM $MgCl_2$, 0.7 mM Na_2HPO_4 (dibasic), 4.8 mM $NaHCO_3$). The virus was then aliquoted and stored at -70°C.

6.3.3. Determination of virus genome titer by slot blot analysis

The virus titer was determined by comparing vector genomes from viral aliquots to vector genomes from plasmids of known concentration. These standards were prepared by serial dilution of the expression cassette generated by NotI restriction digest of pAAV-Igf-I and by MscI restriction digest of pAAV-dys. Virions were also prepared as serial dilution and then subjected to a DNase I (Sigma) digestion for 30 minutes at 37°C to remove residual unpackaged plasmid DNA prior to denaturation. Standards and virus samples were then diluted in denaturing buffer (0.5 M NaOH, 12.5 mM EDTA), boiled for 10 minutes in a water bath and then cooled on ice for another ten minutes. Samples were further diluted to 500 μl in 0.4 M NaOH and transferred to a nylon membrane by vaccum using a slot blot apparatus (Amersham). The membrane was hybridized with a transgene-specific probe that had been denatured and labeled with an alkaline phosphatase direct labeling kit (Amersham). Hybridized bands were visualized using a chemoluminescence imager

(GeneGnome, Syngene Bio Imaging) and quantified with GeneTools software (Syngene Bio Imaging).

6.3.4. Intramuscular injection into *the tibialis anterior*

Nine months-old *mdx* male mice were anesthetized with a combination of Ketamine and Xylazine (animal weight/100 = #ml anesthetic) and shaved to better access the *tibialis anterior* muscle. The *tibialis anterior* muscle was further exposed by opening the skin with a small parallel incision to the muscle. Viral DNA in 30 µl Ringer's salt solution was then carefully injected into the muscle by using a 32-gauge needle attached to a Hamilton syringe. The needle was introduced at the tip of the muscle and pushed straight to the other end of the muscle, then slowly drawn back over a 20-30 second interval whereby the viral solution was injected. After injection, the skin was carefully stretched over the enlarged muscle and glued (Nexaband). Controls for all experiments consisted of sham injections with Ringer's solution. Four months after injection the virus injected and control animals were anesthetized to measure functional properties of the *tibialis anterior* muscle as described in section 6.3.6. Tissue was collected as described in section 6.3.5 and section 6.3.7.

6.3.5. RNA/DNA analysis

RNA and DNA isolation from tissue

Tibialis anterior muscles were frozen in liquid nitrogen and stored at -80^0C until use. Total RNA was isolated and transcribed into cDNA as described in section 6.2.4. DNA was isolated from an aliquot that was taken after tissue lysis and proteinase K treatment and prior to RNA purification over the RNeasy columns (Qiagen). DNA was extracted with a standard phenol/chloroform extraction protocol (Maniatis manual) and residual RNA was removed by RNase A treatment (50 µg/ml).

Quantitative PCR

Igf-I mRNA transcripts and vector genomes were quantified by real-time PCR, using the Applied Biosystems 7700 sequence detection system. The primers and fluorescence labeled probes used are listed in table 2. cDNA templates were prepared and analyzed as described in section 6.2.4. DNA samples were diluted to a final concentration of 100 ng, 10 ng and 1 ng and each reaction was run in duplicate by using DNA specific Igf-I primers. DNA vector persistence was determined by relative quantitation of samples of unknown concentration to a DNA standards curve. DNA standards were prepared by serial dilutions of the Igf-I expression cassette generated by NotI restriction digest of pAAV-Igf-I plasmid DNA. 5 ng/μl standard DNA was diluted 1:10, 1:100, 1:1000, 1:10000 and each reaction was run in duplicate as well.

Table 2. Primers used in quantitative PCR

Igf-I forward exon 3	5'-CAGTTCGTGTGTGGACCGAG
Igf-I reverse exon 4	5'-GCCTGTCTGAGGTGCCCTC
Igf-I probe exon 4	5'-FAM-CCCACAGGCTATGGCTCCAGCATTC-TAMRA
CMV forward exon 1	5'-GGGAACGGTGCATTGGAAC
Igf-I reverse exon 1	5'-CACACAGACCAGCACGTTGC
CMV probe exon 1	5'-FAM-CGGATTCCCCGTGCCAAGAGTGA-TAMRA
CMV intron reverse	5'-GTGGGCCTATAGACTCTATAGGCG
Igf-I reverse exon 5	5'-GCTTCGTTTTCTTGTTTGTCG

6.3.6. Functional properties

Four months post-injection, treated and control mice were anesthetized and the TA muscles were subjected to an *in situ* lengthening contraction protocol as described (DelloRusso et al., 2001). In brief, the optimal muscle length (Lo) and the maximum isometric force were determined for each muscle sample. Muscles were then maximally stimulated and stretched from Lo through 40% of muscle fiber length (Lf) during two lengthening contractions (LC1 and LC2). Maximum isometric force was measured after each lengthening contraction and reported as a percentage of initial maximum isometric force. The forces produced after LC1 and LC2 were indicative of the ability of muscles to resist injury. Muscles were then dissected, weighed, and either frozen in liquid nitrogen

cooled OCT embedding medium for histological analysis, or directly in liquid nitrogen for RNA analysis.

6.3.7. Immunohistochemistry

Tibialis anterior muscles were frozen in liquid nitrogen cooled O.C.T. embedding medium (Tissue-Tek) and stored at -80^0C until use. 5 µm cryosections were cut and mounted on silane-coated slides. For immunohistostaining of dystrophin, sections were blocked with 2% gelatin, 100 µg/ml BSA, 1% Tween 20 in KPBS, then incubated for 1 hour with the N-terminal dystrophin antibody 1/600 (Rafael et al., 1996) diluted in KPBS with 0.2% gelatin and 2% goat serum. After several washes the sections were treated with biotin blocking agent (Molecular probes), before they were stained with 1) the secondary biotinylated antibody 2) streptavidin and 3) DAB according to the manufacturer's instruction (Vector ABC kit). The sections were then fixed in Methanol and counterstained in a 0.5% Neutral Red solution for 10 minutes. Sections were mounted with Paramount mounting media and visualized with a Nikon E1000 microscope connected to a Spot-2 CCD camera.

6.3.8. Image analysis and quantitative measurements

Montage images were photographed by using MONTAGE EXPLORER software (Syncroscopy). IMAGEPRO software (Media Cybernetics) was then used to quantitate the dystrophin-positive area of muscle cross sections as well as to quantify histological features of muscle samples. Total dystrophin-positive area was analyzed by applying the same brightness and contrast thresholds in IMAGEPRO to every sample to exclude background and to calculate the area surrounded by dystrophin immunofluoresence. Total dystrophin-positive area was then normalized to the total area analyzed. For histological analysis, montages of all samples were overlayed with a mask that randomly chose four 400 µm^2 microscopic fields per muscle cross section. These fields were used to determine the percentage of centrally located myofibers as well as the number of muscle fibers per

defined area. Statistical analysis was performed by using STATVIEW software (SAS Institute).

7. LITERATURE

Abmayr, S., R.W. Crawford, and J.S. Chamberlain. 2004. Characterization of ARC, apoptosis repressor interacting with CARD, in normal and dystrophin-deficient skeletal muscle. *Hum Mol Genet*. 13:213-21.

Acsadi, G., G. Dickson, D.R. Love, A. Jani, F.S. Walsh, A. Gurusinghe, J.A. Wolff, and K.E. Davies. 1991. Human dystrophin expression in mdx mice after intramuscular injection of DNA constructs. *Nature*. 352:815-818.

Adamo, M.L., H. Ben-Hur, D. LeRoith, and C.T. Roberts, Jr. 1991. Transcription initiation in the two leader exons of the rat IGF-I gene occurs from disperse versus localized sites. *Biochem Biophys Res Commun*. 176:887-93.

Adamo, M.L., S. Neuenschwander, D. LeRoith, and C.T. Roberts, Jr. 1993. Structure, expression, and regulation of the IGF-I gene. *Adv Exp Med Biol*. 343:1-11.

Adams, G.R. 2002. Autocrine and/or paracrine insulin-like growth factor-I activity in skeletal muscle. *Clin Orthop*:S188-96.

Adams, M.E., N. Kramarcy, S.P. Krall, S.G. Rossi, R.L. Rotundo, R. Sealock, and S.C. Froehner. 2000. Absence of alpha-syntrophin leads to structurally aberrant neuromuscular synapses deficient in utrophin. *J Cell Biol*. 150:1385-98.

Adams, M.E., H.A. Mueller, and S.C. Froehner. 2001. In vivo requirement of the alpha-syntrophin PDZ domain for the sarcolemmal localization of nNOS and aquaporin-4. *J Cell Biol*. 155:113-22.

Ahn, A.H., C.A. Freener, E. Gussoni, M. Yoshida, E. Ozawa, and L.M. Kunkel. 1996. The three human syntrophin genes are expressed in diverse tissues, have distinct chromosomal locations, and each bind to dystrophin and its relatives. *J.Biol.Chem*. 271:2724-2730.

Ahn, A.H., and L.M. Kunkel. 1993. The structural and functional diversity of dystrophin. *Nature Genet*. 3:283-291.

Aihara, H., and J.-i. Miyazaki. 1998. Gene transfer into muscle by electroporation in vivo. *Nature Biotechnology*. Vol. 16 (9):p867.

Albayya, F.P., and J.M. Metzger. 2003. Adenoviral vectors: production and purification. *Methods Mol Biol*. 219:3-17.

Amalfitano, A., C.R. Begy, and J.S. Chamberlain. 1996. Improved adenovirus packaging cell lines to support the growth of replication-defective gene-delivery vectors. *Proc Natl Acad Sci U S A*. 93:3352-3356.

Amalfitano, A., and J.S. Chamberlain. 1997. Isolation and characterization of packaging cell lines that co-express the adenovirus E1, DNA polymerase, and preterminal proteins: implications for gene therapy. *Gene Therapy*. 4:258-263.

Amalfitano, A., J.A. Rafael, and J.S. Chamberlain. 1997. Structure and mutation of the dystrophin gene. *In* Dystrophin: Gene, Protein and Cell Biology. J.A. Lucy and S.C. Brown, editors. Cambridge University Press, Cambridge. 1-26.

Anderson, J.T., R.P. Rogers, and H.W. Jarrett. 1996. Ca^{2+}-calmodulin binds to the carboxyl-terminal domain of dystrophin. *J.Biol.Chem*. 271:6605-6610.

Arahata, K., and A.G. Engel. 1988. Monoclonal antibody analysis of mononuclear cells in myopathies. IV: Cell-mediated cytotoxicity and muscle fiber necrosis. *Ann Neurol*. 23:168-73.

Araishi, K., T. Sasaoka, M. Imamura, S. Noguchi, H. Hama, E. Wakabayashi, M. Yoshida, T. Hori, and E. Ozawa. 1999. Loss of the sarcoglycan complex and sarcospan leads to muscular dystrophy in beta-sarcoglycan-deficient mice. *Human Molecular Genetics*. 8:1589-1598.

Barjot, C., D. Hartigan-O'Connor, G. Salvatori, J.M. Scott, and J.S. Chamberlain. 2002. Gutted adenoviral vector growth using E1/E2b/E3-deleted helper viruses. *J Gene Med*. 4:480-9.

Barton, E.R., L. Morris, A. Musaro, N. Rosenthal, and H.L. Sweeney. 2002. Muscle-specific expression of insulin-like growth factor I counters muscle decline in mdx mice. *J Cell Biol*. 157:137-48.

Barton-Davis, E.R., D.I. Shoturma, A. Musaro, N. Rosenthal, and H.L. Sweeney. 1998. Viral mediated expression of insulin-like growth factor I blocks the aging-related loss of skeletal muscle function. *Proc Natl Acad Sci U S A*. 95:15603-7.

Baserga, R., F. Peruzzi, and K. Reiss. 2003. The IGF-1 receptor in cancer biology. *Int J Cancer*. 107:873-7.

Baumbach, L.L., J.S. Chamberlain, P.A. Ward, N.J. Farwell, and C.T. Caskey. 1989. Molecular and clinical correlations of deletions leading to Duchenne and Becker muscular dystrophies. *Neurology*. 39:465-474.

Bell, G.I., M.M. Stempien, N.M. Fong, and L.B. Rall. 1986. Sequences of liver cDNAs encoding two different mouse insulin-like growth factor I precursors. *Nucleic Acids Res*. 14:7873-82.

Bertoni, C., and T.A. Rando. 2002. Dystrophin Gene Repair in mdx Muscle Precursor Cells In Vitro and In Vivo Mediated by RNA-DNA Chimeric Oligonucleotides. *Hum Gene Ther*. 13:707-18.

Bischoff, R. 1975. Regeneration of single skeletal muscle fibers in vitro. *Anat Rec*. 182:215-35.

Blake, D.J., R. Nawrotzki, M.F. Peters, S.C. Froehner, and K.E. Davies. 1996. Isoform diversity of dystrobrevin, the murine 87-kDa postsynaptic protein. *Journal of Biological Chemistry*. 271:7802-10.

Bogdanovich, S., T.O. Krag, E.R. Barton, L.D. Morris, L.A. Whittemore, R.S. Ahima, and T.S. Khurana. 2002. Functional improvement of dystrophic muscle by myostatin blockade. *Nature*. 420:418-21.

Bonfoco, E., D. Krainc, M. Ankarcrona, P. Nicotera, and S.A. Lipton. 1995. Apoptosis and necrosis: two distinct events induced, respectively, by mild and intense insults with N-methyl-D-aspartate or nitric oxide/superoxide in cortical cell cultures. *Proc Natl Acad Sci U S A*. 92:7162-6.

Bonifati, M.D., G. Ruzza, P. Bonometto, A. Berardinelli, K. Gorni, S. Orcesi, G. Lanzi, and C. Angelini. 2000. A multicenter, double-blind, randomized trial of deflazacort versus prednisone in Duchenne muscular dystrophy. *Muscle Nerve*. 23:1344-7.

Bönnemann, C.G., R. Modi, S. Noguchi, Y. Mizuno, M. Yoshida, E. Gussoni, E.M. McNally, D.J. Duggan, C. Angelini, E.P. Hoffman, E. Ozawa, and L.M. Kunkel. 1995. -Sarcoglycan (A3b) mutations cause autosomal recessive muscular dystrophy with loss of the sarcoglycan complex. *Nature Genet*. 11:266-273.

Bork, P., and M. Sudol. 1994. The WW domain: A signalling site in dystrophin? *Trends Biochem.Sci*. 19:531-533.

Bouri, K., W.G. Feero, M.M. Myerburg, T.J. Wickham, I. Kovesdi, E.P. Hoffman, and P.R. Clemens. 1999. Polylysine modification of adenoviral fiber protein enhances muscle cell transduction. *Hum Gene Ther*. 10:1633-40.

Braun, U., K. Paju, M. Eimre, E. Seppet, E. Orlova, L. Kadaja, S. Trumbeckaite, F.N. Gellerich, S. Zierz, H. Jockusch, and E.K. Seppet. 2001. Lack of dystrophin is associated with altered integration of the mitochondria and ATPases in slow-twitch muscle cells of MDX mice. *Biochim Biophys Acta*. 1505:258-70.

Brenman, J.E., D.S. Chao, S.H. Gee, A.W. McGee, S.E. Craven, D.R. Santillano, Z. Wu, F. Huang, H. Xia, M.F. Peters, S.C. Froehner, and D.S. Bredt. 1996. Interaction of nitric oxide synthase with the postsynaptic density protein PSD-95 and alpha1-syntrophin mediated by PDZ domains. *Cell*. 84:757-67.

Brenman, J.E., D.S. Chao, H.H. Xia, K. Aldape, and D.S. Bredt. 1995. Nitric oxide synthase complexed with dystrophin and absent from skeletal muscle sarcolemma in Duchenne muscular dystrophy. *Cell*. 82:743-752.

Bresolin, N., E. Castelli, G.P. Comi, G. Felisari, A. Bardoni, D. Perani, F. Grassi, A. Turconi, F. Mazzucchelli, and D. Gallotti. 1994. Cognitive impairment in Duchenne muscular dystrophy. *Neuromuscul.Disord*. 4:359-369.

Brooks, S.V. 1998. Rapid recovery following contraction-induced injury to in situ skeletal muscles in mdx mice. *Journal of Muscle Research and Cell Motility*. 19:179-87.

Brooks, S.V., and J.A. Faulkner. 1988. Contractile properties of skeletal muscles from young, adult and aged mice. *Journal of Physiology (London)*. 404:71-82.

Burkin, D.J., G.Q. Wallace, K.J. Nicol, D.J. Kaufman, and S.J. Kaufman. 2001. Enhanced expression of the alpha 7 beta 1 integrin reduces muscular dystrophy and restores viability in dystrophic mice. *J Cell Biol*. 152:1207-18.

Bustin, S.A. 2000. Absolute quantification of mRNA using real-time reverse transcription polymerase chain reaction assays. *J Mol Endocrinol*. 25:169-93.

Byers, T.J., H.G.W. Lidov, and L.M. Kunkel. 1993. An alternative dystrophin transcript specific to peripheral nerve. *Nature Genet*. 4:77-81.

Campbell, K.P. 1995. Three muscular dystrophies: loss of cytoskeleton-extracellular matrix linkage. *Cell*. 80:675-679.

Carpenter, S., and G. Karpati. 1979. Duchenne muscular dystrophy: plasma membrane loss initiates muscle cell necrosis unless it is repaired. *Brain*. 102:147-61.

Chamberlain, J.S. 2002. Gene therapy of muscular dystrophy. *Hum Mol Genet*. 11:2355-62.

Chamberlain, J.S., J.R. Chamberlain, R.G. Fenwick, P.A. Ward, C.T. Caskey, L.S. Dimnick, N.T. Bech-Hansen, D.I. Hoar, and et.al. 1992. Diagnosis of Duchenne and Becker muscular dystrophies by polymerase chain reaction: A multicenter study. *JAMA*. 267:2609-2615.

Chamberlain, J.S., R.A. Gibbs, J.E. Ranier, P.N. Nguyen, and C.T. Caskey. 1988a. Deletion screening of the Duchenne muscular dystrophy locus via multiplex DNA amplification. *Nucleic Acids Res*. 16:11141-11156.

Chamberlain, J.S., J.A. Pearlman, D.M. Muzny, R.A. Gibbs, J.E. Ranier, A.A. Reeves, and C.T. Caskey. 1988b. Expression of the murine Duchenne muscular dystrophy gene in muscle and brain. *Science*. 239:1416-1418.

Chao, D.S., F. Silvagno, and D.S. Bredt. 1998. Muscular dystrophy in mdx mice despite lack of neuronal nitric oxide synthase. *Journal of Neurochemistry*. 71:784-9.

Chao, H., Y. Liu, J. Rabinowitz, C. Li, R.J. Samulski, and C.E. Walsh. 2000. Several Log Increase in Therapeutic Transgene Delivery by Distinct Adeno-Associated Viral Serotype Vectors. *Mol Ther*. 2:619-623.

Chapman, V.M., D.M. Miller, D. Armstrong, and C.T. Caskey. 1989. Recovery of induced mutations for X chromosome-linked muscular dystrophy in mice. *Proc Natl Acad Sci U S A*. 86:1292-1296.

Chatterjee, S., L.T. Bish, V. Jayasankar, A.S. Stewart, Y.J. Woo, M.T. Crow, T.J. Gardner, and H.L. Sweeney. 2003. Blocking the development of postischemic cardiomyopathy with viral gene transfer of the apoptosis repressor with caspase recruitment domain. *J Thorac Cardiovasc Surg*. 125:1461-9.

Chen, H.H., L.M. Mack, R. Kelly, M. Ontell, S. Kochanek, and P.R. Clemens. 1997. Persistence in muscle of an adenoviral vector that lacks all viral genes. *Proc Natl Acad Sci U S A*. 94:1645-1650.

Chen, Y., P. Zhao, R. Borup, and E. Hoffman. 2000. Expression profiling in the muscular dystrophies: Identification of novel aspects of molecular pathophysiology. *Journal of Cell Biology*.151:1321-1336.

Cho, W.K., S. Ebihara, J. Nalbantoglu, R. Gilbert, B. Massie, P. Holland, G. Karpati, and B.J. Petrof. 2000. Modulation of Starling forces and muscle fiber maturity permits adenovirus-mediated gene transfer to adult dystrophic (mdx) mice by the intravascular route. *Human Gene Therapy*. 11:701-14.

Cohn, R.D., M.D. Henry, D.E. Michele, R. Barresi, F. Saito, S.A. Moore, J.D. Flanagan, M.W. Skwarchuk, M.E. Robbins, J.R. Mendell, R.A. Williamson, and K.P. Campbell. 2002. Disruption of DAG1 in differentiated skeletal muscle reveals a role for dystroglycan in muscle regeneration. *Cell*. 110:639-48.

Cordier, L., G. Guang-Ping, A. Hack, E.M. McNally, J.M. Wilson, N. Chirmule, and H.L. Sweeney. 2001. Muscle-specific promoters may be neccesary for adeno-associated virus-mediated gene transfer in the treatment of muscular dystrophies. *Human Gene Therapy*. 12:205-215.

Corrado, K., P.L. Mills, and J.S. Chamberlain. 1994. Deletion analysis of the dystrophin-actin binding domain. *FEBS Lett*. 344:255-260.

Corrado, K., J.A. Rafael, P.L. Mills, N.M. Cole, J.A. Faulkner, K. Wang, and J.S. Chamberlain. 1996. Transgenic *mdx* mice expressing dystrophin with a deletion in the actin-binding domain display a "mild Becker" phenotype. *Journal of Cell Biology*. 134:873-884.

Côté, P., H. Moukhles, M. Lindenbaum, and S. Carbonetto. 1999. Chimeric mice deficient in dystroglycans develop muscular dystrophy and have disrupted myoneural synapses. *Nature Genetics*.

Cox, G.A., N.M. Cole, K. Matsumura, S.F. Phelps, S.D. Hauschka, K.P. Campbell, J.A. Faulkner, and J.S. Chamberlain. 1993a. Overexpression of dystrophin in transgenic mdx mice eliminates dystrophic symptoms without toxicity [see comments]. *Nature*. 364:725-9.

Cox, G.A., S.F. Phelps, V.M. Chapman, and J.S. Chamberlain. 1993b. New *mdx* mutation disrupts expression of muscle and nonmuscle isoforms of dystrophin. *Nature Genet*. 4:87-93.

Cox, G.A., Y. Sunada, K.P. Campbell, and J.S. Chamberlain. 1994. Dp71 can restore the dystrophin-associated glycoprotein complex in muscle but fails to prevent dystrophy [see comments]. *Nat Genet*. 8:333-9.

Crawford, G.E., J.A. Faulkner, R.H. Crosbie, K.P. Campbell, S.C. Froehner, and J.S. Chamberlain. 2000. Assembly of the dystrophin-associated protein complex does not require the dystrophin COOH-terminal domain. *Journal of Cell Biology*. 150:1399-410.

Crawford, G.E., Q.L. Lu, T.A. Partridge, and J.S. Chamberlain. 2001. Suppression of revertant fibers in mdx mice by expression of a functional dystrophin. *Hum Mol Genet*. 10:2745-50.

Crosbie, R.H., R. Barresi, and K.P. Campbell. 2002a. Loss of sarcolemma nNOS in sarcoglycan-deficient muscle. *Faseb J*. 16:1786-91.

Crosbie, R.H., S.A. Dovico, J.D. Flanagan, J.S. Chamberlain, C.L. Ownby, and K.P. Campbell. 2002b. Characterization of aquaporin-4 in muscle and muscular dystrophy. *Faseb J*. 16:943-9.

Crosbie, R.H., L.E. Lim, S.A. Moore, M. Hirano, A.P. Hays, S.W. Maybaum, H. Collin, S.A. Dovico, C.A. Stolle, M. Fardeau, F.M. Tome, and K.P. Campbell. 2000. Molecular and genetic characterization of sarcospan: insights into sarcoglycan-sarcospan interactions. *Hum Mol Genet*. 9:2019-2027.

Crosbie, R.H., V. Straub, H.Y. Yun, J.C. Lee, J.A. Rafael, J.S. Chamberlain, V.L. Dawson, T.M. Dawson, and K.P. Campbell. 1998a. mdx muscle pathology is independent of nNOS perturbation. *Hum Mol Genet*. 7:823-9.

Crosbie, R.H., H. Yamada, D.P. Venzke, M.P. Lisanti, and K.P. Campbell. 1998b. Caveolin-3 is not an integral component of the dystrophin glycoprotein complex. *FEBS Letters*. 427:279-82.

D'Ercole, A.J., A.D. Stiles, and L.E. Underwood. 1984. Tissue concentrations of somatomedin C: further evidence for multiple sites of synthesis and paracrine or autocrine mechanisms of action. *Proc Natl Acad Sci U S A*. 81:935-9.

D'Souza, V.N., N.T. Man, G.E. Morris, W. Karges, D.-A.M. Pillers, and P.N. Ray. 1995. A novel dystrophin isoform is required for normal retinal electrophysiology. *Human Molecular Genetics*. 4:837-842.

Daughaday, W.H., and P. Rotwein. 1989. Insulin-like growth factors I and II. Peptide, messenger ribonucleic acid and gene structures, serum, and tissue concentrations. *Endocr Rev*. 10:68-91.

Deconinck, N., T. Ragot, G. Maréchal, M. Perricaudet, and J.M. Gillis. 1996. Functional protection of dystrophic mouse (*mdx*) muscles after adenovirus-mediated transfer of a dystrophin minigene. *Proc.Natl.Acad.Sci.USA*. 93:3570-3574.

Delaughter, M.C., G.E. Taffet, M.L. Fiorotto, M.L. Entman, and R.J. Schwartz. 1999. Local insulin-like growth factor I expression induces physiologic, then pathologic, cardiac hypertrophy in transgenic mice. *Faseb J*. 13:1923-9.

DelloRusso, C., R. Crawford, J. Chamberlain, and S. Brooks. 2001. Tibialis anterior muscles of *mdx* mice are highly susceptible to contraction-induced injury. *Journal of Muscle Research and Cell Motility*. 22:467-475.

DelloRusso, C., J. Scott, D. Hartigan-O'Connor, G. Salvatori, C. Barjot, A.S. Robinson, R.W. Crawford, S.V. Brooks, and J.S. Chamberlain. 2002. Functional correction of adult

mdx mouse muscle using gutted adenoviral vectors expressing full-length dystrophin. *Proc Natl Acad Sci U S A*. 99:12979-12984.

Deveraux, Q.L., N. Roy, H.R. Stennicke, T. Van Arsdale, Q. Zhou, S.M. Srinivasula, E.S. Alnemri, G.S. Salvesen, and J.C. Reed. 1998. IAPs block apoptotic events induced by caspase-8 and cytochrome c by direct inhibition of distinct caspases. *Embo J*. 17:2215-23.

Deyst, K.A., M.A. Bowe, J.D. Leszyk, and J.R. Fallon. 1995. The □-dystroglycan-□-dystroglycan complex - Membrane organization and relationship to an agrin receptor. *J.Biol.Chem*. 270:25956-25959.

Disatnik, M.H., J.S. Chamberlain, and T.A. Rando. 2000. Dystrophin mutations predict cellular susceptibility to oxidative stress. *Muscle Nerve*. 23:784-92.

Disatnik, M.H., J. Dhawan, Y. Yu, M.F. Beal, M.M. Whirl, A.A. Franco, and T.A. Rando. 1998. Evidence of oxidative stress in mdx mouse muscle: studies of the pre-necrotic state. *Journal of the Neurological Sciences*. 161:77-84.

Dominov, J.A., C.A. Houlihan-Kawamoto, C.J. Swap, and J.B. Miller. 2001. Pro- and anti-apoptotic members of the Bcl-2 family in skeletal muscle: a distinct role for Bcl-2 in later stages of myogenesis. *Dev Dyn*. 220:18-26.

Douglas, J.T., B.E. Rogers, M.E. Rosenfeld, S.I. Michael, M. Feng, and D.T. Curiel. 1996. Targeted gene delivery by tropism-modified adenoviral vectors. *Nature Biotechnology*. 14:1574-8.

Duclos, F., V. Straub, S.A. Moore, D.P. Venzke, R.F. Hrstka, R.H. Crosbie, M. Durbeej, C.S. Lebakken, A.J. Ettinger, J. van der Meulen, K.H. Holt, L.E. Lim, J.R. Sanes, B.L. Davidson, J.A. Faulkner, R. Williamson, and K.P. Campbell. 1998. Progressive muscular dystrophy in alpha-sarcoglycan-deficient mice. *J Cell Biol*. 142:1461-71.

Dunckley, M.G., D.J. Wells, F.S. Walsh, and G. Dickson. 1993. Direct retroviral-mediated transfer of a dystrophin minigene into mdx mouse muscle in vivo. *Hum Mol Genet*. 2:717-23.

Durbeej, M., R.D. Cohn, R.F. Hrstka, S.A. Moore, V. Allamand, B.L. Davidson, R.A. Williamson, and K.P. Campbell. 2000. Disruption of the beta-sarcoglycan gene reveals pathogenetic complexity of limb-girdle muscular dystrophy type 2E. *Mol Cell*. 5:141-51.

Ebihara, S., G.H. Guibinga, R. Gilbert, J. Nalbantoglu, B. Massie, G. Karpati, and B.J. Petrof. 2000. Differential effects of dystrophin and utrophin gene transfer in immunocompetent muscular dystrophy (mdx) mice. *Physiol Genomics*. 3:133-44.

Eguchi, Y., S. Shimizu, and Y. Tsujimoto. 1997. Intracellular ATP levels determine cell death fate by apoptosis or necrosis. *Cancer Res*. 57:1835-40.

Ekhterae, D., Z. Lin, M.S. Lundberg, M.T. Crow, F.C. Brosius, 3rd, and G. Nunez. 1999. ARC inhibits cytochrome c release from mitochondria and protects against hypoxia-induced apoptosis in heart-derived H9c2 cells. *Circ Res*. 85:e70-7.

Emery, A.E.H. 1993. Duchenne Muscular Dystrophy. Oxford Medical Publications, Oxford.

Engert, J.C., E.B. Berglund, and N. Rosenthal. 1996. Proliferation precedes differentiation in IGF-I-stimulated myogenesis. *J Cell Biol*. 135:431-40.

England, S.B., L.V. Nicholson, M.A. Johnson, S.M. Forrest, D.R. Love, E.E. Zubrzycka-Gaarn, D.E. Bulman, J.B. Harris, and K.E. Davies. 1990. Very mild muscular dystrophy associated with the deletion of 46% of dystrophin. *Nature*. 343:180-182.

Ervasti, J.M., and K.P. Campbell. 1993. A role for the dystrophin-glycoprotein complex as a transmembrane linker between laminin and actin. *J.Cell Biol.* 122:809-823.

Ervasti, J.M., K. Ohlendieck, S.D. Kahl, M.G. Gaver, and K.P. Campbell. 1990. Deficiency of a glycoprotein component of the dystrophin complex in dystrophic muscle. *Nature*. 345:315-319.

Ewton, D.Z., and J.R. Florini. 1981. Effects of the somatomedins and insulin on myoblast differentiation in vitro. *Dev Biol.* 86:31-9.

Ferrari, G., G. Cusella-De Angelis, M. Coletta, E. Paolucci, A. Stornaiuolo, G. Cossu, and F. Mavilio. 1998. Muscle regeneration by bone marrow-derived myogenic progenitors [see comments] [published erratum appears in Science 1998 Aug 14;281(5379):923]. *Science*. 279:1528-30.

Fisher, K.J., K. Jooss, J. Alston, Y. Yang, S.E. Haecker, K. High, R. Pathak, S.E. Raper, and J.M. Wilson. 1997. Recombinant adeno-associated virus for muscle directed gene therapy. *Nat Med.* 3:306-12.

Florini, J.R., and D.Z. Ewton. 1990. Highly specific inhibition of IGF-I-stimulated differentiation by an antisense oligodeoxyribonucleotide to myogenin mRNA. No effects on other actions of IGF-T. *J Biol Chem.* 265:13435-7.

Florini, J.R., D.Z. Ewton, and K.A. Magri. 1991. Hormones, growth factors, and myogenic differentiation. *Annu Rev Physiol.* 53:201-16.

Florini, J.R., and K.A. Magri. 1989. Effects of growth factors on myogenic differentiation. *Am J Physiol.* 256:C701-11.

Francke, U., H.D. Ochs, B. de Martinville, J. Giacalone, V. Lindgren, C. Disteche, R.A. Pagon, M.H. Hofker, G.J. van Ommen, P.L. Pearson, and et al. 1985. Minor Xp21 chromosome deletion in a male associated with expression of Duchenne muscular dystrophy, chronic granulomatous disease, retinitis pigmentosa, and McLeod syndrome. *Am J Hum Genet.* 37:250-67.

Franco, A., Jr., and J.B. Lansman. 1990. Calcium entry through stretch-inactivated ion channels in mdx myotubes. *Nature*. 344:670-673.

Freeman, W.M., S.J. Walker, and K.E. Vrana. 1999. Quantitative RT-PCR: pitfalls and potential. *Biotechniques*. 26:112-22, 124-5.

Gee, S.H., R. Madhavan, S.R. Levinson, J.H. Caldwell, R. Sealock, and S.C. Froehner. 1998. Interaction of muscle and brain sodium channels with multiple members of the syntrophin family of dystrophin-associated proteins. *J.Neurosci.* 18:128-137.

Geertman, R., A. McMahon, and E.L. Sabban. 1996. Cloning and characterization of cDNAs for novel proteins with glutamic acid-proline dipeptide tandem repeats. *Biochim Biophys Acta*. 1306:147-52.

Gibson, U.E., C.A. Heid, and P.M. Williams. 1996. A novel method for real time quantitative RT-PCR. *Genome Res.* 6:995-1001.

Gilbert, R., J. Nalbantoglu, J.M. Howell, L. Davies, S. Fletcher, A. Amalfitano, B.J. Petrof, A. Kamen, B. Massie, and G. Karpati. 2001. Dystrophin expression in muscle following gene transfer with a fully deleted ("gutted") adenovirus is markedly improved by trans-acting adenoviral gene products. *Hum Gene Ther.* 12:1741-55.

Gilbert, R., J. Nalbantoglu, B.J. Petrof, S. Ebihara, G.H. Guibinga, J.M. Tinsley, A. Kamen, B. Massie, K.E. Davies, and G. Karpati. 1999. Adenovirus-mediated utrophin gene transfer mitigates the dystrophic phenotype of mdx mouse muscles. *Human Gene Therapy.* 10:1299-310.

Glover, D.M., and B.D. Hames. 1995. DNA cloning : a practical approach. IRL, Oxford.
Goldspink, G., P. Williams, and H. Simpson. 2002. Gene expression in response to muscle stretch. *Clin Orthop*:S146-52.
Grady, R.M., R.W. Grange, K.S. Lau, M.M. Maimone, M.C. Nichol, J.T. Stull, and J.R. Sanes. 1999. Role for alpha-dystrobrevin in the pathogenesis of dystrophin-dependent muscular dystrophies. *Nat Cell Biol*. 1:215-20.
Grady, R.M., H. Zhou, J.M. Cunningham, M.D. Henry, K.P. Campbell, and J.R. Sanes. 2000. Maturation and maintenance of the neuromuscular synapse: Genetic evidence for roles of the dystrophin-glycoprotein complex. *Neuron*. 25:279-293.
Graham, F.L., and L. Prevec. 1991. Manipulation of Adenovirus Vectors. *In* Methods in Molecular Biology, Vol. 7: Gene Transfer and Expression Protocols. E.J. Murray, editor. The Humana Press Inc., Clifton, NJ. 109-128.
Greelish, J.P., L.T. Su, E.B. Lankford, J.M. Burkman, H. Chen, S.K. Konig, I.M. Mercier, P.R. Desjardins, M.A. Mitchell, X.G. Zheng, J. Leferovich, G.P. Gao, R.J. Balice-Gordon, J.M. Wilson, and H.H. Stedman. 1999. Stable restoration of the sarcoglycan complex in dystrophic muscle perfused with histamine and a recombinant adeno-associated viral vector. *Nat Med*. 5:439-43.
Greenberg, D.S., Y. Sunada, K.P. Campbell, D. Yaffe, and U. Nudel. 1994. Exogenous Dp71 restores the levels of dystrophin associated proteins but does not alleviate muscle damage in *mdx* mice. *Nature Genet*. 8:340-344.
Gregorevic, P., D.R. Plant, K.S. Leeding, L.A. Bach, and G.S. Lynch. 2002. Improved contractile function of the mdx dystrophic mouse diaphragm muscle after insulin-like growth factor-I administration. *Am J Pathol*. 161:2263-72.
Gussoni, E., Y. Soneoka, C.D. Strickland, E.A. Buzney, M.K. Khan, A.F. Flint, L.M. Kunkel, and R.C. Mulligan. 1999. Dystrophin expression in the mdx mouse restored by stem cell transplantation. *Nature*. 401:390-4.
Gustafsson, A.B., M.R. Sayen, S.D. Williams, M.T. Crow, and R.A. Gottlieb. 2002. TAT protein transduction into isolated perfused hearts: TAT-apoptosis repressor with caspase recruitment domain is cardioprotective. *Circulation*. 106:735-9.
Hack, A.A., L. Cordier, D.I. Shoturma, M.Y. Lam, H.L. Sweeney, and E.M. McNally. 1999. Muscle degeneration without mechanical injury in sarcoglycan deficiency. *Proc Natl Acad Sci U S A*. 96:10723-8.
Hack, A.A., M.E. Groh, and E.M. McNally. 2000. Sarcoglycans in muscular dystrophy. *Microsc Res Tech*. 48:167-80.
Hack, A.A., C.T. Ly, F. Jiang, C.J. Clendenin, K.S. Sigrist, R.L. Wollmann, and E.M. McNally. 1998. Gamma-sarcoglycan deficiency leads to muscle membrane defects and apoptosis independent of dystrophin. *J.Cell Biol*. 142:1279-87.
Hagiwara, Y., T. Sasaoka, K. Araishi, M. Imamura, H. Yorifuji, I. Nonaka, E. Ozawa, and T. Kikuchi. 2000. Caveolin-3 deficiency causes muscle degeneration in mice. *Hum Mol Genet*. 9:3047-54.
Harper, S.Q., R.W. Crawford, C. DelloRusso, and J.S. Chamberlain. 2002a. Spectrin-like repeats from dystrophin and alpha-actinin-2 are not functionally interchangeable. *Hum Mol Genet*. 11:1807-15.
Harper, S.Q., M.A. Hauser, C. DelloRusso, D. Duan, R.W. Crawford, S.F. Phelps, H.A. Harper, A.S. Robinson, J.F. Engelhardt, S.V. Brooks, and J.S. Chamberlain. 2002b.

Modular flexibility of dystrophin: Implications for gene therapy of Duchenne muscular dystrophy. *Nature Medicine*. 8:253-61.

Hartigan-O'Connor, D., C. Barjot, G. Salvatori, and J.S. Chamberlain. 2002. Generation and growth of gutted adenoviral vectors. *Methods in Enzymology*. 346:224-46.

Hartigan-O'Connor, D., C.J. Kirk, R. Crawford, J.J. Mule, and J.S. Chamberlain. 2001. Immune evasion by muscle-specific gene expression in dystrophic muscle. *Molecular Therapy*. 4:525-33.

Hasegawa, M., A. Cuenda, M.G. Spillantini, G.M. Thomas, V. Buee-Scherrer, P. Cohen, and M. Goedert. 1999. Stress-activated protein kinase-3 interacts with the PDZ domain of alpha 1-syntrophin - A mechanism for specific substrate recognition. *J.Biol.Chem.* 274:12626-12631.

Hauser, M.A., D.L. Gregory, M.A. Shields, S. Apone, A.M. Saulino, S.D. Hauschka, and J.S. Chamberlain. 1995. Development of muscle-specific expression cassettes for recombinant adenoviral vectors. *Am.J.Hum.Genet*. 57(S).

Henry, M.D., and K.P. Campbell. 1996. An extracellular matrix receptor linked to the cytoskeleton. *Curr.Opin.Cell Biol*. 8:625-631.

Higuchi, M., T. Honda, R.J. Proske, and E.T. Yeh. 1998. Regulation of reactive oxygen species-induced apoptosis and necrosis by caspase 3-like proteases. *Oncogene*. 17:2753-60.

Higuchi, R. 1990. Recombinant PCR. *In* PCR Protocols- A Guide to Methods and Applications. M.A. Innis, D.H. Gelfand, J.J. Sninsky, and T.J. White, editors. Academic Press, Inc, San Diego. 177-183.

Hildinger, M., A. Auricchio, G. Gao, L. Wang, N. Chirmule, and J.M. Wilson. 2001. Hybrid vectors based on adeno-associated virus serotypes 2 and 5 for muscle-directed gene transfer. *J Virol*. 75:6199-203.

Hoffman, E.P., R.H. Brown, Jr., and L.M. Kunkel. 1987. Dystrophin: the protein product of the Duchenne muscular dystrophy locus. *Cell*. 51:919-928.

Hoffman, E.P., K.H. Fischbeck, R.H. Brown, M. Johnson, R. Medori, J.D. Loike, J.B. Harris, R. Waterston, M. Brooke, L. Specht, J.S. Chamberlain, C.T. Caskey, F. Shapiro, and L.M. Kunkel. 1988. Characterization of dystrophin in muscle-biopsy specimens from patients with Duchenne's or Becker's muscular dystrophy. *N.Engl.J.Med*. 318:1363-1368.

Hofmann, K., P. Bucher, and J. Tschopp. 1997. The CARD domain: a new apoptotic signalling motif. *Trends Biochem Sci*. 22:155-6.

Hosaka, Y., T. Yokota, Y. Miyagoe-Suzuki, K. Yuasa, M. Imamura, R. Matsuda, T. Ikemoto, S. Kameya, and S. Takeda. 2002. Alpha1-syntrophin-deficient skeletal muscle exhibits hypertrophy and aberrant formation of neuromuscular junctions during regeneration. *J Cell Biol*. 158:1097-107.

Im, W.B., S.F. Phelps, E.H. Copen, E.G. Adams, J.L. Slightom, and J.S. Chamberlain. 1996. Differential expression of dystrophin isoforms in strains of mdx mice with different mutations. *Hum Mol Genet*. 5:1149-53.

James, M., A. Nuttall, J.L. Ilsley, K. Ottersbach, J.M. Tinsley, M. Sudol, and S.J. Winder. 2000. Adhesion-dependent tyrosine phosphorylation of (beta)-dystroglycan regulates its interaction with utrophin. *J Cell Sci*. 113:1717-26.

Jansen, M., F.M. van Schaik, A.T. Ricker, B. Bullock, D.E. Woods, K.H. Gabbay, A.L. Nussbaum, J.S. Sussenbach, and J.L. Van den Brande. 1983. Sequence of cDNA encoding human insulin-like growth factor I precursor. *Nature*. 306:609-11.

Jarrett, H.W., and J.L. Foster. 1995. Alternate binding of actin and calmodulin to multiple sites on dystrophin. *J.Biol.Chem*. 270:5578-5586.

Jones, K.J., A.G. Compton, N. Yang, M.A. Mills, M.F. Peters, D. Mowat, L.M. Kunkel, S.C. Froehner, and K.N. North. 2003. Deficiency of the syntrophins and alpha-dystrobrevin in patients with inherited myopathy. *Neuromuscul Disord*. 13:456-67.

Jung, D., B. Yang, J. Meyer, J.S. Chamberlain, and K.P. Campbell. 1995. Identification and characterization of the dystrophin anchoring site on β-dystroglycan. *J.Biol.Chem*. 270:27305-27310.

Kahana, E., and W.B. Gratzer. 1995. Minimum folding unit of dystrophin rod domain. *Biochemistry*. 34:8110-8114.

Kahana, E., P.J. Marsh, A.J. Henry, M. Way, and W.B. Gratzer. 1994. Conformation and phasing of dystrophin structural repeats. *J.Mol.Biol*. 235:1271-1277.

Kameya, S., Y. Miyagoe, I. Nonaka, T. Ikemoto, M. Endo, K. Hanaoka, Y. Nabeshima, and S. Takeda. 1999. alpha1-syntrophin gene disruption results in the absence of neuronal-type nitric-oxide synthase at the sarcolemma but does not induce muscle degeneration. *J.Biol.Chem*. 274:2193-200.

Kemp, G.J., D.J. Taylor, G.K. Radda, and B. Rajagopalan. 1992. Bio-energetic changes in human gastrocnemius muscle 1-2 days after strenuous exercise. *Acta Physiol Scand*. 146:11-4.

Khurana, T.S., E.P. Hoffman, and L.M. Kunkel. 1990. Identification of a chromosome 6-encoded dystrophin-related protein. *J. Biol. Chem*. 265:16717-16720.

Kirk, C.J., D. Hartigan-O'Connor, B.J. Nickoloff, J.S. Chamberlain, M. Giedlin, L. Aukerman, and J.J. Mule. 2001. T cell-dependent antitumor immunity mediated by secondary lymphoid tissue chemokine: augmentation of dendritic cell-based immunotherapy. *Cancer Res*. 61:2062-70.

Koenig, M., E.P. Hoffman, C.J. Bertelson, A.P. Monaco, C. Feener, and L.M. Kunkel. 1987. Complete cloning of the Duchenne muscular dystrophy (DMD) cDNA and preliminary genomic organization of the DMD gene in normal and affected individuals. *Cell*. 50:509-517.

Koenig, M., and L.M. Kunkel. 1990. Detailed analysis of the repeat domain of dystrophin reveals four potential hinge segments that may confer flexibility. *J.Biol.Chem*. 265:4560-4566.

Koenig, M., A.P. Monaco, and L.M. Kunkel. 1988. The complete sequence of dystrophin predicts a rod-shaped cytoskeletal protein. *Cell*. 53:219-226.

Koseki, T., N. Inohara, S. Chen, and G. Nunez. 1998. ARC, an inhibitor of apoptosis expressed in skeletal muscle and heart that interacts selectively with caspases. *Proc Natl Acad Sci U S A*. 95:5156-60.

Kunkel, L.M., et.al. 1986. Analysis of deletions in DNA from patients with Becker and Duchenne muscular dystrophy. *Nature*. 322:73-77.

Kunkel, L.M., A.P. Monaco, W. Middlesworth, H.D. Ochs, and S.A. Latt. 1985. Specific cloning of DNA fragments absent from the DNA of a male patient with an X chromosome deletion. *Proc Natl Acad Sci U S A*. 82:4778-82.

Kuznetsov, A.V., K. Winkler, F.R. Wiedemann, P. von Bossanyi, K. Dietzmann, and W.S. Kunz. 1998. Impaired mitochondrial oxidative phosphorylation in skeletal muscle of the dystrophin-deficient mdx mouse. *Molecular & Cellular Biochemistry*. 183:87-96.

Landin-Wilhelmsen, K., L. Wilhelmsen, G. Lappas, T. Rosen, G. Lindstedt, P.A. Lundberg, and B.A. Bengtsson. 1994. Serum insulin-like growth factor I in a random population sample of men and women: relation to age, sex, smoking habits, coffee consumption and physical activity, blood pressure and concentrations of plasma lipids, fibrinogen, parathyroid hormone and osteocalcin. *Clin Endocrinol (Oxf)*. 41:351-7.

Lederfein, D., Z. Levy, N. Augier, D. Mornet, G. Morris, O. Fuchs, D. Yaffe, and U. Nudel. 1992. A 71-kilodalton protein is a major product of the Duchenne muscular dystrophy gene in brain and other nonmuscle tissues. *Proc.Natl.Acad.Sci.(U.S.A.)*. 89:5346-5350.

LeRoith, D., and C.T. Roberts, Jr. 1991. Insulin-like growth factor I (IGF-I): a molecular basis for endocrine versus local action? *Mol Cell Endocrinol*. 77:C57-61.

LeRoith, D., and C.T. Roberts, Jr. 2003. The insulin-like growth factor system and cancer. *Cancer Lett*. 195:127-37.

Levine, B.A., A.J. Moir, V.B. Patchell, and S.V. Perry. 1990. The interaction of actin with dystrophin. *FEBS Lett*. 263:159-162.

Li, P., D. Nijhawan, I. Budihardjo, S.M. Srinivasula, M. Ahmad, E.S. Alnemri, and X. Wang. 1997. Cytochrome c and dATP-dependent formation of Apaf-1/caspase-9 complex initiates an apoptotic protease cascade. *Cell*. 91:479-89.

Li, P.F., J. Li, E.C. Muller, A. Otto, R. Dietz, and R. von Harsdorf. 2002. Phosphorylation by protein kinase CK2: a signaling switch for the caspase-inhibiting protein ARC. *Mol Cell*. 10:247-58.

Lidov, H.G.W., S. Selig, and L.M. Kunkel. 1995. Dp140: A novel 140 kDa CNS transcript from the dystrophin locus. *Hum.Mol.Genet*. 4:329-335.

Lim, L.E., and K.P. Campbell. 1998. The sarcoglycan complex in limb-girdle muscular dystrophy. *Current Opinion in Neurology*. 11:443-52.

Louis, M., J. Lebacq, J.R. Poortmans, M.C. Belpaire-Dethiou, J.P. Devogelaer, P. Van Hecke, F. Goubel, and M. Francaux. 2003. Beneficial effects of creatine supplementation in dystrophic patients. *Muscle Nerve*. 27:604-10.

Lowe, W.L., Jr., C.T. Roberts, Jr., S.R. Lasky, and D. LeRoith. 1987. Differential expression of alternative 5' untranslated regions in mRNAs encoding rat insulin-like growth factor I. *Proc Natl Acad Sci U S A*. 84:8946-50.

Lu, Q.L., G. Bou-Gharios, and T.A. Partridge. 2003a. Non-viral gene delivery in skeletal muscle: a protein factory. *Gene Ther*. 10:131-42.

Lu, Q.L., H.D. Liang, T. Partridge, and M.J. Blomley. 2003b. Microbubble ultrasound improves the efficiency of gene transduction in skeletal muscle in vivo with reduced tissue damage. *Gene Ther*. 10:396-405.

Lu, Q.L., C.J. Mann, F. Lou, G. Bou-Gharios, G.E. Morris, S.A. Xue, S. Fletcher, T.A. Partridge, and S.D. Wilton. 2003c. Functional amounts of dystrophin produced by skipping the mutated exon in the mdx dystrophic mouse. *Nat Med*.

Lu, Q.L., G.E. Morris, S.D. Wilton, T. Ly, O.V. Artem'yeva, P. Strong, and T.A. Partridge. 2000. Massive idiosyncratic exon skipping corrects the nonsense mutation in dystrophic mouse muscle and produces functional revertant fibers by clonal expansion. *J Cell Biol*. 148:985-96.

Lumeng, C., S. Phelps, G.E. Crawford, P.D. Walden, K. Barald, and J.S. Chamberlain. 1999. Interactions between beta 2-syntrophin and a family of microtubule-associated serine/threonine kinases. *Nature Neuroscience*. 2:611-7.

Lund, P.K. 1994. Insulin-like growth factor I: molecular biology and relevance to tissue-specific expression and action. *Recent Prog Horm Res*. 49:125-48.

Lynch, G.S., S.A. Cuffe, D.R. Plant, and P. Gregorevic. 2001a. IGF-I treatment improves the functional properties of fast- and slow-twitch skeletal muscles from dystrophic mice. *Neuromuscul Disord*. 11:260-8.

Lynch, G.S., R.T. Hinkle, J.S. Chamberlain, S.V. Brooks, and J.A. Faulkner. 2001b. Force and power output of fast and slow skeletal muscles from mdx mice 6-28 months old. *J Physiol*. 535:591-600.

Madhavan, R., and H.W. Jarrett. 1994. Calmodulin-activated phosphorylation of dystrophin. *Biochemistry*. 33:5797-5804.

Madhavan, R., L.R. Massom, and H.W. Jarrett. 1992. Calmodulin specifically binds three proteins of the dystrophin-glycoprotein complex. *Biochem Biophys Res Commun*. 185:753-9.

Maichele, A.J., and J.S. Chamberlain. 1992. Cross-species conservation of a polymorphic dinucleotide repeat in the 3' non-translated region of the dystrophin gene. *Submitted*.

Mann, C.J., K. Honeyman, A.J. Cheng, T. Ly, F. Lloyd, S. Fletcher, J.E. Morgan, T.A. Partridge, and S.D. Wilton. 2001. Antisense-induced exon skipping and synthesis of dystrophin in the mdx mouse. *Proc Natl Acad Sci U S A*. 98:42-7.

Mathews, K.D., and S.A. Moore. 2003. Limb-girdle muscular dystrophy. *Curr Neurol Neurosci Rep*. 3:78-85.

Matsuda, R., A. Nishikawa, and H. Tanaka. 1995. Visualization of dystrophic muscle fibers in Mdx mouse by vital staining with evans blue: Evidence of apoptosis in dystrophin-deficient muscle. *J.Biochem.(Tokyo)*. 118:959-964.

McKoy, G., W. Ashley, J. Mander, S.Y. Yang, N. Williams, B. Russell, and G. Goldspink. 1999. Expression of insulin growth factor-1 splice variants and structural genes in rabbit skeletal muscle induced by stretch and stimulation. *J Physiol*. 516 (Pt 2):583-92.

Merlini, L., A. Cicognani, E. Malaspina, M. Gennari, S. Gnudi, B. Talim, and E. Franzoni. 2003. Early prednisone treatment in Duchenne muscular dystrophy. *Muscle Nerve*. 27:222-7.

Minetti, C., F. Sotgia, C. Bruno, P. Scartezzini, P. Broda, M. Bado, E. Masetti, M. Mazzocco, A. Egeo, M.A. Donati, D. Volonte, F. Galbiati, G. Cordone, F.D. Bricarelli, M.P. Lisanti, and F. Zara. 1998. Mutations in the caveolin-3 gene cause autosomal dominant limb-girdle muscular dystrophy. *Nature Genetics*. 18:365-8.

Mizuno, Y., T.G. Thompson, J.R. Guyon, H.G. Lidov, M. Brosius, M. Imamura, E. Ozawa, S.C. Watkins, and L.M. Kunkel. 2001. Desmuslin, an intermediate filament protein that interacts with alpha - dystrobrevin and desmin. *Proc Natl Acad Sci U S A*. 98:6156-61.

Monaco, A.P., C.J. Bertelson, S. Liechti-Gallati, H. Moser, and L.M. Kunkel. 1988. An explanation for the phenotypic differences between patients bearing partial deletions of the DMD locus. *Genomics*. 2:90-95.

Monaco, A.P., R.L. Neve, C. Coletti-Feener, C.J. Bertelson, D.M. Kurnit, and L.M. Kunkel. 1986. Isolation of candidate cDNA clones for portions of the Duchenne muscular dystrophy gene. *Nature*. 323:646-650.

Moser, H. 1984. Review of studies on the proportion and origin of new mutants in Duchenne muscular dystrophy. *In* Current Clinical Practices, series 20. L.P. Ten Tate, P.L. Pearson, and A.M. Stadhouders, editors. Excerpta Medica, Amsterdam. 41-52.

Musaro, A., K. McCullagh, A. Paul, L. Houghton, G. Dobrowolny, M. Molinaro, E.R. Barton, H.L. Sweeney, and N. Rosenthal. 2001. Localized Igf-1 transgene expression sustains hypertrophy and regeneration in senescent skeletal muscle. *Nat Genet*. 27:195-200.

Naldini, L., U. Blomer, P. Gallay, D. Ory, R. Mulligan, F.H. Gage, I.M. Verma, and D. Trono. 1996. In vivo gene delivery and stable transduction of nondividing cells by a lentiviral vector. *Science*. 272:263-267.

Neely, J.D., M. Amiry-Moghaddam, O.P. Ottersen, S.C. Froehner, P. Agre, and M.E. Adams. 2001. Syntrophin-dependent expression and localization of Aquaporin-4 water channel protein. *Proc Natl Acad Sci U S A*. 98:14108-13.

Neuss, M., R. Monticone, M.S. Lundberg, A. Chesley, E. Fleck, and M.T. Crow. 2001. The apoptotic regulatory CARD protein, ARC, prevents oxidant stress- mediated cell death by preserving mitochondrial function. *J Biol Chem*. 3:3.

Newey, S.E., E.V. Howman, C.P. Ponting, M.A. Benson, R. Nawrotzki, N.Y. Loh, K.E. Davies, and D.J. Blake. 2001. Syncoilin, a novel member of the intermediate filament superfamily that interacts with alpha-dystrobrevin in skeletal muscle. *J Biol Chem*. 276:6645-55.

Nguyen, H.H., V. Jayasinha, B. Xia, K. Hoyte, and P.T. Martin. 2002. Overexpression of the cytotoxic T cell GalNAc transferase in skeletal muscle inhibits muscular dystrophy in mdx mice. *Proc Natl Acad Sci U S A*. 99:5616-21.

Nguyen, H.X., and J.G. Tidball. 2003. Expression of a muscle-specific, nitric oxide synthase transgene prevents muscle membrane injury and reduces muscle inflammation during modified muscle use in mice. *J Physiol*. 550:347-56.

Nigro, V., E.D. Moreira, G. Piluso, M. Vainzof, A. Belsito, L. Politano, A.A. Puca, M.R. Passos-Bueno, and M. Zatz. 1996. Autosomal recessive limb-girdle muscular dystrophy, LGMD2F is caused by a mutation in the & sarcoglycan gene. *Nature Genet*. 14:195-198.

Noguchi, S., E.M. McNally, K. Ben Othmane, Y. Hagiwara, Y. Mizuno, M. Yoshida, H. Yamamoto, C.G. Bönnemann, E. Gussoni, P.H. Denton, T. Kyriakides, L. Middleton, F. Hentati, M. Ben Hamida, I. Nonaka, J.M. Vance, L.M. Kunkel, and E. Ozawa. 1995. Mutations in the dystrophin-associated protein gamma-sarcoglycan in chromosome 13 muscular dystrophy. *Science*. 270:819-822.

Nolan, M.A., O.D. Jones, R.L. Pedersen, and H.M. Johnston. 2003. Cardiac assessment in childhood carriers of Duchenne and Becker muscular dystrophies. *Neuromuscul Disord*. 13:129-32.

Nonaka, I. 1998. Animal models of muscular dystrophies. *Lab Anim Sci*. 48:8-17.

Nudel, U., D. Zuk, P. Einet, E. Zeelon, Z. Levy, S. Neuman, and D. Yaffe. 1989. Duchenne muscular dystrophy gene product is not identical in muscle and brain. *Nature*. 337:76-78.

Oak, S.A., K. Russo, T.C. Petrucci, and H.W. Jarrett. 2001. Mouse alpha1-syntrophin binding to Grb2: further evidence of a role for syntrophin in cell signaling. *Biochemistry*. 40:11270-8.

Oak, S.A., Y.W. Zhou, and H.W. Jarrett. 2003. Skeletal muscle signaling pathway through the dystrophin glycoprotein complex and Rac1. *J Biol Chem*. 278:39287-95.

Okamoto, T., A. Schlegel, P.E. Scherer, and M.P. Lisanti. 1998. Caveolins, a family of scaffolding proteins for organizing "preassembled signaling complexes" at the plasma membrane. *J Biol Chem*. 273:5419-22.

Ozawa, E., M. Yoshida, A. Suzuki, Y. Mizuno, Y. Hagiwara, and S. Noguchi. 1995. Dystrophin-associated proteins in muscular dystrophy. *Hum.Mol.Genet*. 4:1711-1716.

Parks, R.J., L. Chen, M. Anton, U. Sankar, M.A. Rudnicki, and F.L. Graham. 1996. A helper-dependent adenovirus vector system: removal of helper virus by Cre-mediated excision of the viral packaging signal. *Proc Natl Acad Sci U S A*. 93:13565-70.

Pastore, L., N. Morral, H.S. Zhou, R. Garcia, R.J. Parks, S. Kochanek, F.L. Graham, B. Lee, and A.L. Beaudet. 1999. Use of a liver-specific promoter reduces immune response to the transgene in adenoviral vectors. *Human Gene Therapy*. 10:1773-1781.

Peters, M.F., M.E. Adams, and S.C. Froehner. 1997. Differential association of syntrophin pairs with the dystrophin complex. *J. Cell Biol*. 138:81-93.

Peters, M.F., N.R. Kramarcy, R. Sealock, and S.C. Froehner. 1994. □2-syntrophin: Localization at the neuromuscular junction in skeletal muscle. *NeuroReport*. 5:1577-1580.

Peters, M.F., H.M. Sadoulet-Puccio, M.R. Grady, N.R. Kramarcy, L.M. Kunkel, J.R. Sanes, R. Sealock, and S.C. Froehner. 1998. Differential membrane localization and intermolecular associations of alpha-dystrobrevin isoforms in skeletal muscle. *Journal of Cell Biology*. 142:1269-78.

Petley, T., K. Graff, W. Jiang, H. Yang, and J. Florini. 1999. Variation among cell types in the signaling pathways by which IGF-I stimulates specific cellular responses. *Horm Metab Res*. 31:70-6.

Petrof, B.J., J.B. Shrager, H.H. Stedman, A.M. Kelly, and H.L. Sweeney. 1993. Dystrophin protects the sarcolemma from stresses developed during muscle contraction. *Proc Natl Acad Sci U S A*. 90:3710-3714.

Phelps, S.F., M.A. Hauser, N.M. Cole, J.A. Rafael, R.T. Hinkle, J.A. Faulkner, and J.S. Chamberlain. 1995. Expression of full-length and truncated dystrophin mini-genes in transgenic *mdx* mice. *Hum.Mol.Genet*. 4:1251-1258.

Piluso, G., M. Mirabella, E. Ricci, A. Belsito, C. Abbondanza, S. Servidei, A.A. Puca, P. Tonali, G.A. Puca, and V. Nigro. 2000. Gamma1- and gamma2-syntrophins, two novel dystrophin-binding proteins localized in neuronal cells. *J Biol Chem*. 275:15851-60.

Podhorska-Okolow, M., M. Sandri, S. Zampieri, B. Brun, K. Rossini, and U. Carraro. 1998. Apoptosis of myofibres and satellite cells: exercise-induced damage in skeletal muscle of the mouse. *Neuropathol Appl Neurobiol*. 24:518-31.

Pulido, a.S.M., a.A.C. Passaquin, a.W.J. Leijendekker, a.C. Challet, b.T. Wallimann, and a.U.T. Rüegg. 1998. Creatine supplementation improves intracellular Ca2+ handling and survival in mdx skeletal muscle cells. *Febs Letters*. 439: pp. 357-362.

Qin, Z.H., Y. Wang, K.K. Kikly, E. Sapp, K.B. Kegel, N. Aronin, and M. DiFiglia. 2001. Procaspase-8 is predominantly localized in mitochondria and released into cytoplasm upon apoptotic stimulation. *J Biol Chem*. 276:8079-86.

Rafael, J.A., G.A. Cox, K. Corrado, D. Jung, K.P. Campbell, and J.S. Chamberlain. 1996. Forced expression of dystrophin deletion constructs reveals structure-function correlations. *Journal of Cell Biology*. 134:93-102.

Rafael, J.A., E.R. Townsend, S.E. Squire, A.C. Potter, J.S. Chamberlain, and K.E. Davies. 2000. Dystrophin and utrophin influence fiber type composition and post-synaptic membrane structure. *Hum Mol Genet*. 9:1357-67.

Ragot, T., N. Vincent, P. Chafey, E. Vigne, H. Gilggenkrantz, D. Couton, J. Cartaud, P. Briand, J. Kaplan, M. Perricaudet, and A. Kahn. 1993. Efficient adenovirus-mediated transfer of a human minidystrophin gene to skeletal muscle of mdx mice. *Nature*. 361:647-650.

Rando, T.A., M.H. Disatnik, Y. Yu, and A. Franco. 1998. Muscle cells from mdx mice have an increased susceptibility to oxidative stress. *Neuromuscul Disord*. 8:14-21.

Ray, P.N., B. Belfall, C. Duff, C. Logan, V. Kean, M.W. Thompson, J.E. Sylvester, J.L. Gorski, R.D. Schmickel, and R.G. Worton. 1985. Cloning of the breakpoint of an X;21 translocation associated with Duchenne muscular dystrophy. *Nature*. 318:672-675.

Rinderknecht, E., and R.E. Humbel. 1978. The amino acid sequence of human insulin-like growth factor I and its structural homology with proinsulin. *J Biol Chem*. 253:2769-76.

Roberts, M.L., D.J. Wells, I.R. Graham, S.A. Fabb, V.J. Hill, G. Duisit, K. Yuasa, S. Takeda, F.L. Cosset, and G. Dickson. 2002. Stable micro-dystrophin gene transfer using an integrating adeno-retroviral hybrid vector ameliorates the dystrophic pathology in mdx mouse muscle. *Hum Mol Genet*. 11:1719-1730.

Roberts, R.G., A.J. Coffey, M. Bobrow, and D.R. Bentley. 1993. Exon structure of the human dystrophin gene. *Genomics*. 16:536-538.

Rosen, K.M., B.M. Wentworth, N. Rosenthal, and L. Villa-Komaroff. 1993. Specific, temporally regulated expression of the insulin-like growth factor II gene during muscle cell differentiation. *Endocrinology*. 133:474-81.

Rotwein, P. 1986. Two insulin-like growth factor I messenger RNAs are expressed in human liver. *Proc Natl Acad Sci U S A*. 83:77-81.

Rotwein, P., K.M. Pollock, D.K. Didier, and G.G. Krivi. 1986. Organization and sequence of the human insulin-like growth factor I gene. Alternative RNA processing produces two insulin-like growth factor I precursor peptides. *J Biol Chem*. 261:4828-32.

Rowe, L.B., J.H. Nadeau, R. Turner, W.N. Frankel, V.A. Letts, J.T. Eppig, M.S. Ko, S.J. Thurston, and E.H. Birkenmeier. 1994. Maps from two interspecific backcross DNA panels available as a community genetic mapping resource. *Mamm Genome*. 5:253-74.

Sadoulet-Puccio, H.M., M. Rajala, and L.M. Kunkel. 1997. Dystrobrevin and dystrophin: An interaction through coiled-coil motifs. *Proc Natl Acad Sci U S A*. 94:12413-12418.

Sakamoto, M., K. Yuasa, M. Yoshimura, T. Yokota, T. Ikemoto, M. Suzuki, G. Dickson, Y. Miyagoe-Suzuki, and S. Takeda. 2002. Micro-dystrophin cDNA ameliorates dystrophic phenotypes when introduced into mdx mice as a transgene. *Biochem Biophys Res Commun*. 293:1265-72.

Sampaolesi, M., Y. Torrente, A. Innocenzi, R. Tonlorenzi, G. D'Antona, M.A. Pellegrino, R. Barresi, N. Bresolin, M.G. De Angelis, K.P. Campbell, R. Bottinelli, and G. Cossu. 2003. Cell therapy of alpha-sarcoglycan null dystrophic mice through intra-arterial delivery of mesoangioblasts. *Science*. 301:487-92.

Sander, M., B. Chavoshan, S.A. Harris, S.T. Iannaccone, J.T. Stull, G.D. Thomas, and R.G. Victor. 2000. Functional muscle ischemia in neuronal nitric oxide synthase-deficient skeletal muscle of children with Duchenne muscular dystrophy. *Proc Natl Acad Sci U S A*. 97:13818-23.

Sandri, M., and U. Carraro. 1999. Apoptosis of skeletal muscles during development and disease. *Int J Biochem Cell Biol*. 31:1373-90.

Sandri, M., C. Minetti, M. Pedemonte, and U. Carraro. 1998. Apoptotic myonuclei in human Duchenne muscular dystrophy. *Laboratory Investigation*. 78:1005-16.

Sandri, M., M. Podhorska-Okolow, V. Geromel, C. Rizzi, P. Arslan, C. Franceschi, and U. Carraro. 1997. Exercise induces myonuclear ubiquitination and apoptosis in dystrophin- deficient muscle of mice. *J Neuropathol Exp Neurol*. 56:45-57.

Sara, V.R., and K. Hall. 1990. Insulin-like growth factors and their binding proteins. *Physiol Rev*. 70:591-614.

Sarukhan, A., S. Camugli, B. Gjata, H. von Boehmer, O. Danos, and K. Jooss. 2001a. Successful interference with cellular immune responses to immunogenic proteins encoded by recombinant viral vectors. *J Virol*. 75:269-77.

Sarukhan, A., C. Soudais, O. Danos, and K. Jooss. 2001b. Factors influencing cross-presentation of non-self antigens expressed from recombinant adeno-associated virus vectors. *J Gene Med*. 3:260-70.

Schiaffino, S., and C. Reggiani. 1994. Myosin isoforms in mammalian skeletal muscle. *J Appl Physiol*. 77:493-501.

Schiedner, G., N. Morral, R.J. Parks, Y. Wu, S.C. Koopmans, C. Langston, F.L. Graham, A.L. Beaudet, and S. Kochanek. 1998. Genomic DNA transfer with a high-capacity adenovirus vector results in improved in vivo gene expression and decreased toxicity. *Nature Genetics*. 18:180-3.

Schultz, J., U. Hoffmuller, G. Krause, J. Ashurst, M.J. Macias, P. Schmieder, J. Schneider-Mergener, and H. Oschkinat. 1998. Specific interactions between the syntrophin PDZ domain and voltage- gated sodium channels. *Nat Struct Biol*. 5:19-24.

Scott, J.M., S. Li, S.Q. Harper, D. Welikson, D. Bourque, C. DelloRusso, S.D. Hauschka, and J.S. Chamberlain. 2002. Viral vectors for gene transfer of micro-, mini-, or full-length dystrophin. *Neuromuscular Disorders*. 12(S):S23-S29.

Screaton, G.R., J.F. Caceres, A. Mayeda, M.V. Bell, M. Plebanski, D.G. Jackson, J.I. Bell, and A.R. Krainer. 1995. Identification and characterization of three members of the human SR family of pre-mRNA splicing factors. *Embo J*. 14:4336-49.

Shayakhmetov, D.M., C.A. Carlson, H. Stecher, Q. Li, G. Stamatoyannopoulos, and A. Lieber. 2002. A high-capacity, capsid-modified hybrid adenovirus/adeno-associated virus vector for stable transduction of human hematopoietic cells. *J Virol*. 76:1135-43.

Shimatsu, A., and P. Rotwein. 1987. Mosaic evolution of the insulin-like growth factors. Organization, sequence, and expression of the rat insulin-like growth factor I gene. *J Biol Chem*. 262:7894-900.

Shimizu, T., K. Matsumura, Y. Sunada, and T. Mannen. 1989. Dense immunostaining of both neuromuscular and myotendon junctions with an anti-dystrophin antibody. *Biomedical Research*. 10:405-409.

Sicinski, P., Y. Geng, A.S. Ryder-Cook, E.A. Barnard, M.G. Darlison, and P.J. Barnard. 1989. The molecular basis of muscular dystrophy in the mdx mouse: a point mutation. *Science*. 244:1578-1580.

Singleton, J.R., and E.L. Feldman. 1999. Insulin-like growth factor-1 in muscle metabolism and myotherapies. *Trends Endo. Metab. in press*.

Sjogren, K., J.L. Liu, K. Blad, S. Skrtic, O. Vidal, V. Wallenius, D. LeRoith, J. Tornell, O.G. Isaksson, J.O. Jansson, and C. Ohlsson. 1999. Liver-derived insulin-like growth factor I (IGF-I) is the principal source of IGF-I in blood but is not required for postnatal body growth in mice. *Proc Natl Acad Sci U S A*. 96:7088-92.

Song, K.S., P.E. Scherer, Z.L. Tang, T. Okamoto, S.W. Li, M. Chafel, C. Chu, D.S. Kohtz, and M.P. Lisanti. 1996. Expression of caveolin-3 in skeletal, cardiac, and smooth muscle cells - Caveolin-3 is a component of the sarcolemma and co-fractionates with dystrophin and dystrophin-associated glycoproteins. *J.Biol.Chem.* 271:15160-15165.

Spencer, M.J., E. Montecino-Rodriguez, K. Dorshkind, and J.G. Tidball. 2001. Helper (CD4(+)) and cytotoxic (CD8(+)) T cells promote the pathology of dystrophin-deficient muscle. *Clin Immunol*. 98:235-43.

Spencer, M.J., C.M. Walsh, K.A. Dorshkind, E.M. Rodriquez, and J.G. Tidball. 1997. Myonuclear apoptosis in dystrophic muscle occurs by perforin-mediated cytotoxicity. *FASEB J*. 11:2944.

Stedman, H.H., H.L. Sweeney, J.B. Shrager, H.C. Maguire, R.A. Panettieri, B. Petrof, M. Narusawa, J.M. Leferovich, J.T. Sladky, and A.M. Kelly. 1991. The mdx mouse diaphragm reproduces the degenerative changes of Duchenne muscular dystrophy. *Nature*. 352:536-539.

Stewart, C.E., and P. Rotwein. 1996. Growth, differentiation, and survival: multiple physiological functions for insulin-like growth factors. *Physiol Rev*. 76:1005-26.

Stoss, O., F.W. Schwaiger, T.A. Cooper, and S. Stamm. 1999. Alternative splicing determines the intracellular localization of the novel nuclear protein Nop30 and its interaction with the splicing factor SRp30c. *J Biol Chem*. 274:10951-62.

Straub, V., J.A. Rafael, J.S. Chamberlain, and K.P. Campbell. 1997. Animal models for muscular dystrophy show different patterns of sarcolemmal disruption. *J.Cell Biol*. 139:375-385.

Sunada, Y., and K.P. Campbell. 1995. Dystrophin-glycoprotein complex: molecular organization and critical roles in skeletal muscle. *Curr Opin Neurol*. 8:379-384.

Susin, S.A., H.K. Lorenzo, N. Zamzami, I. Marzo, C. Brenner, N. Larochette, M.C. Prevost, P.M. Alzari, and G. Kroemer. 1999. Mitochondrial release of caspase-2 and -9 during the apoptotic process. *J Exp Med*. 189:381-94.

Sussenbach, J.S. 1989. The gene structure of the insulin-like growth factor family. *Prog Growth Factor Res*. 1:33-48.

Tews, D.S., and H.H. Goebel. 1997a. Apoptosis-related proteins in skeletal muscle fibers of spinal muscular atrophy. *J Neuropathol Exp Neurol*. 56:150-6.

Tews, D.S., and H.H. Goebel. 1997b. DNA-fragmentation and expression of apoptosis-related proteins in muscular dystrophies. *Neuropathol Appl Neurobiol*. 23:331-8.

Thomas, G.D., M. Sander, K.S. Lau, P.L. Huang, J.T. Stull, and R.G. Victor. 1998. Impaired metabolic modulation of alpha-adrenergic vasoconstriction in dystrophin-deficient skeletal muscle [see comments]. *Proc Natl Acad Sci U S A*. 95:15090-5.

Tidball, J.G., D.E. Albrecht, B.E. Lokensgard, and M.J. Spencer. 1995. Apoptosis precedes necrosis of dystrophin-deficient muscle. *J.Cell Sci*. 108:2197-2204.

Tinsley, J., N. Deconinck, R. Fisher, D. Kahn, S. Phelps, J.M. Gillis, and K. Davies. 1998. Expression of full-length utrophin prevents muscular dystrophy in mdx mice. *Nat Med*. 4:1441-4.

Tinsley, J.M., D.J. Blake, A. Roche, U. Fairbrother, J. Riss, B.C. Byth, A.E. Knight, J. Kendrick-Jones, G.K. Suthers, D.R. Love, Y.H. Edwards, and K.E. Davies. 1992. Primary structure of dystrophin-related protein. *Nature*. 360:591-593.

Torres, L.F., and L.W. Duchen. 1987. The mutant mdx: inherited myopathy in the mouse. Morphological studies of nerves, muscles and end-plates. *Brain*. 110:269-299.

Tripathy, S.K., H.B. Black, E. Goldwasser, and J.M. Leiden. 1996. Immune responses to transgene-encoded proteins limit the stability of gene expression after injection of replication-defective adenovirus vectors. *Nature Med*. 2:545-550.

Turner, P.R., R. Schultz, B. Ganguly, and R.A. Steinhardt. 1993. Proteolysis results in altered leak channel kinetics and elevated free calcium in *mdx* muscle. *J.Membr.Biol*. 133:243-251.

van Deutekom, J.C., M. Bremmer-Bout, A.A. Janson, I.B. Ginjaar, F. Baas, J.T. den Dunnen, and G.J. van Ommen. 2001. Antisense-induced exon skipping restores dystrophin expression in DMD patient derived muscle cells. *Hum Mol Genet*. 10:1547-54.

Veal, E.A., and M.J. Jackson. 1996. Expression of programmed cell death-related genes in dystrophic *mdx* and control mouse muscle. *Biochem.Soc.Trans*. 24:S486.

Vincent, N., T. Ragot, H. Gilgenkrantz, D. Couton, P. Chafey, A. Grégoire, P. Briand, J.-C. Kaplan, A. Kahn, and M. Perricaudet. 1993. Long-term correction of mouse dystrophic degeneration by adenovirus-mediated transfer of a minidystrophin gene. *Nature Genet*. 5:130-134.

Vincent-Lacaze, N., R.O. Snyder, R. Gluzman, D. Bohl, C. Lagarde, and O. Danos. 1999. Structure of adeno-associated virus vector DNA following transduction of the skeletal muscle. *J Virol*. 73:1949-55.

Wang, B., J. Li, and X. Xiao. 2000. Adeno-associated virus vector carrying human minidystrophin genes effectively ameliorates muscular dystrophy in mdx mouse model. *Proceedings of the National Academy of Sciences of the United States of America*. 97:13714-9.

Warner, L.E., C. DelloRusso, R.W. Crawford, I.N. Rybakova, J.R. Patel, J.M. Ervasti, and J.S. Chamberlain. 2002. Expression of Dp260 in muscle tethers the actin cytoskeleton to the dystrophin-glycoprotein complex and partially prevents dystrophy. *Hum Mol Genet*. 11:1095-105.

Wells, K.E., J. Maule, R. Kingston, K. Foster, J. McMahon, E. Damien, A. Poole, and D.J. Wells. 1997. Immune responses, not promoter inactivation, are responsible for decreased long-term expression following plasmid gene transfer into skeletal muscle. *FEBS Lett*. 407:164-168.

Wells, K.E., S. Torelli, Q. Lu, S.C. Brown, T. Partridge, F. Muntoni, and D.J. Wells. 2003. Relocalization of neuronal nitric oxide synthase (nNOS) as a marker for complete

restoration of the dystrophin associated protein complex in skeletal muscle. *Neuromuscul Disord*. 13:21-31.

Wickham, T. 2000. Targeting adenovirus. *Gene Therapy*. 7:110-114.

Williamson, R.A., M.D. Henry, K.J. Daniels, R.F. Hrstka, J.C. Lee, Y. Sunada, O. Ibraghimov-Beskrovnaya, and K.P. Campbell. 1997. Dystroglycan is essential for early embryonic development: Disruption of Reichert's membrane in Dag1-null mice. *Hum.Mol.Genet*. 6:831-841.

Wolff, J.A., R.W. Malone, P. Williams, W. Chong, G. Acsadi, A. Jani, and P.L. Felgner. 1990. Direct gene transfer into mouse muscle in vivo. *Science*. 247:1465-8.

Xiao, X., J. Li, and R.J. Samulski. 1996. Efficient long-term gene transfer into muscle tissue of immunocompetent mice by adeno-associated virus vector. *Journal of Virology*. 70:8098-108.

Yakar, S., Y. Wu, J. Setser, and C.J. Rosen. 2002. The role of circulating IGF-I: lessons from human and animal models. *Endocrine*. 19:239-48.

Yang, B., D. Jung, D. Motto, J. Meyer, G. Koretzky, and K.P. Campbell. 1995a. SH3 domain-mediated interaction of dystroglycan and Grb2. *J.Biol.Chem*. 270:11711-11714.

Yang, B., D. Jung, J.A. Rafael, J.S. Chamberlain, and K.P. Campbell. 1995b. Identification of □-syntrophin binding to syntrophin triplet, dystrophin, and utrophin. *J.Biol.Chem*. 270:4975-4978.

Yang, L., H. Lochmuller, J. Luo, B. Massie, J. Nalbantoglu, G. Karpati, and B.J. Petrof. 1998. Adenovirus-mediated dystrophin minigene transfer improves muscle strength in adult dystrophic (MDX) mice. *Gene Ther*. 5:369-79.

Yang, S., M. Alnaqeeb, H. Simpson, and G. Goldspink. 1996. Cloning and characterization of an IGF-1 isoform expressed in skeletal muscle subjected to stretch. *Journal of Muscle Research & Cell Motility*. 17:487-95.

Yang, S.Y., and G. Goldspink. 2002. Different roles of the IGF-I Ec peptide (MGF) and mature IGF-I in myoblast proliferation and differentiation. *FEBS Lett*. 522:156-60.

Yang, Y., F.A. Nunes, K. Berencsi, E.E. Furth, E. Gonczol, and J.M. Wilson. 1994. Cellular immunity to viral antigens limits E1-deleted adenoviruses for gene therapy. *Proc Natl Acad Sci U S A*. 91:4407-4411.

Yoshida, M., H. Hama, M. Ishikawa-Sakurai, M. Imamura, Y. Mizuno, K. Araishi, E. Wakabayashi-Takai, S. Noguchi, T. Sasaoka, and E. Ozawa. 2000. Biochemical evidence for association of dystrobrevin with the sarcoglycan-sarcospan complex as a basis for understanding sarcoglycanopathy. *Hum Mol Genet*. 9:1033-40.

Yuasa, K., M. Sakamoto, Y. Miyagoe-Suzuki, A. Tanouchi, H. Yamamoto, J. Li, J.S. Chamberlain, X. Xiao, and S. Takeda. 2002. Adeno-associated virus vector-mediated gene transfer into dystrophin-deficient skeletal muscles evokes enhanced immune response against the transgene product. *Gene Ther*. 9:1576-88.

Zhang, Y., N. Chirmule, G. Gao, and J. Wilson. 2000. CD40 ligand-dependent activation of cytotoxic T lymphocytes by adeno-associated virus vectors in vivo: role of immature dendritic cells. *J Virol*. 74:8003-10.

Zubrzycka-Gaarn, E.E., D.E. Bulman, G. Karpati, A.H. Burghes, B. Belfall, H.J. Klamut, J. Talbot, R.S. Hodges, P.N. Ray, and R.G. Worton. 1988. The Duchenne muscular dystrophy gene product is localized in sarcolemma of human skeletal muscle. *Nature*. 333:466-469.

8. ACKNOWLEDGMENTS

There are many people whom I would like to thank. Their continuous support and encouragement helped me enjoy my time as a graduate student in Ann Arbor and Seattle and made this thesis possible.

I feel deeply appreciative to my thesis advisor Jeffrey Chamberlain for giving me the opportunity to conduct this work in his lab. I am very grateful for his tremendous support and guidance over the past five years, which has made my research enjoyable and very rewarding. Thanks for all the valuable advice, good ideas and encouragements throughout my time as a graduate student.

I am very grateful to Charalampos Aslanidis for his continuous interest in my project and for supervising this work at the University of Regensburg.

I would like to thank Steve Hauschka for giving me a great introduction to the world of myoblast cell culture and for many inspiring discussions.

A big thank you to all past and present Chamberlain lab members for creating such a pleasant lab atmosphere, for many stimulating discussions and for making my day in the lab so cheerful. In particular, I would like to thank James Allen for his support and guidance in generating AAV and to Paul Gregorevic for giving me valuable support in measuring functional contractile properties.

I am very grateful to all of my friends from Ann Arbor and Seattle. Thank you for all the good times we spent together and all the support and encouragements, which were so important to complete this thesis. My special thanks to Martin, who never stopped believing in me and whose help and patience was crucial in getting this far. Finally, thanks to my parents, my brother and all my friends from Munich for their continuous support, and patience for seeing me only once a year.

Die vorliegende Arbeit wurde am Institut für Neurologie an der Universität von Washington, Seattle unter der Betreuung von Prof. Dr. Jeffrey Chamberlain durchgeführt.

Die vorliegende Arbeit wurde selbstständig, ohne unzulässige Hilfe angefertigt.

_____

Simone Abmayr